Karina. L. New

The Role of Subunit Interfaces in the Function of $(\alpha4\beta2)_2\beta2$ nAChRs

A thesis submitted in partial fulfilment of the requirement of Oxford Brookes University for the degree of Doctor of Philosophy

September 2016

Contents

Chapter 1 - Introduction

Chapter 2 - Materials and Methods

Chapter 3 - Is there an agonist site at the β2(+)/β2(-) interface of the HS α4β2 nAChR?

List of Publications

Mantione E, Micheloni S, Alcaino C, **New K**, Mazzaferro S and Bermudez. (2012) Allosteric modulators of α4β2 nicotinic acetylcholine receptors: A new direction for antidepressant drug discovery. *Future Medicinal Chemistry* 4(17): 2217-30

Mazzaferro S, Gasparri F, **New K**, Alcaino C, Faundez M, Vasquez P.I, Vijayan, R, Biggin, P.C, Bermudez I (2014). Non-equivalent ligand selectivity of agonist sites in $(\alpha4\beta2)_2\alpha4$ nicotinic acetylcholine Receptors: A key determinant of agonist efficacy. *Journal of Biological Chemistry* 289(31): 21795-806.

Manuscripts in Preparation

New K, Garcia del Villar, S, Mazzaferro S, Biggin P, Bermudez I. (2016) The fifth subunit in the high sensitivity α4β2 nicotinic acetylcholine receptor contributes to agonist-driven channel gating.

New K, Biggin P, Muusgard M, Bermudez I (2016) Structural determinants of TC-2559 agonism on HS α4β2 nicotinic acetylcholine receptor

Poster Presentations

Biophysical Society Annual Meeting 2013, San Francisco, CA, USA. **The agonist binding sites in (α4β2)2α4 nicotinic receptors display different agonist pharmacology.**

Nicotinic Acetylcholine Receptors Meeting. Cambridge, UK, 2014. **Does the auxiliary subunit in $(\alpha4\beta2)_2\beta2$ nicotinic acetylcholine receptors affect ACh sensitivity?**

List of Abbreviations

ACh	Acetylcholine
AChBP	Acetylcholine binding protein
ABS	Agonist binding site
ADNFLE	Autosomal dominant nocturnal frontal lobe epilepsy
ANOVA	Analysis of variance
cDNA	Complementary deoxyribose nucleic acid
CNS	Central nervous system
CRC	Concentration response curve
cRNA	Complementary ribonucleic acid
dNTP	Deoxyribonucleotide triphosphate
DhβE	Dihydro-β-erythroidine
DMSO	Dimethylsulphoxide
DTT	Dithioerythritol
EC_{20}	Concentration producing 20% of maximal effect.
EC_{50}	Concentration producing half maximal effect
EC_{80}	Concentration producing 80% maximal effect
EC_{50_1}	Concentration producing half-maximal high sensitivity stimulatory effect in a biphasic CRC
EC_{50_2}	Concentrations producing half-maximal low sensitivity stimulatory effects in a biphasic CRC
ECD	Extracellular domain
ELIC	Prokaryotic pentameric ligand-gated ion channels from *Erwinia chrysanthemi*
EPSP	Excitatory postsynaptic potential
GABA	γ-aminobutyric acid
$GABA_A$	γ-aminobutyric acid receptor type A

GLIC	Prokaryotic pentameric ligand-gated ion channels from *Gloeobacter violaceus*
GluCl	Glutamate-gated chloride channels
Gly	Glycine
GlyR	Glycine receptor
HEPES	N-2-hydroxyethylpiperazine-N'-2-ethansulphonic acid
HS	High sensitivity
IC_{50}	Concentration producing half maximal inhibition
IPSP	Inhibitory postsynaptic potential
Ki	Binding affinity constants
kDA	Kilo Dalton
LGIC	Ligand-gated ion channel
LS	Low sensitivity
MTS	Methenothiosulphate reagents
MTS-ET	[2-(Trimethylammonium)ethyl] methanethiosulfonate
N-terminal	Amino-terminus
nAChR	Nicotinic acetylcholine receptor
nH	Hill coefficient
PCR	Polymerase chain reaction
pLGIC	Pentameric ligand-gated ion channel
REFER	Rate-equilibrium free energy relationships
SCAM	Substituted Cysteine Accessibility Method
SEM	Standard error of the mean
TC-2559	4-(5-ethoxy-3-pyridinyl)-N-methyl-(3E)-3-buten 1aminedifumarate
TMD	Transmembrane domain

List of Figures

Chapter 1.

Chapter 2.

Chapter 3.

Chapter 4.

Chapter 5.

List of Tables

Chapter 3.

Chapter 4.

Chapter 5

Abstract

Nicotinic acetylcholine receptors (nAChRs) are pentameric ligand-gated ion channels formed from homologous subunits, of which there are many different subtypes. The ability to combine different types of subunits into an individual pentamer enables a wide diversity of functional properties to meet a range of physiological needs. In the brain, the vast majority of high-sensitivity ^{3}H-nicotine binding sites are due to nAChRs containing α4 and β2 subunits. These subunits assemble into pentamers with alternate stoichiometries $(\alpha4\beta2)_2\beta2$ and $(\alpha4\beta2)_2\alpha4$. These two receptors differ in sensitivity to ACh, unitary current amplitude, selectivity for different agonists, antagonists an, and potentiation by ions or drugs. The alternate stoichiometries are present in neurones and although they tend to co-express, there are regions in the brain such as the striatum, where only one stoichiometry is present.

Recent studies of the $(\alpha4\beta2)_2\alpha4$ nAChR have shown that this receptor type functions with three agonist sites, two of these are on the α4/β2 interfaces of the receptor and are thus classical nAChR agonist sites, whereas the other site is on the α4/α4 interface, the signature interface of this receptor type. Pharmacological studies have shown convincingly that the site at the α4/α4 interface accounts for the unique pharmacology of the $(\alpha4\beta2)_2\alpha4$ nAChRs. In the case of the $(\alpha4\beta2)_2\beta2$, there is a signature β2(+)/β2(-) interface that homology models suggest may house an agonist site. The β2(+)/β2(-) interface forms between the fifth subunit of the receptor and another β2 subunit that also contributes, through its complementary face, to an agonist site. In common with the $(\alpha4\beta2)_2\alpha4$ nAChR, the α4/β2 interfaces of $(\alpha4\beta2)_2\beta2$ house each an agonist site. To test the possibility of an operational agonsit site at the β2(+)/β2(-) interface, and to answer the question of whether the unique functional behaviour of the $(\alpha4\beta2)_2\beta2$ can be ascribed to an additional agonist site, the work presented here used targeted single point-mutations, functional analysis and the substituted cysteine scanning approach. By using these approaches, it was found that the β2(+)/β2(-) interface does not house an agonist site; however, it was found that this interface is an important site for inter-subunit communication and that this communication encodes agonist efficacy elements.

The inter-subunit communication occurs between residues of the E loop of the fifth subunit of the receptor and conserved aromatic residues in loop B of the complementary subunit of one of the agonist sites found on α/β interfaces. By alanine substituting agonist sites on the α4/β2 interfaces and determining the consequences of the mutations on the pattern of covalent reaction between a methanethiosulphonate compound and one of the β2 subunits contributing to the β2(+)/β2(-) interface, it was found that the agonist sites communicate with the β2(+)/β2(-) interface via the interactions between the E loop residues and conserved aromatic residues. Further studies with a compound that enabled direct measurements of changes in agonist efficacy relative to that ACh established that agonist efficacy is dependent on primarily on binding of the agonist to the agonist sites on the α4/β2 interfaces and then on the E loop-conserved aromatic residues interactions. The results are discussed in the context of recent cryo-electron microscopy structures of the muscle nAChR that show, for the first time, that the fifth subunit of nAChRs may play a key role in gating of the ion channel.

Chapter 1

-Introduction-

1.1 Study of the Mind and Brain

The final frontier of medical science is often referred to as the challenge of providing biological explanation of complex high order processes such as consciousness and behaviour; how these arise from apparently simple physical matter and how they differ between individuals.

The earliest recording of study of the brain dates back to ancient Egyptian civilisation, in a document known as the Edwin Smith Surgical Papyrus. This not only contains accurate descriptions of cranial structures including the external brain surface, but accounts of somatic disorders caused by damage to the brain, historically introducing its power to govern widespread effects (Wilkins, 1992).

Roughly 10 centuries later, over two millennia ago, Hippocrates proposed that in order to begin to understand the mind, we must first study the brain; a historical notion re-enforced by 20th century neural science. More recently in western science, at the turn of the 19th century, Auguste Comte, the French philosopher recognised that studies of the mind required objective observation, and thus investigations into psychological phenomena should be integrated in biological sciences (Gardner and Martin, 2000).

Recently, advancement of scientific techniques and interdisciplinary research has seen remarkable progress of research that although still largely concerned with internal representations of information and subjective states of mind, has firm empirical grounding in biological science. Revelations of genetics, allowing sequencing of proteins integral to specialised cell function has enabled us to study the complex composition of the brain, greatly expanding our knowledge of the physical processes from which senses, learning and perceiving arise.

1.1.2 - Insight to "Building Blocks" of the Brain and its Behaviours

Towards the end of the 19th century, anatomist Santiago Ramon y Cajal observed that the reality of the composition of cortical communication networks are discrete units, neurons, with spaces between them termed synapses (Ramon y Cajal, 1988, Boya and Alamo, 2006). These specialised cells communicate to one another, transmitting signals across the synapses between neurons in precise fashion and are connected in functional groups.

Ramon y Cajal realised two important factors of cell signalling and brain function. The first, the 'principle of dynamic polarization' states that signals transmitted along these connections of neurons can only travel in one direction. Secondly, the 'principle of connectional specificity' encompasses the fact that network formation is not random, but specific and functional connections are made between cells (Kandel, 2000). These core principles are still at the center of our understanding of processes occurring in the brain.

At this point it was long known that live muscle and nerve cells have inherent abilities to produce electricity. This idea was later developed by experiments showing that this electrical activity of a given cell could predictably affect that of an adjacent cell, leading to conclusions that it was these electrical properties that governed transmission of information through and between neurons (Kandel, 2000). This was famously investigated by British physiologists Hodgkin and Huxley in 1965. Through their studies of the giant squid axon they revealed the existence of the action potential; electrical signals conducted through nervous tissue by the movement of ions.

Dependent on their physiology, signals from neurons can be excitatory or inhibitory and one neuron may have up to 10,000 inputs of both inhibitory and

excitatory signals from other cells. Dependent on the pattern of these signals that accumulates at a given time, the post synaptic cell may or may not reach the depolarisation threshold required to initiate an action potential that will then in turn inhibit or excite any of the 1000s of neurons they are pre-synaptic to. With a total of around 100 billion cells in the human brain, the intricacies of particular pathways begin to be seen.

1.2 Synaptic Signalling in the Nervous System

Neurones communicate with each other and target cells using structures termed synapses. There are electrical synapses and chemical synapses. The former are gap junctions that allow cytoplasmic continuity between synapsed cells; they are rare in mammalian neurones (Kandel, 2000). Chemical synapses are the predominant structure by which mammalian neurones signal (Kandel, 2000). Chemical synapses consist of a presynaptic terminal and a postsynaptic cell separated by a narrow space termed synaptic gap. The presynaptic terminal, the end part of an axon, contains vesicles filled with neurotransmitter and the apparatus needed for the release of the neurotransmitter into the synaptic gap. The post-synaptic cell contains postsynaptic receptors in the membrane facing the synaptic gap. The key functional feature of chemical synapses is the interaction between the released neurotransmitter and the neurotransmitter receptors of the post-synaptic cell. Membrane depolarisation brought about by the arrival of action potentials to the presynaptic terminal causes influx of calcium ions through voltage gated calcium channels, prompting vesicles containing neurotransmitter to fuse with the presynaptic membrane facing the synaptic gap. Fusion releases neurotransmitter into the synaptic cleft, which

increases the concentration of the neurotransmitter in the gap, thus favouring the diffusion of the chemical messenger towards the post synaptic cell where it will bind the postsynaptic gap receptors.

A major class of post-synaptic receptors are ligand gated ion channels (LGIC's). These proteins are ion channels integrated into the cell membrane; they are not only found in neurones but also in muscle cells, cells of the auto-immune system, hormone-releasing cells (e.g. pancreatic cells), where they also play key roles in cell signalling. Binding of neurotransmitters to the agonist site in LGIC's gates the ion channel allows influx or outflow of ion across the channel. As a result of the movement of ions through the channel, the post-synaptic neuron generates post-synaptic potentials, which can be excitatory (EPSP) or inhibitory (IPSP), depending on the nature of the ionic current that passed through the ion channel. EPSP may lead to the generation of action potentials, depending if the level of overall membrane depolarisation is sufficient to elicit action potentials. Conversely, IPSP cause membrane hyperpolarization as it defers from the threshold value for transmission of excitatory stimuli, thus these events are seen as inhibitory. Considering the vast number of cells synapsing onto a single neuron and the probability of action potential transmission being a result of the summation of this alteration of membrane potential, this can be a very fine tuned process.

Neurotransmitter-receptor complexes dissociate within milliseconds and the receptors return to a resting state. The ligands are then recycled back into the presynaptic neuron through transporters and diffusion. Many chemical structures act as neurotransmitters, including amino acids and hormones. A major neurotransmitter system is the cholinergic system and this thesis focuses on one component of this system, the α4β2 nicotinic acetylcholine receptor.

1.3 The Cholinergic System

The cholinergic system is a widespread system implicated in many central nervous system (CNS) functions and pathologies. In the peripheral nervous system, the action of ACh on its receptors is the predominant form of fast acting point to point contact across the synapses in autonomic ganglia and the neuromuscular junction. Conversely, the role of ACh and the cholinergic system in the brain is said to be mostly neuromodulatory (Wonnacott, 1997).

The neurotransmitter used by the cholinergic system is acetylcholine (ACh). ACh was the first neurotransmitter to be discovered, which occurred in 1914. At that time, it was termed "Vagustoff" due to its origins from the vagus nerve (Tansey, 2006). The modern name is derived from the fact that it is an acetylated choline molecule, synthesised from choline and acetyl-CoA by the enzyme choline acetyltransferase. Once ACh dissociates from the receptors to which it binds and activates, it is broken down into choline and acetate by the enzyme acetylcholinesterase. This facilitates ACh clearance from the synapse once the synaptic transmission is complete as choline is then taken up into the presynaptic cell by the choline transporter.

1.3.1- Neuromodulation by Cholinergic Neurons

Neuromodulation is described as the alteration of a neuron or group of neurons signalling by external excitatory or inhibitory inputs. A neuromodulator modifies behaviour of target cells by changing their state without directly causing excitation or inhibition (Ito and Schuman 2008). ACh modulates neuronal signalling

by number of ways such as influencing presynaptic neurotransmitter release, altering neuronal firing patterns, or combinations of these (Exley and Cragg 2008; Rice and Cragg, 2004; Zhang and Sulzer, 2004); however, these effects are always mediated through ACh-selective receptors located in the cell body, axon or presynaptic terminals of the target neuron (Wonnacott, 1998)

Many studies have revealed the neuromodulatory effects of ACh in the brain via these processes and shown their mechanisms pertaining to cognition and behaviour (Poorthuis et al, 2014). Letzkus et al, (2011) demonstrated rapid ACh mediated alteration of neuron excitation required for fear conditioning alongside direct activation of cholinergic neurons in regions of the cortex contributing to learning. ACh has also been shown to amplify sensory signals to the cortex while inhibiting excitatory feedback of a stimulus in order to aid information retrieval, reinforcing learning and memory processes (Hasselmo, 2006), as well as improving the signal-to-noise ratio in a learning environment (Yu and Dayan, 2005). Activation of cholinergic receptors has also been shown to co-ordinate firing of neurons suggesting its importance in synchronisation of neuronal activity (Bucher and Goaillard 2011; Kawai et al., 2007). Differences in the time-scale of ACh release at the local microcircuit level may further refine the role of ACh in complex behaviours, highlighting in turn the intricacies and complexities of processes underlying them (Hasselmo and Sarter, 2011; Giocomo and Hasselmo, 2007; Yu and Dayan, 2005). It is this complex neuromodulatory role of ACh in the brain that has made it difficult to use the cholinergic system for therapeutic intervention in diseases in which ACh signalling is involved, in comparison to neurotransmitter systems that signal predominantly post-synaptically (e.g., GABA, glutamate)

1.3.2 Receptors of the Cholinergic System

In common with many signalling systems in the brain, the cholinergic system signals through metabotropic (muscarinic acetylcholine receptors, mAChRs) and ligand-gated ion channels (nicotinic acetylcholine receptors, nAChRs). These receptors have been named according to their ability to bind the plant alkaloid nicotine and mushroom toxin muscarine respectively. mAChRs are G-protien coupled receptors initiating and mediating long lasting intracellular metabolic responses, whereas nAChRs are ligand-gated ion channels that mediate fast ionic currents when bound to ACh.

Neuromodulation is typically attributed to metabotropic receptors due to their ability to alter many downstream cellular processes and their long term effects. However, nAChRs in the brain also appear to play primarily modulatory roles (Wonnacott, 1997). In addition, mAChR alteration of nAChR mediated of neurotransmitter release in the CNS and interaction of the two receptor classes as a mode of neuromodulation has been reported (Luchicchi et al, 2014; Grili et. al., 2008). This has suggested that the overall cholinergic effect exerted upon specific circuits greatly depends on the expression patterns of both nAChRs and mAChRs (Wilkie et al., 1996). mAChR-nAChR interactions appear to modulate activity in the pre-limbic area of the rat prefrontal cortex, a cortical region known to be involved in cognitive processes (Vidal and Changeux, 1993).

Cross-talk between mACh and nAChRs has been demonstrated to exist particularly in the presynaptic location of the modulatory receptors studied (Marchi and Grilli, 2010). Thus, it stands that presynaptic nAChRs interact with other metabotropic or ionotropic receptors on the same cell, producing an integrated

response of the neuron with antagonistic or synergistic outcomes. Additionally this can then have a resultant effect upon consequences at the post synaptic cell and its receptors. mAChR activation has been shown to be instigated by activity of nAChRs coexisting on the same dopamine releasing terminals. Conversely, co-ordinated activation of mAChRs and nAChRs has been shown to modulate pre-synaptic GABA release (Grilli et al., 2008; Grilli et al., 2009). Functional effects of receptor type interplay has also been shown experimentally such as regulation of muscarinic receptor signalling via cholinergic interneurons being critical in decision making behaviours modulated by striatal activity (Goldberg, Ding and Surmeier, 2012).

Overall control and specificity of cholinergic signalling appears to be mediated by many interlinked factors including differences in sites of receptor expression, interplay of both mAChRs and nAChRs and their affinities for ACh, concentration of ACh in and around the synapse, rates of synaptic clearance and the interconnection of all these contributors. Additionally time-scale differences of ACh release further refines the action of ACh at the local microcircuit level in complex behaviours (Zhang et. al., 2010; McQuiston, 2014) .

1.4 nAChRs

nAChRs belong to the superfamily of pentameric ligand gated ion channels (pLGICs). In humans, this superfamily comprises the Cys loop receptors (including muscle and neuronal nAChR, 5-HT_3, GABA-A, and glycine receptors), which mediate all fast CNS synaptic inhibition and much of fast peripheral excitation (Miller and Smart, 2010). Cys loop receptor subunits assemble as a pentamer of identical (homomeric receptors) or different (heteromeric receptors) subunits around

a central ion channel. These receptors exist in at least four distinct, interconvertible states: resting (agonist unbound, closed), flipped (agonist-bound, closed), open (agonist-bound, open) and desensitised (agonist-bound, closed), and the binding of agonists, antagonist and allosteric compounds alters the equilibrium between these states. Agonists such as neurotransmitters bind the agonist site, which is located in the extracellular domain (ECD) of the receptors, and this triggers rapid opening of an intrinsic ion channel. Prolonged exposure to the agonist induces the non-conducting (desensitised) state of the ion pore.

1.4.1 Cellular Expression of nAChRs

In the brain, nAChRs have been found dispersed along the cell body, processes, axons and pre-synaptic terminals (Wonnacott, 1997; Léna et al. 1999; McGehee et al. 1995; Kawai et al. 2007; Galindo-Charles et al. 2008). In these regions, α4β2 nAChRs have been shown to be modulatory rather than synaptic (Wonnacott *et al.*, 1989; Dickinson et al., 2008). As non-synaptic receptors, they have been found to modulate the pre-synaptic release of ACh as well neurotransmitters such as dopamine, serotonin**,** GABA and ATP (Marchi and Grilli 2010; Grilli et al. 2009; Exley and Cragg 2008; Galindo-Charles et al. 2008; Gurano et al., 2012).

Anatomical studies of rats and humans have also identified cholinergic synapses of comparable structure to those of other point-to-point neurotransmitters, in the neocortex and anterior temporal lobe (Turrini *et al.*, 2001). In a number of brain areas, nicotine directly applied to neurons has been shown to consequentially induce significant nAChR inward currents, mediated β2 subunit containing nAChRs

(Picciotto et al., 1995; Picciotto et al., 1998; Léna and Changeux 1999). Also, post-synaptic nAChRs expressed on serotonergic neurons have been shown to be important in their funtiuon (Galindo-Charles *et al.*, 2008). This further supports nAChRs directly influencing cell polarisation by postsynaptic receptors.

Although debated in the literature, another cellular location derived mechanism of ACh action is volume transmission via extra synaptically expressed nAChRs (Descarries et al. 1997; Descarries and Mechawar 2000). This raises the question of whether cholinergic signalling can occur at a distance from its site of release, following its diffusion through the extracellular space, or, strictly via regular synapses comprising compatible pre- and postsynaptic cells in close proximity (Agnati et al., 1995; Sarter et al, 2009). The idea of ACh volume transmission in the brain has been suggested by many lines of evidence such as the diffuse nature of cholinergic innervation, lack of post-synaptic specialisation of cells within the cholinergic system and anatomical and temporal mismatches between of ACh release and cholinergic receptor stimulation (Contant *et al.*, 1996; Zhang et al, 2010).

1.4.2 pLGIC Structure

In the last 16 years extraordinary progress has been made in resolving the atomic structures that underlie the function of the pLGICs. The current view of the function and structure of the pLGICs is based on cryo-electro microscopy (EM) structures of the *Torpedo* muscle nAChR in an agonist unbound presumed closed state (4Å) (Unwin, 2005) and agonist-bound presumed desensitised state (6.2Å resolution) (Unwin and Fujiyoshi, 2012), cryo-EM structures of the glycine receptors in presumed open, closed and desensitised states (Du et al., 2015), high-resolution

crystal structures of the snail homologue ACh binding protein (AChBP) (Brejc et al., 2001; Celie et al., 2005), extracellular binding domains of the nAChR α1 (Dellisanti et al., 2007), α7 (Li et al., 2011), α9 (Zouridakis et al., 2014) and α2 (Kouvatsos et al., 2016) subunits, full-length crystal structures of prokaryotic pLGICs homologues from *Erwina chrysanthemi* (ELIC) (Hilf et al., 2008) and *Gliobacter violaceous* (GLIC) (Boquet et al., 2009), solved in presumed closed and open channel conformation, the *Caenorhabditis elegans* glutamate-gated ion channel in an open channel conformation (Althoff et al., 2014), full-length human GABA-A (Miller and Ariescu, 2014), murine 5-HT3 (Hassaine et al., 2014) and human α4β2 nACh (Morales-Perez et al., 2016) receptors in a presumed desensitised conformation, as well as molecular dynamics analysis of pLGICs (Calimet et al., 2013). The discussion that follows focuses on current views of the structure and function of the pLGICs.

The recently reported ECD and full-length structures mentioned above have provided significant insight into the structure of the pLGICs. In agreement with the structure of the AChBP (Brejc et al., 2001; Celie et al., 2005), all pLGICs share a conserved organisation with five identical or homologous subunits arranged around a central ion pore **(Figure 1.1).** Each subunit has a large hydrophilic extracellular N terminal domain (ECD) that is folded in a highly conserved immunoglobulin-like β-sandwich made of 10 β-strands (β1-β10) that arrange into an inner and outer β-sheet, stabilised through highly conserved hydrophobic amino acids (Corringer et al., 2012) **(Figure 1.1).** The strands are connected through loops that play a critical role in agonist binding, structure and coupling agonist binding to gating (Corringer et al., 2012). The loops vary in length and structure among the pLGICs. For example,

prokaryotic pLGICs lack the name-sake Cys loop (joining β strands β6 and β7) found in all Cys-loop pLGICs (Hilf et al., 2008; Bocquet et al., 2009).

The transmembrane domain (TMD) of pLGICs comprises four transmembrane α helices (M1 to M4) connected by linkers (M1-M2, M2-M3, M3-M4), as well as intracellular domains and a highly variable extracellular C-terminal (post-M4) (Corringer et al., 2012) **(Figure 1.1).** M2 α-helices form the walls of the ion channel and each subunit contributes to it (Unwin, 2005). M1, M3 and M4 face the lipid bilayer and have been shown to host binding site for allosteric modulators (Young et al., 2008; Olsen et al., 2013; Nury et al., 2011) and lipids (Bocquet et al., 2009). In common with the ECD loops, the TMD α-helices are linked by loops, which play a key role in such aspects of receptor function as gating (Corringer et al., 2012) and coupling agonist-triggered agonist binding site movements to channel gating (Miller and Smart, 2010).

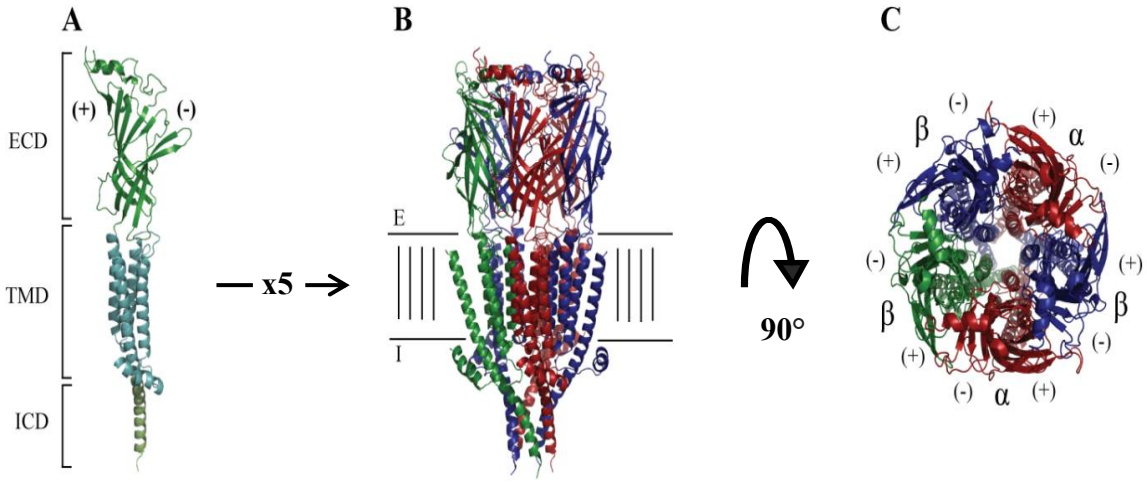

Figure 1.1. Ribbon diagrams of nAChR β2 subunit and α4β2 pentamer to demonstrate assembly. (A) Single (β2) subunit of nAChR highlighting the three structural domains; the ECD (extracellular domain - green), TMD (trans-membrane domain - teal) and ICD (intracellular domain – pale green) Orientation of the principal (+) and complimentary (-) faces is also shown**. (B)** Five subunits come together to form pentamer in membrane. Cartoon of membrane is shown and extracellular (E) and intracellular (I) spaces labled. **(C)** View of pentamer from extracellular space. Pseudo symmetrical arrangement around ion pore can be seen as well as orientation of the principal (+) and complementary (-) faces of each subunit and subunit interfaces.

1.4.3 - Extracellular domain (ECD) and Agonist Binding Site

The binding site is located at the interface between two subunits. The best functionally and biochemically characterised agonist site is that of the muscle nAChR. Early affinity labelling, together with extensive mutagenesis studies, identified and mapped the ACh binding site at the interface between two adjacent subunits with the contribution from three regions from a principal subunit (α1), termed loops A, B and C and four regions of a complementary subunit (γ or and δ) termed loops D, E, F and G (Corringer et al., 2000) **(Figure 1.2)**.

X-ray structures of the agonist site have been resolved for the AChBP (Brejc et al., 2001), GLIC (Hilf and Dutzler, 2009; Bocquet et al., 2009), ELIC (Hilf and Dutzler, 2008), GluCl (Hibbs and Gouaux, 2011), human GABA-A (Miller and Aricescu, 2014), murine 5-HT3 (Hassaine et al., 2014) and human α4β2 nACh

receptors (Morales-Perez et. al., 2016). Binding loop structures of nAChR α1 (Dellisanti et al., 2007), α7 (Li et al., 2011), α9 (Zouridakis et al., 2014) and α2 (Kouvatsos et al., 2016) subunits have also been resolved. In human α4β2 nAChR and AChBP, loops A (Y), B (W), C (two Y), and D (W) form an aromatic pocket that stabilises the agonist occupation of the pocket by chelating the ammonium group of ACh with the tryptophan residue from loop B establishing a direct cation-π interaction (Morales-Perez et. al., 2016, Zhong et al., 1998; Xiu et al, 2009) **(Figure 1.2).** Recent crystallisation of human α4β2 nAChR further showed residues contributed by the complimentary subunit of the interface to protrude into the binding pocket with possible roles in stabilising the binding interaction. These include V110, F119, L121 of the E-loop and the D170 residue from loop F serving an important role to stabilise C-loop interactions (Morales-Perez et. al., 2016).

There are small differences in the overall binding of agonist across the pLGICs family. For example, in GluCl, the neurotransmitter L-glutamate binds through its ammonium group to corresponding aromatic residues from loop A (F), B (Y), and C (Y), whereas the lateral carboxylate groups form salt-bridging interactions with Arg and Lys residues from loops D and F of the complementary subunit (Hibbs and Gouaux, 2011). In the GABA-A homomeric receptor β3, the agonist site is also formed by four aromatic residues protruding from both the principal and complementary subunit, one from loop B (Y), two from loop C (Y and F) and one from loop D (Y), along with Glu155 delimiting the top of the binding pocket. Electrophysiological studies have shown previously that Glu155 was implicated in gating (Newell et al., 2004). Analogous interactions are required for ligand binding and activation in nAChRs (Miller and Aricescu, 2014; Purohit et al., 2012). Thus, electrophysiological studies have shown that only three aromatic

residues are crucial in adult nAChRs, whereas the four of them are important in the foetal form (Auerbach, 2015). Co-crystallization of ELIC in complex with the mild agonist bromopropylamine at 4.0 Å resolution (Zimmermann and Dutzler, 2011) or its competitive antagonist ACh (Pan et al., 2012) showed that agonist binding also occurs at subunit interfaces in the bacterial homologues. Thus, the overall architecture of the agonist site is highly conserved in the pLGIC family.

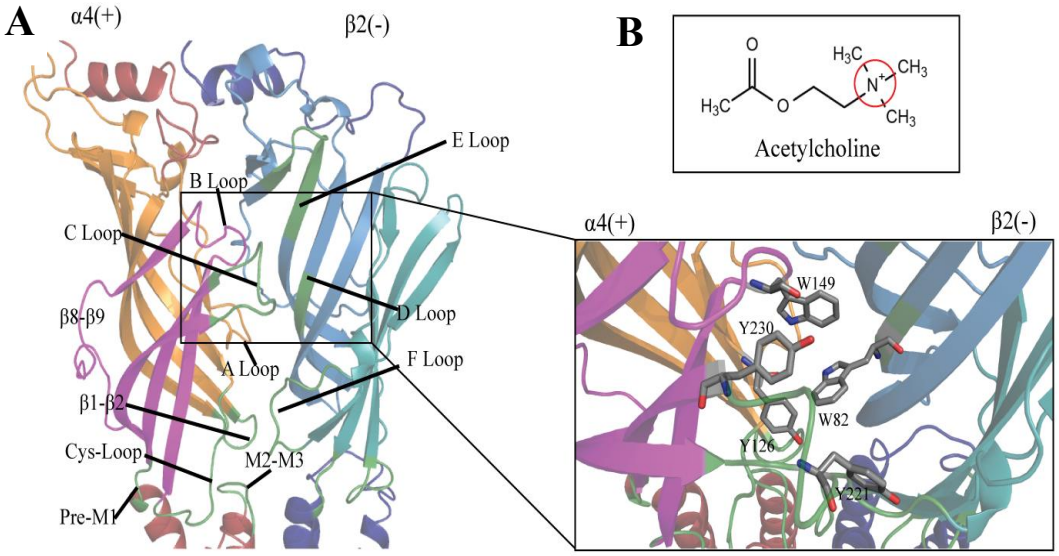

Figure 1.2. Cartoon of ECD subunit interface of α4β2 nAChR. (A) Inner and outer β-sheets are distinct colours for clarity, α4 subunit outter sheet in magenta, inner sheet in orange; β2 subunit outer sheet in teal, inner sheet in light blue. Functional loops also highlighted as green, except for loop A (orange) and loop B (magenta) for clarity. Close up region highlights important aromatic residues of binding pocket. α4β2 numbering used but homology to torpedo as follows; Y126 = Y93, W149 = W182, Y190 = Y221, Y198 = Y230 and W55/W57 = W82. **(B)** Structure of acetylcholine, highlighting quaternary ammonium group central to pi-cation interactions of ligand with the agonist binding residues.

1.4.4 The Ion Pore

The hydrophobic region that spans the cell membrane forms the ion channel. This region, the transmembrane domain (TMD) is covalently linked to the ECD. The TMD of each subunit is a cluster of 4 membrane spanning α-helices, termed M1-M4, dictated by the order in which they continue in amino acid sequence **(Figure 1.3).** They are structurally connected by functionally important loops that add flexibility to this region, allowing its movement during activation of the receptor complex and opening of the ion pore (Miyazawa et al, 2003; Miller and Smart, 2010). The pre-M1 region joins ECD to the M1 α-helix. This helix traverses the membrane towards the cell cytoplasm with the rest following roughly parallel in alternate directions. The loop M1-M2 between M1 and M2 is the first intracellular section and features a glycine residue conferring to its flexibility (Miyazawa et al, 2003; Miller and Smart, 2010). M2-M3 loop also boasts this functional feature and sits in the region between the ECD and TMD known as the coupling ECD-TMD interface. A larger intracellular loop (M3-M4) and intracellular helix (MX) adjoins the final helices M4, which ends with the final short C-terminal region that is extracellular (Unwin, 2005, Morales-Perez et. al., 2016).

The ion channel is lined with the M2 α-helices from each subunit. Lining of the pore is achieved by presence of conserved residues that form concentric circles of amino acid side chains with important properties once the subunits come together. These are numerated upto 20' – 20' being residues forming the ring at the position adjacent to the ECD (Miyazawa et al., 2003). The pore-lining helices contain three rings of charged/polar amino acids that confer ion selectivity. In the closed conformation of the muscle nAChR, the helices bend towards the centre of the

channel leading to a narrow region formed by three rings of hydrophobic amino acids at the 9'-14' region: αL251, αV255, αV259, and the corresponding residues from the other four subunits (White and Cohen, 1992; Miyazawa et al, 2003; Arevalo et al, 2005; Unwin, 2005). At the level of αL251 and αV255, the channel constriction is too narrow (approx. 6Å) and too hydrophobic to allow hydrated sodium or potassium ions passing through, which has led to the view that this area is the ion channel gate (Miyazawa et al., 2003). The gate is stabilised by hydrophobic interactions between residues.

In the α4β2 nAChR crystal, the narrowest point is shown to be further down the pore away from the ECD at the -1' ring. Here each subunit contributes a glutamate side chain protruding to pore (α4E247 and β2E239), resulting in a 3.8Å diameter and increased electronegative environment (serving to attract positive charge ions to gate thus acting as selectivity filter). Here the 'gate' is stabilised in the closed conformation via hydrogen bond interactions with the backbone of -2' glycine residues from adjacent subunit (Morales-Perez et. al., 2016).

It is thought that conformational changes induced by gating break these interactions stabilising the constricted pore, resulting in the widening of the pore (Miyazawa et al., 2003; Unwin and Fujiyoshi, 2012). This type of ionic permeation is conserved across the cationic pLGICs. Thus, for example, permeation through the prokaryotic GLIC is similar to that just described for the nAChR (Sauguet et al., 2013).

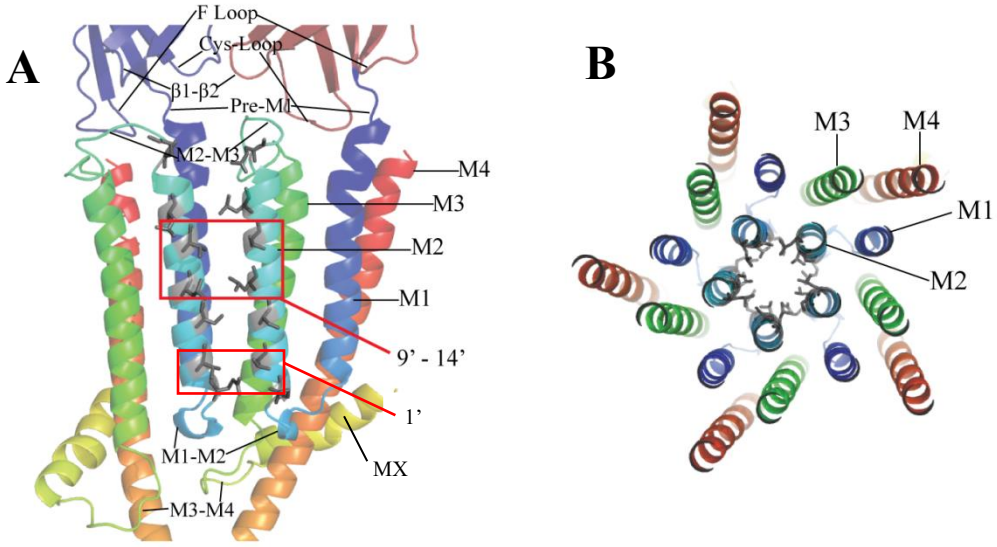

Figure 1.3. Cartoon of α4β2 nAChR showing alpha helices of TMD. **(A)** View of membrane spanning helices of an α4(+)/β2(-) interface from inside pore. M2 of each subunit can be seen as closest together as well as closest to inner channel pore. Residues of M2 that come together to form concentric rings of side-chains that line the pore are shown as grey sticks. Connecting loops of TMD are highlighted, as well as important loops of ECD-TMD interface. **(B)** Pentamer TMD helices as viewed from extracellular space. It is clearly seen here that M2 helices line the pore with functionally important residues coming together to form gate, and M4 of subunits positioned farthest away from channel and in most contact with cell membrane.

As previously mentioned, the nAChR receptors are selective to cations, and it is properties of the pore lining M2 region that governs this. Structurally the M2 regions are furthest apart at the top of the channel, next to the ECD, where it is lined with aspartate and glutamate residues (Unwin, 2005; Hilf & Dutzler, 2008). This creates a large electronegative space ideal for accumulation of positively charged Na^+, K^+ and dependent on stoichiometry, Ca^{++} ions. It has additionally been suggested that these structural features are associated with activation profiles and functional states of the receptor such as desensitisation in which an agonist is bound, but pore remains in the closed state (Yakel, 2010). Differences in properties of the 20' side chain ring are further suggested to account for differences in conductance across stiochiometries (Tapia et al., 2007)

1.4.5 - Gating

Agonist binding is coupled to gating and this is achieved through the recruitment of several ECD and TMD loops and regions (Prevost et al., 2012; Corringer et al., 2000, 2010). Coupling is achieved at the ECD-TMD interface by a principal pathway that couples the pre-M1 region in the ECD to the M2-M3 linker through the β1-β2 loop (Lee and Sine, 2005; Jha et al., 2007) and the canonical FPF motif of the β6-β7 loop (the Cys loop) (Lee et al., 2009) **(Figure 1.3).** More recently, it has been shown that gating is also affected by more peripheral pathways that couple M4 to M1 and M3 (Carswell et al., 2015) and, post-M4 to the Cys loop (daCosta and Baenziger, 2009; daCosta et. al., 2011). It is movement of these structures and interactions between them that drives the agonist binding signal to the ion channel gate. For example in the muscle nAChR, following application of agonist, a salt bridge between a lysine in β-strand 7 and an aspartate at β-strand 10 associated with the receptor at resting closed state is interrupted by activation mediated movement of a tyrosine of the ECD to a close enough proximity (Mukhtasimova et al., 2005). This shows ECD movement elicited by agonist will affect interactions in this region that will in turn cause changes in M2-M3 and eventually in the TMD. These movements, starting in β-strand 7 and β-strand 10, are thought to start the series of conformational changes prior to channel gating (Mukhtasimova et al., 2005).

The extraordinary progress that have been made in the last 10 years in terms of atomic structure, analysis of the microscopic function of pLGICs (e.g., rate-equilibrium free energy relationship [REFER] analysis) and molecular dynamics have led to the current view that a progressive stepwise isomerization (previously considered as conformational wave) that starts from the principal subunit of the

agonist binding site (loops A, B, and C), propagates to the ECD/TMD interface by a rigid-body rearrangement of the extracellular β-sandwich and travels down to the TMD (first M2, then M4 and M3) to eventually open the gate (Calimet et al., 2013; Sauguet et al., 2014a; Grosman et al., 2000; Purohit et al., 2007). The X-ray structures of the prokaryotic GLIC pH4 (open channel) and ELIC or GLIC pH7 (closed channel) showed a global twist on receptor's activation (Bocquet et al., 2009). This structural rearrangement has been described as a concerted anti-clockwise movement of the ECD relative to the TMD. The X-ray structure of the prokaryotic pLGICs (Hilf and Dutzler, 2008, 2009; Bocquet et al., 2009) also showed that the important conformational changes on activation as well as the significant tilting of the M2 helices observed in cryo-EM structures of the nAChR (Unwin, 2005) were not accounted for by the twisting model. Molecular Dynamics studies of the GluCl pLGIC contributed new insight into the molecular mechanism for gating of the receptor channel (Nury et al., 2010; Calimet et al., 2013). By monitoring the spontaneous relaxation of the open-channel structure upon agonist (or positive allosteric modulator such as ivermectin) unbinding (Nury et al., 2010; Calimet et al., 2013), these studies showed that global twisting initiates the closing transition by facilitating the un-tilting of the M2 helices, which does not occur in the untwisted (active) state of the receptor. Thus receptor un-twisting appears to contribute to activation by “locking” the ion channel in its open state. Furthermore, the simulation of GluCl with ivermectin removed (Calimet et al., 2013) predicted that a tilting of the extracellular β-sandwich in the outward direction would be implicated in coupling the agonist binding site and the ion channel. This tilting is nowadays termed blooming of the ECD domain in the resting state and has been recently demonstrated by the X-ray structure of GLIC at pH 7 (Sauguet et al.,

2014).). Also, the most recent structure of GluCl solved in the absence of agonist confirmed that that the rearrangements of the ECD during receptor activation resemble "the closure of a blossom" (Althoff et al., 2014). Thus, together, these studies confirm the occurrence of both twisting and blooming during the conformational transitions through which pLGICs undergo during gating. Of importance, the postulation of twisting and blooming implies that agonists as well as positive allosteric modulator binding should promote activation by favouring the contracted form of the ECD, whereas antagonist or negative allosteric modulators should favour the blooming conformation **(Figure 1.4).**

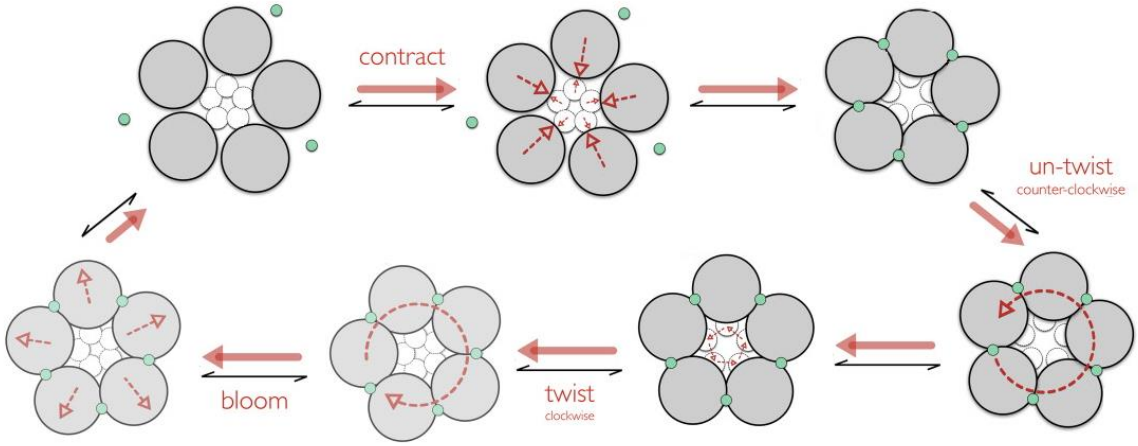

Figure 1.4. Cartoon showing the twisting and blooming conformation changes sassociated to gating isomerisation. Adapted from Cechinni and Changeux, 2015.

1.4.5.1- The molecular events behind twisting and blooming

In the current model, from data of multiple studies, the movements leading to channel activation are initiated by re-arrangement of hydrogen bonds of conserved residues close to the aromatic residues co-ordinating the agonist in the agonist pocket (Unwin, 2005; Xiu et al, 2005; Absalom et al, 2003; Lee and Sine, 2005). This includes the central binding residue α1W149, often being shown as the hydrogen

bond acceptor of the protonated nitrogen of agonists (Hibbs et al., 2009). Following this, residues from both the principal and complementary faces of the agonist site move inwards towards the bound agonist, creating distances between them suitable for van der Waals interactions. The most significant of these is the 11Å movement of loop C in an anti-clockwise motion, towards the channel pore. This is known as loop C capping of agonist as the ligand that becomes 'trapped' in the binding cavity. Here the signature cysteines of loop C (Cys192-Cys193) interact with the ligand and the now closer F loop of the complementary binding face (Celie et al., 2004; Hansen et al., 2005; Billen et al, 2012).

Although these subsequent interactions are important events, it is the exaggerated loop C movement that appears to initiate re-arrangement of the β-sandwich that results in energy transition and structural alterations down to the coupling region at its base. In line with considerations of the ECD re-arrangement occurring as a rigid twisting movement, Unwin and Fujiyoshi (2012) supposed from their data that the capping of loop C pulls the outer sheet of the β sandwich in the direction of its rotation. This would cause the adjustment of outer sheet comparative to the inner sheet and prompt the re-organisation of residues involved in interactions that stabilise the closed and open states. An important example of this is re-location of the conserved aromatic residues αW149 in loop B and αY190 in loop B and C loop (Cadugan and Auerbach, 2010). Substitutions of these side chains showed a direct correlation between the mutations of residues and the presence of long-lived spontaneous openings (Purohit, et al, 2007), supporting the importance of the positioning of these aromatic residues and their interactions in stabilising the closed state. When this is compromised (by substitutions or structural re-arrangements prompted by binding) the conformational change of nAChR is initiated.

Although all three binding loops of the principal subunit face are shown to move following ligand binding, loop A, closest to the gate, appears to move the least. Loop B and loop C undergo synchronised movement towards the bound agonist; loop B by rotating clockwise and loop C by a twisting and rotating movement (Unwin, 2005). Loop B importantly joins the outer to the inner β-sheets of the ECD, thus participating directly in effecting their relative displacements, shown to lead to opening of the channel (Unwin and Fujiyoshi , 2012; Cecchini and Changeux, 2015).

It has been proposed that in the closed channel, α subunits assume tense and "distorted" configurations relative to non-α subunits. The region showing largest disparities between α and non-α subunit structure was seen close to the centre of the β sheet sandwich, resulting from larger degree of separation between the inner and outer-sheet arrangements of α subunits. The tense conformation of α subunits are stabilised by residue interactions only present within the β sheets of α subunits (Unwin, 2002). Inter-subunit interactions also appear to stabilise the closed conformations. In the muscle nAChR, the α subunit loop B faces the inner sheet strands β5 and β6 of the (-) face γ and δ. Likewise, inner sheet residues on the complementary face of α subunits are within distance to interact with A, B and C loops of β and γ subunits. Several putative contacts are seen between subunits in these regions, the majority being salt bridges; for example possibly between αD152 and γR78 or δR81 and αR79 with βD155 or γE154 (Unwin, 2002, Unwin, 2005). No such structural features are seen at the δ(+)/β(-) interface, supporting proposal that these interactions would serve to stabilise α subunit conformation (Unwin, 2005).

Following agonist binding dependent re-structuring of the ECD, these interactions are broken and the α subunits "relax". This reduces the distortion,

making α and non-α subunits of a similar configuration, promoting symmetry of the open pentamer (Unwin, 2002). Conversion of the α subunits to a non-α like pose involves rotational movements of the inner β sheets of approximately 10º in both α subunits relative to the non-α subunits, thought to play a key role in the gating mechanism due to the close association of inner sheets with the pore-lining M2 helices through the loop β1–β2 (Unwin, 2002).

In this process, both inner and outer-sheets of the β-sandwich move independently but as rigid bodies, accompanied by small readjustments of their connecting loops. The inner sheet is thought to be the primary structural element determining the gating function of the channel, rotating to displace the β1–β2 loop adjacent to the M2 helix lining the channel pore. The outer sheet appears to provide the structural framework required to instigate the inner sheet rotation, accommodating the displacements involved. The rotation axis of each α subunit was shown to be similar; 8–9Å from the disulphide bridge of the Cys loop, passing through the hydrophobic core of the ligand-binding domain, through the base of the β9–β10 hairpin and between helices M1, M3 and M4 (Unwin, 2002). Together these data suggest the occurrence of conformational transitions in the α subunits prior to their non-α counterparts, and a similarity between the axis of all subunits to show the accumulative concerted movement of the pentamer as a whole.

An additional set of interactions unique to α subunit may stabilise the "untwisted" configuration of the β9-β10 hairpin within the open state. A salt-bridge between Y190 on β9–β10 and K145 on β7 at one end, and a hydrophobic contact between αI210 on β9–β10 and the Cys loop at the other end, both shown to be important to receptor gating (Akk et. al., 1996; Mukhtasimova et al., 2005). In the rest (unbound, closed) state, K145 is bridged with D200, importantly suggesting the

formation of new bonds and inter-subunit interactions of the ECD stabilising the open channel conformation of the receptor following activation (Mukhtasimova et al., 2005). This may occur within all subunit interfaces throughout the pentamer.

The β9 and β10 hairpin of the α subunits incorporates the C loop, and its capping is also said to importantly disrupt a salt bridge residue between αR109 and αE45 at the base of strands β9 and β10 (Lee and Sine, 2005). As this is in close proximity to the coupling interface between ECD and TMD, a direct connection between movement of loop C and transmission of binding signal down to the region of the channel gate is proposed.

In summary, the "twist and bloom" mechanism comprises two distinct stages of activation, the first (binding and rearrangement of ECD) involving finer movements and alterations finalises in an intermediate activation state. The following pore opening movement is on a global scale, at which level individual subunits may sterically interact in a concerted movement of the whole pentamer as seen with pushing movments of ECD (Unwin & Fujiyoshi, 2012). From studies of the muscle nAChR, the only subunit in which ECD displacement is coupled tightly to TMD helices displacement through the loops of the coupling region appears to be the β subunit (Unwin & Fujiyoshi, 2012). The unique outward displacement of β subunit ECD relative to TMD is as an exaggerated movement causing an equal tilting of the TMD helices in the opposite sense **(Figure 1.5).** This movement is prompted by movements of the αγ subunit following binding. The β subunit movement is thus thought to be central to gating as Unwin & Fujiyoshi's (2012) comparison of open and closed conformations of nAChR isolated this as the only structural alteration accross the two domains that coud communicate the effect of ACh binding downwards to the membrane and thus channel gate.

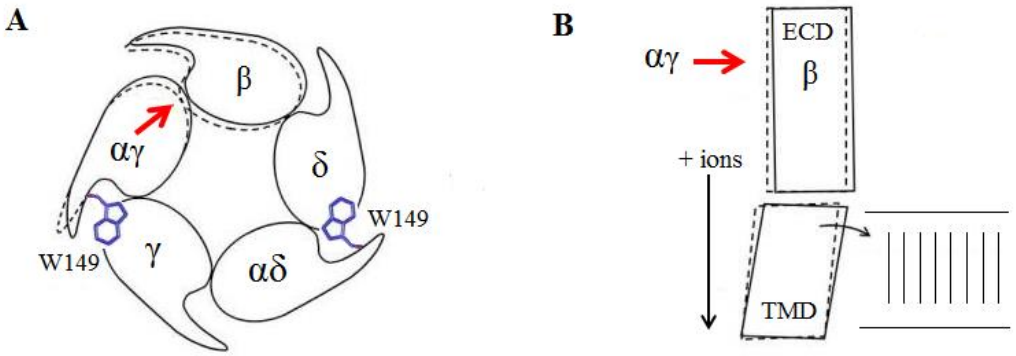

Figure 1.5. Rigid subunit domain movement of nAChRs. A and B depicts the rigid movements in bound *Torpedo* nAChR that lead to gating. Adapted from Unwin and Fujiyoshi, 2012.

1.4.5.2 - Gating and agonist efficacy

Monod-Wyman-Changeux model of agonist activation of allosteric proteins defines a symmetry in the protein in absence of ligands, and state that ligands are able to displace the equilibrium between the different active and inactive conformations, stabilizing the state for which they have a higher affinity (Changeux 2013; Changeux, 2012). It is this that distinguishes ligands as agonists or antagonists.

The efficacy of a given agonist is defined by its ability to elicit a response at maximum concentration, often defined in relation to the endogenous neurotransmitter as = 1. For example, the maximum response of a nAChR to ACh is known as 1. Any full agonist will have a maximum response level the same as the endogenous neurotransmitter, and therefore = 1. A partial agonist however, would produce a response lower than this at any given concentration, and not be able to equal or surpass 1, thus expressing an efficacy value as a fraction. Conversely, a super agonist is able to produce maximum responses larger than that of the

endogenous neurotransmitter, expressing a maximum efficacy value of greater than 1.

A breakthrough in the understanding of what determines agonist efficacy was made independently by Lucia Sivilotti and her team in London (Lape et al., 2008) and Stephen Sine in the USA (Mukhtasimova et al., 2009). Using advanced kinetic analysis of microscopic currents elicited by agonists it was found that agonist efficacy is not related to the ability of agonist to induce gating, agonist and partial agonists showed the same ability, but rather it is the ability of agonist-bound receptors to reach closed conformation immediately preceding the open conformation (Lape et al, 2008). Sivilotti and her team termed these closed states "flipping states" (Lape et al, 2008; Colquhoun and Lape, 2012). The flipping states are equivalent to functional states termed priming states by Mukhtasimova et al. (2009) **(Figure 1.6).**

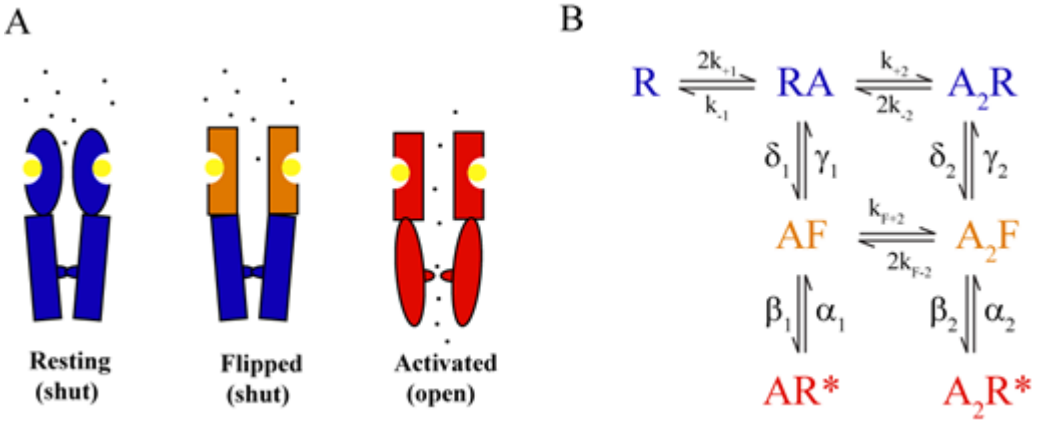

Figure 1.6 The flipped state. **(A)** Agonist binds to the receptor at rest state. This induces conformational changes resulting in receptor reaching the flipped state. This flipped state has increased affinity for agonist but the channel remains closed. Following the flipped state the receptor switches to the open conformation. **(B)** Schematic of the flipping mechanism in tetramethylammonium (TMA) activated muscle nAChR. 'A' represents agonist, 'R' and 'R*' represent the receptor in the resting closed and activated ipen states respectively and 'F'denotes the flipped conformation (Adapted from Lape et al., 2008)

The studies by Lape et al. (2008) and Mukhtasimova et al. (2009) imply that partial agonism is a reduced ability to flip, rather than a reduced ability to open the receptor. In terms of affinity, it is a ligands low affinity for the flipped state, relative to the resting state, that makes an agonist partial, rather than low affinity for the open state, relative to the resting state, as previously supposed. Overall, this places interaction energies defining agonist efficacies earlier in the chain of events that follow binding than if defining state was an open state.

1.5 nAChR Subunits and the Receptors They Form

Of the nAChR's there are many subtypes, each with individual pharmacological characteristics and physiological roles. The diversity and subsequent complexity of this array of receptors is primarily down to the fact that there are many genes encoding for various subunits that come together in multiple combinations to form unique pentamers. The subunits are classified as α (1-10) and non α (β1- β4, δ, γ and ε), primarily based on presence (α) or absence (non α) of an enlarged loop C. The subunits are then further grouped into 4 sub families (I, II, III, IV), based on sequence, structure and anatomical expression.

Sub family I contains the α9 and α10 found in epithelial and nervous tissue and is considered alongside sub family II as ancient proteins. α9α10 nAChRs display a unique pharmacology, somewhere between that of nicotinic and muscarinic receptors (Verbitsky et al, 2000) and are the exclusive stoichiometry of α9 and α10 subunits, despite the ability of α9 to form homomeric receptors (Sgard et al, 2002). These are found in the organ of Corti in the inner ear (Elgoyhen et al, 2001) but also

in the pain perception pathway, specifically in dorsal root ganglion neurons (Lips et al, 2002) as well as in epithelial tissue (Kummer et al, 2008)

Sub family II contains α7 and α8 subunits. Insofar, α7 and α8 subunits are the only nAChR subunits found to be able to form functional homomeric nAChRs. α8 subtype has only been located in avian neurons. α7 pentamers have been shown to express widely in the mammalian brain and are highly permeable to Ca^{2+} ions as well as Na^{+} and K^{+}. α7β2 nAChRs have recently been suggested to exist via detection of this pentamer mRNA(Azam et al, 2003) in rat brain cholinergic neurons and heterologous co-expression of these two subunits in oocytes or brain slices yields receptors that display slower desensitisation than that of α7 homomers (Murray et al, 2012; Khiroug et al, 2002). A physiological role of these heteromeric α7β2 nAChRs, mainly expressed in prefrontal cortex and forebrain (Moretti et. al., 2014, Tamsen et. al., 2015), has been shown as presynaptic modulation of glutamate release (Dickinson et al, 2008). Until these studies it was thought that members of subfamily II and III did not combine to assemble receptors, but this reveals possibilities of existence of many more pharmacologically and structurally distinct nAChRs.

Sub family III encompasses the remaining subunits; α2- α5 and β2 - β4 that form heteromeric receptors in many combinations and include autonomic, peripheral and CNS nAChRs. Expression of several different types of heteromeric nAChR containing α2, α3, α4,α5, β2 and β4 subunits has been ascertained, and biochemical and immunoprecipitation studies suggest that they assemble to form α2β2*, α3β2* and α4β2*nAChRs (* noting that some other subunit assembles with the subunits denoted), spread in equivalent amounts (Grady *et al.*, 2009). α3 and β4 subunits come together to form α3β4 receptors, the nAChRs responsible for synaptic

transmission in autonomic neurons. These may further combine with α5 subunits and are accordingly referred to as α3β4* with * indicating the presence of one or more additional types of subunit (Lukas *et al.*, 1999). α3β4* nAChRs are present mostly in adrenal and dorsal medulla and autonomic ganglia and can also be found in areas such as retina, interpeduncular nucleus and pineal gland (Grady *et al.*, 2009, 2010). *α5* and *β3* are known to be unable to generate functional ACh binding sites as they need to assemble with either α4-β2, α6* or α3-β4/β2 subunits to generate functional receptors. β2 subunit is also found in many cortical areas and may combine with many other subunits to form functional receptors, including α3, α4, α6, and β3. This is the subunit primarily responsible for nicotine binding and often confers a high sensitivity profile to receptors. Studies have shown the α2β2* nAChR type widely expressed in primate brain regions (Han *et al.*, 2003) although in mice this receptor subtype is mainly co-localised with α3β4* nAChRs in retina and IPn (Moretti *et al.*, 2004). *α6*- containing receptors have more restricted distribution in the CNS; they are present in the ventral tegmental area, striatum and retina (Gotti *et al.*, 2009). α6 KO mice from the ventral tegmental area have shown a direct correlation between the rewarding effects of nicotine and the expression of these subunit types in midbrain.

The α4 subunit is exclusively and widely expressed in the CNS and α4β2 nAChRs are the most abundant and widespread nAChR subtypes in the brain, where they exhibit high affinity for nicotine (Gotti *et al.*, 2009). The α4β2 pair may also combine with additional subunit types to be α4β2* for example α4β2α5. The α4-β2 pair has been also found co-localised with α6β3* receptors in the striatum, forming receptors with a mix of binding sites of α4 and β2 subunits and α6 and β2 subunits. This area receives innervation from midbrain dopaminergic neurons, and both

subtypes of receptors are key elements in the regulation of mesostriatal dopamine dopamine release (Laviolette and van der Kooy, 2004).

Sub family IV comprises the α1, β1, δ, γ and ε subunits, grouped so due to their exclusive assembly into the adult skeletal (α1γα1δβ1) and embryonic (α1εα1δβ1) muscle nAChRs and was the latest group to evolve.

The existence of nine neuronal types of α subunits and three types of β subunits indicates a high structural and functional diversity of nAChRs in CNS, supported by experimental studies (Chavez-noriega et al. 1997; Gotti et al. 2009; Wu and Lukas 2011). These will in turn present differing roles in the cholinergic system, increasing its modulatory capabilities and complexity. For example, evidence supports the possibility that α7 and α4β2 nAChR subtypes, which are differently permeable to Ca^{2+} ions, trigger neurotransmitter release via different mechanisms (Dickinson et al, 2008; Bancila et al., 2009).

1.6 The α4β2 nAChRs

This thesis focuses on α4β2 nAChRs. The most abundant and widely expressed nAChR in the brain are nAChRs containing α4 and β2 nAChR subunits, which include the α4β2, α5α4β2, α6α4β2 and α6β2α4β2 nAChRs (Dani and Bertrand 2007; Gotti et al. 2007) **(Figure 1.7).** The α4β2 receptors exist in two alternate stoichiometries. These are known as the high sensitivity (HS) $(\alpha4\beta2)_2\beta2$ and low sensitivity (LS) $(\alpha4\beta2)_2\alpha4$ nAChRs, reflecting marked differences in ACh sensitivity.

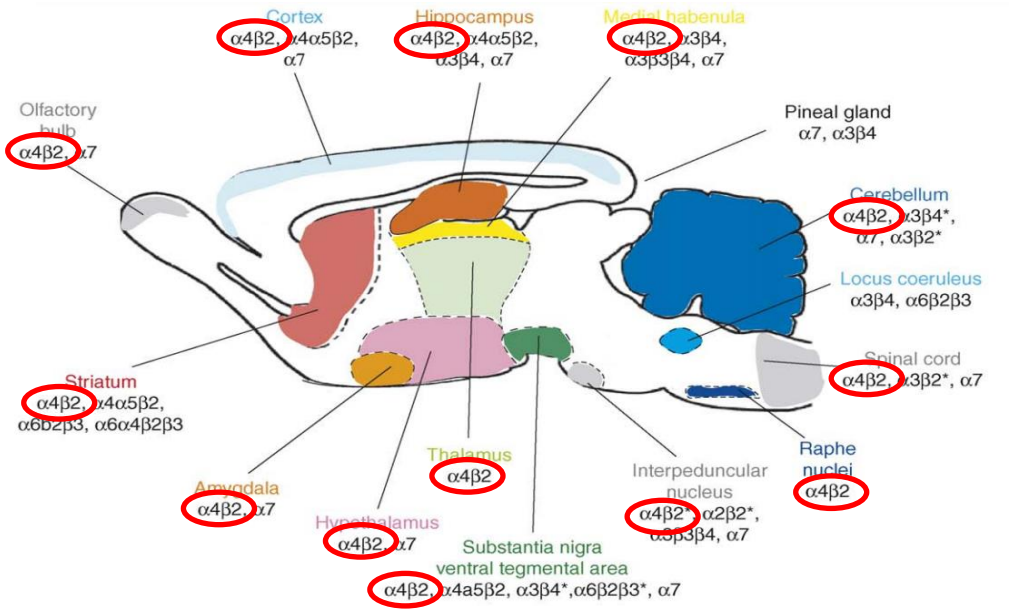

Figure 1.7. Diagram of rat brain demonstrating regional expression patterns of nAChRs. As can be seen the α4β2 pair subtype is the most widely expressed nAChR (adapted from Gotti et al., 2006)

1.6.1. Expression of α4 and β2 nAChR Subunits in the CNS

Receptors containing the α4β2 pair account for about 90% of the high affinity central nAChRs in the brain (Grady et al. 2009, 2010) and, as mentioned previously, these may combine with additional subunits to produce pentamers, forming further functionally distinct receptors. As it is known, α7 and α4β2* subtypes are the predominant nAChRs in the brain (Albuquerque *et al.*, 2009) and about 20% of the α4β2 containing nAChRs present an α5 subunit in the accessory position to give $(\alpha4\beta2)_2\alpha5$ stoichiometry (Brown *et al.*, 2007). This $(\alpha4\beta2)_2\alpha5$ receptor subtype has proved difficult to localize in the brain, as it shows a very similar pharmacological profile to that of $(\alpha4\beta2)_2\beta2$ receptors (Kuryatov, Onksen and Lindstrom, 2008).

Both the $(\alpha4\beta2)_2\beta2$ and $(\alpha4\beta2)_2\alpha4$ nAChR stoichiometries have been shown

to be present and functional in brain regions such as the thalamus and the cortex (Marks et al. 1999; Gotti et al., 2008; Marks et al. 2010). The use of the novel $(\alpha4\beta2)_2\alpha4$ selective allosteric modulator NS9283 confirmed that thalamo-cortical neurones express both $(\alpha4\beta2)_2\beta2$ and $(\alpha4\beta2)_2\alpha4$ nAChRs (Rode *et al.*, 2012; Timmermann *et al.*, 2012). Of importance, these studies also showed that striatal neurones express solely high-sensitivity $(\alpha4\beta2)_2\beta2$ receptors. This implies that in the striatum the release of dopamine is controlled by the HS isoform but not by its LS counterpart. More recently, a study of the synapse between motoneurons and Renshaw cells, identified the LS $(\alpha4\beta2)_2\alpha4$ receptor as predominant in this type of signalling, suggesting a post-synaptic location and novel role for this stoichiometry in central synapses (d'Incamps and Ascher 2014).

Chronic exposure of α4β2 nAChRs to competitive ligands such as nicotine increases the number of receptors in the cell membrane (up-regulation). Interestingly, up-regulation affects the HS $(\alpha4\beta2)_2\beta2$ nAChRs (Kuryatov *et al.*, 2005; Moroni *et al.*, 2006; Srinivasan *et al.*, 2011). The expression of the HS isoform is also increased by reduced temperature, subunit mutations pertaining to adult nocturnal frontal lobe epilepsy (ADNFLE), or polymorphism on the α4 subunit, and absolute or relative increased levels of β2 subunit (Lester et al. 2009; Exley et al. 2006; Nelson et al. 2003, Kim et al., 2003). What it is interesting in this phenomenon is that the increase can occur at the expense of the expression of the LS isoform (Nelson et al., 2003; Exley et al., 2006; Lester et. al., 2009), suggesting that expression of the α4β2 nAChR isoforms may respond to environmental cues.

Further work is needed to determine the distribution of α4β2 nAChRs throughout the brain, which will aid elucidating the contribution of each stoichiometry to brain functions and behaviours modulated by α4β2 nAChRs. The

success of such studies largely rests on the availability of α4β2 stoichiometry-specific compounds and so far, few agonists have been developed that show preference for high sensivity $(\alpha4\beta2)_2\beta2$ nAChRs such as TC-2559 (4-(5-ethoxy-3-pyridinyl)-N-methyl-(3E)-3-buten-1-amine difumarate, developed by the now defunct Targacept drug discovery company (Gatto et al. 2004; Carbone et al. 2009; Moroni et al. 2006)

1.6.2 α4β2 nAChRs and Brain Function and Pathology

α4β2 nAChRs are involved in a wide range of brain functions, including cognition, attention, mood noniception and reward (Taly et al., 2009) and are thus attractive targets for therapeutic intervention. Although the last 10-15 years have witnessed the development of many drug discovery projects based on the naChR, there has been little success, with the exeption of anti-smoking drugs such as varenicline. Perhaps, this lack of success is due to the lack of understanding of how the alternate stoichiometries of the α4β2 nAChRs contribute to function or disease, or, perhaps, the high level of homology between the nAChR family is an unsurmountable obstacle to highly specific drugs. Despite these problems that need to be considered when developing drugs, the α4β2 nAChRs is still an interesting drug target. The discussion that follows focuses on the functions or diseases that have been widely target for drug discovery exercises.

1.6.2.1 - Nicotine Addiction

α4β2 nAChRs exhibit high-affinity for nicotine as well as showing involvement in cognitive pathways central to reward and addiction (Picciotto et al. 2001). Studies investigating the Habenulo-Interpeduncular pathway have found this to be relevant for nicotine withdrawal symptoms mediated by β2 containing receptors (Moretti et al., 2004; Grady et al., 2009).

Early studies of β2 gene knock out mice suggested a central role in nicotine addiction of receptors featuring this subunit as these mice do not self-administer nicotine (Picciotto et al., 1999). Nicotine also does not appear to exert any effect on dopamine release in the ventral tegmental area or the nucleus accumbens of these mice – a cholinergic mediated brain processes central to reward (Picciotto et al., 1999). This is further supported by viral re-introduction of the β2 subunit to these knock out mice. This restores the behavioural and neurophysiological aspects of this previously eradicated nicotine "addiction" as self-administration was resumed alongside nicotine determined dopamine release in the ventral tegmental area and the nucleus accumbens (Maskos et al., 2005). Moreover these experiments with β2 knock out mice have shown expression of these subunit types in midbrain to be directly correlated with rewarding effects of nicotine and these knock out mice exhibiting hyperactivity as a result of altered dopamine release show reversal of these behaviours following re-expression of the β2 subunit in the striatum (Maskos, 2005).

GABA has also been implicated in the nicotinic regulation of reward pathways within the ventral tegmental area, mediated by α4 containing receptors. In mice expressing a gain of function mutation, L9'S, of the α4 subunits in GABAergic neurons of the ventral tegmental area, lower doses of nicotine were sufficient to

activate these neurons and promote reward seeking behaviour. These studies also support the role of the α4 subunit in mechanisms of addiction to nicotine (Ngolab et al., 2015). Similarly, an α4L9'A mutation of the α4 subunit increases receptor sensitivity to nicotine activation. Incorporation of this subunit to receptors in mice caused nicotine addiction behaviours to manifest at a nicotine concentration 50-fold lower than the concentration needed to induce the same response in wild type mice. As other nAChRs are not activated at such a low concentrations this highlights which behaviours are a result of nicotine evoked responses of α4-containing receptors, distinguishing their role in addictive behaviour (Tapper *et al.*, 2004).

α5 subunit knock out mice have shown a decrease in the affinity for acute nicotine administration, suggesting this type of receptors could account for the regulation of the rate of response to large doses of nicotine in mice (Kedmi et al., 2004). A single-nucleotide polymorphism in the gene coding for the α5 subunit has been linked to propensity to nicotine addiction although how this polymorphism may affect the addiction and reward pathways is unknown (Kuryatov et al., 2011). These effects of the α5 subunit can further implicate the α4β2 pair in cigarette addiction while asserting a role for its presence within pentamers as the accessory subunit to modulate receptor activity.

These α4β2 receptors may also be implicated in memories associated with smoking that re-enforces the addictive behaviour as the nicotine-evoked ACh release in hippocampal synaptosomes was shown to be due to the stimulation of α4β2 subtype (Wilkie *et al.*, 1996). This also implicates this subtype in learning and memory processes. The upregulation of the high sensitivity $(\alpha4\beta2)_2\beta2$ isoform by nicotine may also play a significant role in nicotine craving by smokers. If this stoichiometry is dominantly expressed due to chronic exposure to nicotine from

cigarette smoke, the dopaminergic reward pathways activated by nicotine are more likely to be elicited to a greater degree eliciting a greater degree of reward.

Another pharmacological mechanism governing nicotine addictive properties could be its desensitisation of α4β2 nAChRs as opposed to their activation. As a result of chronic exposure to agonists such as the nicotine self-administered by smokers, α4β2 nAChRs undergo long-term desensitisation. This is a state in which the pore is closed but ligand remains bound, preventing binding and thus receptor activation (Benallegue et al., 2013). When these receptors undergo such effects and are temporarily non-functional, it can reduce the activation of inhibitory GABAergic neurones in the ventral tegmental area. This will cause a down-stream effect of diminished inhibition of the dopaminergic neuronal activity in the ventral tegmental area and nucleus accumbens that these GABA neurons mediate, thus increasing and maintaining high levels of activity in the reward pathway, also caused by the initial activation of pre-synaptic α4β2 nAChRs of the DA neurons in these areas (Mansvelder and McGehee 2002a; Laviolette and van der Kooy 2004). The nicotinic modulation of the GABAergic system was antagonized by dihydro-β-erythroidine (DhβE), a selective antagonist of the α4β2 nAChRs, supporting presynaptic α4β2 nAChRs involvement, (Grilli et al. 2009). Subtype dependent desensitisation kinetics and distribution has also been shown to be an important mechanism of modulating dopaminergic activity and transmission in areas associated with addiction and reward; the striatum, ventral tegmental area and substantia nigra compacta (Exley and Cragg 2008; Wooltorton et al. 2003)

These processes may too involve the high sensitivity $(\alpha4\beta2)_2\beta2$ nAChR dominance up regulated by nicotine in smokers as this stoichiometry has shown greater levels of chronic desensitisation compared to its low sensitivity $(\alpha4\beta2)_2\alpha4$

counterpart (Marks et al., 2010; Benallegue et al., 2013). The most likely scenario is of both activation and desensitisation of α4β2 nAChR contributing to nicotine addiction through the key aspects of addiction, reward, withdrawal and tolerance (Mansvelder and McGehee, 2002; Picciotto *et al.*, 2008).

1.6.2.2 - Anxiety and Depression

The α4β2 nAChR subtypes have been implicated in the mood functions of the brain, thus making them targets for the chemical treatment of anxiety and depressive disorders (Levin and Simon 1998; Ashare and McKee 2012; McKee et al. 2012; Mineur & Picciotto 2010; Mantione et al. 2012).

Presynaptic α4β2* nAChRs are known to express within brain regions highly associated with mood and stress such as the ventral tegmental area, nucleus accumbens, locus coerelus, dorsal raphe nucleus, pre-frontal cortex, amygdala and hippocampus, from where they have been shown to modulate the release of ACh and other important neurotransmitters involved in mood such as serotonin, GABA, and dopamine (Picciotto et al. 2012; Garduno et al. 2012). Pharmacological studies of knock-out β2 mice suggest that α4β2 receptors are essential for dopamine release in the mid brain often linked to affective and mood disorders (Mineur et al. 2016, 2010; Maskos 2010). Paterson and Nordberg (2000) attributed the anxiolytic effects of nicotine to GABAergic modulation by α4β2 nAChRs as this is reversed following blockage of GABA activity. α4β2 nAChRs have also been shown to alter glutamate activity within these regions and systems which through long-term potentiation and long-term depression may mediate long-term depressive effects and subsequent physiological alterations associated with learned negative emotionality and maintenance of the depressive state (Garduno et al. 2012).

In the dorsal raphe nucleus, the primary region associated with serotoninergic system and thus depression, the activation of β2-containing nAChRs, located at glutamate terminals, produces changes in synaptic efficacy through a mechanism involving voltage gated calcium chanels (Lambe et al. 2003; Mansvelder amd McGehee 2002b). According to findings of Garduno et al., (2012), both nicotine and exogenous ACh increased the frequency of glutamate-dependent sEPSCs recorded from identified 5-HT neurons. This effect was mediated by high sensitivity α4β2 nAChRs because it was manifest at low nicotine concentrations (300 nM) characteristic of this subtype (Zoli *et al.*, 1998; Lambe et al, 2003), blocked by low concentrations of the α4β2 preferring antagonist DHβE (100 nM), and unaffected by a selective α7 nAChR blocker.

Genetic deletion of the α4 subunit from dopaminergic neurons has shown the α4-containing nAChRs are necessary for the anxiolytic effects of nicotine (Mineur *et al.*, 2013). Point mutant mice with hypersensitive α4 subunit display dopaminergic impairment in the substantia nigra alongside altered basal levels of anxiety (Labarca *et al.*, 2001), supporting links between α4β2 nAChRs, dopamine and depression. Also, a polymorphism in the α4 subunit gene (rs1044396) is associated with negative emotionality (Markett et al., 2011).

Scope of treatment of mood and anxiety disorders by targeting the activity of α4β2 nAChRs has been supported by both clinical and preclinical data and these are the nAChRs showing greatest potential for this therapeutic use (Mineur and Picciotto 2010). α4β2 nAChR preferring competitive antagonists, such as DhβE, have demonstrated antidepressant-like effects in mice (Andreasen et al. 2009). The non-selective nAChR channel blocker mecamylamine also reduced depressive-like behaviours (Rabenstein et al, 2006; Andreasen et al., 2009), but this effect was not

seen in β2 knock out mice, supporting involvement of β2 containing nAChRs in depression and its alleviation (Rabenstein et al, 2006) . However, treatment of mecamylamine does not enhance the outcomes of treatment with antidepressants in mice, whereas chronic exposure to nicotine does have this effect (Andreasen and Redrobe, 2009b). Considering this alongside findings that nicotine treatment alone has anti-depressive properties (Andreasen and Redrobe 2009a) suggests different mechanisms behind mood modulation by these compounds and furthermore that nAChR desensitisation is involved. This is supported by lack of effect following acute treatment with agonists that do not desensitise the nAChR as potently as nicotine (Andreasen *et al.*, 2009). Together, these findings suggest that a reduced but not abolished activity of α4β2 nAChRs is key to reduction of depressive behaviours, in turn highlighting the complexity and importance of fine balance of receptor activity.

1.6.2.3 - Nociception

Analgesia constitutes a promising therapeutic application of nAChR agonists as nicotinic compounds such as nicotine and epibatidine have been found to have analgesic properties (Daly et al., 2000). α4β2 nAChRs in particular have been implicated in nociception by knock-out studies of both α4 and β2 subunits showing reduced nociception (Picciotto et al., 1999). The absence of analgesic effects of nicotine in α5 knock out mice also supports a role of the (α4β2)2α5 subtype in these systems (Jackson *et al.*, 2010).

Similar to nicotine addiction, the role of α4β2* nAChRs in nociception may be mediated via their activation or desensitisation, as suggested by activation of α4β2 nAChRs being necessary but not sufficient to produce analgesia in vivo and in

vitro (Gao *et al.*, 2010). Additionally compounds that more potently desensitise α4β2* nAChRs have been shown to be more effective at producing analgesia, suggesting that desensitisation contributes to the efficacy of nicotinic analgesics (Zhang et al. 2012). It appears that both activation and desensitisation will contribute to nociception but may work synergistically to bring about these effects in contrast to addiction in which they function in separate mechanisms.

1.6.2.4. - Adult Nocturnal Frontal Lobe Epilepsy (ADNFLE)

ADNFLE is a rare familial epilepsy characterized by brief nocturnal seizures that originate in the frontal lobe and occur mainly during stage II of non-rapid-eye-movement sleep (Scheffer et al., 1995). ADNFLE is well associated with mutations in the α4β2 nAChR as four α4 and five β2 mutations have been linked to ADNFLE (Steinlein et al. 2012; Becchetti et al. 2015; Kurahashi and Hirose 1993). Little is known about the mechanisms that may induce seizures in ADFNLE patients due to the complexity of the cholinergic system, but its involvement in the mediation of sleep/wake states may be implicated. As most of the mutations linked to ADFNLE are gain of function mutations that increase receptor sensitivity to ACh (Bertrand *et al.*, 2002), the consequent over-stimulation of neurons could lead to seizures. An alternative hypothesis considers the involvement of GABA in other forms of epilepsy and its linkages with the cholinergic system, suggesting alterations to pre-frontal GABA release behind seizure onset, possibly arising during maturation of neural circuits (Becchetti *et al.*, 2015). This implicates disturbances of the fine balance between excitatory and inhibitory modulation of pre-frontal circuits as a mechanism of seizure causation, a notion that could aid explanation of cholinergic and nAChR involvement in other pathologies.

1.6.2.5 – Alzheimer's Disease (AD)

Alzheimer's disease (AD) is the most common form of dementia, characterised by cell malfunction and death in the hippocampus and cortex, leading to cognitive decline of sufferers. In initial progression of the disease, the cholinergic neurons projecting from the basal forebrain to these areas are amongst the first cells to deterirate.

1.6.3 Alternate Stoichiometries of α4β2 nAChRs

As previously mentioned, the α4 and β2 subunits assemble into alternate stoichiometries. The two predominant subunit stoichiometries differ in their sensitivity to ACh (Nelson et al., 2003; Moroni et al., 2006) and are accordingly labled as low sensitivity (LS) α4β2 nAChR [$(\alpha4\beta2)_2\alpha4$] and high sensitivity (HS α4β2 nAChR [$(\alpha4\beta2)_2\beta2$].

These receptors also display distinct unitary current amplitude (Nelson et al., 2003), selectivity for different agonists and antagonists (Moroni et al., 2006; Zwart et al., 2006; Carbone et al., 2009; Timmermann et al., 2012), potentiation by ions or drugs (Moroni et al., 2008; Timmermann et al., 2012; Olsen et al., 2013) and pattern of desensitisation (Marks et al., 2010; Benallegue et al., 2013).

Biochemical (Nelson et al. 2003), electrophysiological (Moroni et al., 2009) and concatenated receptor (Carbone et al., 2009; Mazzaferro et al., 2011) studies have shown the α4β2 to consist of two equivalent α4β2 subunit pairs and a fifth α4 or β2 subunit. The canonical agonist binding sites are located on the α4/β2 interface of the subunit pairs. The principal or (+) face of the binding site is contributed by the

α4 subunit, whilst the β2 subunit contributes the complementary or (-) face (Mazzaferro et al., 2011).

Additional to the structurally identical α4(+)/β2(-) binding interfaces, the isoforms each contain two structurally equivalent β2(+)/α4(-) interfaces in both receptor forms (Mazzaferro *et al.*, 2011, 2014). These interfaces house binding sites for inhibitory Zn^{2+} (Moroni *et al*., 2008) and the anthelmintic compound morantel (Cesa et al.,2011). In contrast, the fifth subunit, contributor varies being an α4 in the $(\alpha4\beta2)_2\alpha4$ nAChR and a β2 subunit in the $(\alpha4\beta2)_2\beta2$ nAChR (Carbone et al., 2009; Mazzaferro et al. 2011), which results in the signature β2(+)/β2(-) interface of the $(\alpha4\beta2)_2\beta2$ receptors and the α4(+)/α4(-) binding interface in $(\alpha4\beta2)_2\alpha4$ receptors that likely underlie the functional differences between the receptors (Moroni et al., 2008). Significant strides have been made towards understanding the role of the α4(+)/α4(-) in receptor function. This interface contains major determinants for sensitivity to potentiation by Zn^{2+} (Moroni et al., 2008) and NS8293 (Harpsoe et al., 2011; Olsen et al.,2013) and, critically, it also houses an operational agonist site that plays a dominant role in the overall function of the LS isoform (Harpsoe et al., 2011; Mazzaferro et al., 2011; Benallegue et al., 2013).

Because the agonist binding sites form at interfaces between the principal face of an α4 subunit and the complementary face of either a β2 or α4 subunit (Harpsoe et al., 2011; Mazzaferro et al., 2011), changes in subunit stoichiometry alter the number of agonist binding sites per pentamer. In addition, at non-agonist binding interfaces, changes in subunit pairing can alter receptor function via allosteric effects. Thus understanding the functional consequences of changes in stoichiometry of α4 and β2 subunits is of paramount significance towards the design

of drugs to treat the various brain diseases in which this family of receptors have been implicated, and understanding how cys-loop LGIC's function.

1.6.4 Concatenated α4β2 nAChRs

Insight into the relationship between the stoichiometry of α4β2 nAChR function has been achieved using concatemeric receptors in which five subunits are covalently linked head to tail in a prederetimed order and stoichiometry (Carbone et al., 2009; Mazzaferro et al., 2011; Benallegue et al., 2013; Mazzaferro et al., 2014; Lucero et al., 2016). Concatemeric receptors containing two non-consecutive α4 and three β2 subunits activate in response to low concentrations of ACh, and mimic the high agonist sensitivity of HS $(\alpha4\beta2)_2\beta2$ receptors (Carbone et al., 2009; Lucero et al., 2016). On the other hand, concatemeric receptors containing three α4 and two non-consecutive β2 subunits activate in response to high concentrations of ACh, and mimic the low sensitivity of LS $(\alpha4\beta2)_2\alpha4$ receptors (Carbone et al., 2009; Mazzaferro et al., 2011; 2014). Likewise, the agonists sazetidine-A and TC-2559 activate concatemeric HS $(\alpha4\beta2)_2\beta2$ receptors, but not LS $(\alpha4\beta2)_2\alpha4$ receptors, in accord with studies of receptors assembled in the presence of an excess of either the β2 or α4 subunit (Moroni et al., 2006; Zwart et al., 2006; Carbone et al., 2009). Finally, zinc potentiates agonist-elicited responses of concatemeric LS $(\alpha4\beta2)_2\alpha4$ receptor, but not those of concatenated HS $(\alpha4\beta2)_2\beta2$ receptors (Carbone et al., 2009), in agreement with studies of receptors assembled in the presence of an excess of either α4 or β2 subunits, respectively (Moroni et al., 2008). This work supports the likeness of concatemers to loose subunit assemblies of the α4β2 nAChR as well

as confirming subunit composition and order around pore. This was confirmed in the case of the $(\alpha4\beta2)_2\beta2$ by x-ray crystallography (Morales-Perez et al., 2016).

The studies that will be described in the following chapters of this thesis have used the concatemeric HS $(\alpha4\beta2)_2\beta2$ receptors to address the role of the signature β2(+)/β2(-) interface of this receptor type. By using homology models of this receptor, subunit-targeted mutagenesis and the covalent modification of substituted cysteines by a methanethiosulphonate reagent (MTS), this study found that the β2(+)/β2(-) interface encodes elements of efficacy. This is the first time that efficacy is shown to be affected by subunits not directly involved in agonist binding. The results are discussed in terms of their significance for gating and agonist efficacy.

1.7 Aims of the Thesis

The broad consideration of this thesis is how the non-binding interfaces contribute to the pharmacological signatures of the $(\alpha4\beta2)_2\beta2$ nAChRs, in particular the stoichiometry specific β2(+)/β2(-) interface. In line with this specific aims were to address the following questions:

1) Does the β2(+)/β2(-) interface of HS α4β2 contribute to receptor function and pharmacological characteristics?
2) If so, how is this conducted? Through operational ligand binding site analogous to the α4(+)/α4(-) binding interface?
3) Do the two the β2(+)/α4(-) interfaces act in a comparable manner to the β2(+)/β2(-) interface?
4) What are α4β2 nAChR stoichiometry specific mechanisms underlying pharmacological differences that cannot be accounted for by the presence of an additional binding site on LS α4β2?
5) What are the implications for this on current view of allosteric nature of receptor activation?

Chapter 2

-Materials and Methods-

2.1 Reagents

Standard laboratory chemicals were of Analar grade. Collagenase Type IA, ACh, and DhβE were purchased from Sigma-Aldrich (UK). TC-2559 was purchased from Tocris Chemicals (UK). MTS, aminoethylmethanethiosulfonate (MTSEA), Sodium (2-Sulfonatoethyl)methanethiosulfonate (MTS-ES) and [2-Trimethylammonium)ethyl]methanethiosulfonate (MTSET) were purchased from Toronto Research Chemicals (Canada).

2.2 Animals

Xenopus laevis (*X. laevis*) were purchased from *Xenopus* one (Chicago, USA), *Xenopus* Express, (France) or Portsmouth University (UK). *Xenopus* care and experimental procedures were in accordance with the Home Office regulations and were approved by the Animal Use Committee of Oxford Brookes University. Briefly, *X. laevis* were housed in the animal house of Oxford University in black tanks filled with dechlorinated water (>15L per toad) kept in a temperature-controlled room (18˚C). The animals were kept under a fixed 12 h light/dark cycle. Frogs were fed twice a week with amphibian food pellets.

2.3 Molecular Biology

DNA ligations, maintenance and growth of *Escherichia coli* bacterial strains and the use of restriction enzymes were carried out following the procedures described by Sambrook *et al.,* (1989). Plasmid isolation and DNA gel purification were carried out using commercially available kits (Omega Biotech, USA and

Promega, UK respectively). Capped cRNA coding for wild type and mutant concatemeric receptors was transcribed *in vitro* from SwaI-linearized cDNA template using the mMessage mMachine T7 kit (Ambion, UK.). The integrity and size of the cRNA transcripts was confirmed using RNA gel electrophoresis.

2.3.1 - Single Point Mutations

Point mutations were carried out using the QuikChange™ Site-Directed Mutagenesis Kit (Stratagene, The Netherlands). Oligonucleotides for polymerase chain reactions (PCR) were purchased from Eurofins (UK). The full-length sequence of wild type and mutated subunit cDNAs were verified by DNA sequencing (BiosourceScience, Oxford and Eurofins, UK). In order to increase the number of positive clones, the protocol used was slightly modified from the manufacturer's instructions, as described below.

1. Oligonucleotides primers (35 to 45 long, Melting TM > 80˚C) were synthesised carrying the desired mutations in the middle.
2. The synthesised primers were diluted to a final concentration of 125 ng/µl and used in the subsequent PCR reaction.
3. The PCR mix consisted of the following:

DNA template (stock 50 ng/µl)	->	1 µl
sense primer (125 ng)	->	1 µl
antisense primer (125 ng)	->	1 µl
dimethyl sulphoxide	->	3 µl
dNTPs (2 mM)	->	5 µl
Pfu Buffer 10X	->	5 µl
High Fidelity Pfu Polymerase	->	1 µl
Nuclease free water	->	33 µl
Total		50 µl

The parameters for the PCR run were as follows:

Stage	Number of Cycles	Holding Temperature (C)	Time (minutes)
1	1	95	1
		95	0.5
2	16	55	1
		68	1 min per kbp
3	1	68	1 min per kbp

4. 1µl of the enzyme DpnI was added to the PCR mixture and incubated at 37˚C for one hour. This was in order to degrade the parental methylated DNA, which corresponds to the template (non-mutated DNA), and to leave intact only the newly formed DNA (non-methylated and likely containing the desired mutation).

5. X-Gold competent *E. coli* cells were transformed with 30 µl of the digestion product. After overnight incubation at 37˚C, 3-5 colonies were picked and amplified by growing them in 10 ml of Terrific Broth medium (Sigma-Aldritch, USA) with ampicillin (80 µg/mL) at 37˚C. After overnight growth, the plasmid was isolated from the bacteria using commercially available DNA purification kits (Omega, USA), and fully sequenced to confirm the presence of the desired mutation and verify the sequence of the non-mutated regions. The residue numbering used throughout this thesis includes the signal sequence. To obtain the position in the mature form, subtract 28 for α4 and 26 for β2.

2.3.2 - Concatenated $(\alpha4\beta2)_2\alpha4$ and $(\alpha4\beta2)_2\beta2$ Receptors

The fully concatenated form of the $(\alpha4\beta2)_2\alpha4$ and $(\alpha4\beta2)_2\beta2$ isoforms, constructs β2_α4_β2_α4_α4 and β2_α4_β2_α4_β2 were engineered as previously described by Carbone et al. (2009). Briefly, the signal peptide and start codon were removed from all the subunits but the first (a β2 subunit) and the subunits were bridged by AGS (alanine, glycine, serine) linkers. The number of AGS triplets was 6 between β2 and α4 subunits, and 9 between α4 and β2 subunits or between α4 subunits. Only the last subunit in the construct (an α4 or β2 subunit, dependent on isoform) contained a stop codon. The subunits were subcloned into a modified pCI plasmid vector (Promega, UK) using unique restriction enzyme sites flanking the N- and C- terminals of each subunit.

Wild type or mutant concatenated receptors were assayed for integrity by determining the ACh sensitivity of concatenated receptors co-expressed with an excess of β2 or α4 monomers carrying the LT reporter mutation (L9'T in the second transmembrane domain). This mutation impacts gating activity of the receptor, increasing the receptor sensitivity to agonist to give an observable change to function should these substituted subunits be incorporated into the pentamers (Groot-Kormelink et al., 2004; Carbone et al., 2009). No changes were observed in comparison to receptors expressed in the absence of L9'T mutant subunits. This indicates that the concatenated constructs used in this study did not degrade into lower-order concatemers or monomers as such degradation products would incorporate the β2L9'T or α4L9'T monomers into receptors of higher sensitivity to ACh than the intact concatenated $(\alpha4\beta2)_2\alpha4$ and $(\alpha4\beta2)_2\beta2$ receptors (Groot-Kormelink et al., 2004; Carbone et al., 2009). This thesis focuses on the functional properties of the $(\alpha4\beta2)_2\beta2$ receptor. Unless otherwise stated, the studies described

here were carried out using the concatenated form of the $(\beta2\alpha4)_2\beta2$ and this will be referred to as β2_α4_β2_α4_ β2.

2.3.3 - Engineering Mutant β2_α4_β2_α4_ β2 Receptors

To introduce mutations into specific subunits of β2_α4_β2_α4_ β2 receptors, the mutation was first introduced into the appropriate individual subunit subcloned into a modified pCI plasmid as described in section 2.3. After confirming the presence of the desired mutation and verifying the sequence of the non-mutated regions, the subunit cDNA was digested with appropriate unique flanking restriction enzymes and then ligated into the desired position in the concatemer using standard cDNA ligation protocols with T4 ligase (New England Biolabs, UK). To verify incorporation of the mutated subunit into the concatemer, the subunit was excised by enzyme restriction digest from the concatemer and then sequenced by standard DNA sequencing. For clarity, mutations in the concatemeric receptors are shown as superscript positioned in the (+) or (-) face of the mutated subunit (e.g., in β2_^{W182A}α4_β2_α4_ β2 the mutation W182A is located in the (+) face of the α4 subunit occupying the second position of the linear sequence of the concatemer.

2.3.4 - Chimeric β2_α4_β2_α4_β2/α4 and β2_α4_β2_α4_α4/β2 Receptors

Subunits made of either the N-terminal of the α4 or the β2 subunit and the remaining TMD part of the α4 or the β2 subunit, as appropriate, was ligated to β2_α4_β2_α4 to construct chimeras β2_α4_β2_α4_β2/α4 and β2_α4_β2_α4_α4/β2. Chimeric subunits were constructed by first adding to both the α4 and β2 subunits a

BspEI restriction enzyme site at the interface between the ECD and TMD within a sequence motif, IRR, that is conserved in the nAChR family. The site was used to cut the subunits into two portions, the ECD-IR and the remaining subunit containing the four TMDs and the C-terminus (R-TMD-C-terminus). After digestion of the subunits with BspEI and after gel purification, the restricted sites were ligated using standard DNA ligation procedures to form β2/α4 or α4/β2 chimeras.

2.4 *Xenopus laevis* Oocyte Preparation

Xenopus oocytes were collected from adult female *Xenopus laevis*, anaesthetised and sacrificed according to Home Office guidelines. A visceral incision was made through the skin and body wall. The ovaries were removed and stored in OR2 solution (82 mM NaCl, 2 mM KCl, 2 mM $MgCl_2$ 2.5 mM HEPES (N-2-hydroxyethylpiperazine-N'-2-ethansulphonic acid) adjusted to pH 7.6 with NaOH). Only oocytes at the stage V and VI of maturation were isolated. The theca and epithelial layers were removed enzymatically by incubating the oocytes in Type IA collagenase (2 mg/ml) dissolved in OR2 and placed on a belly dancer rotator for 1.5 – 2 hours at room temperature. Oocytes were maintained at 18˚C in an incubator in a modified Barth's medium (88 mM NaCl, 1 mM KCl, 2.4 mM $NaHCO_3$, 0.3 mM $Ca(NO_3)_2$, 0.41 mM $CaCl_2$, 0.82 mM MgSO4, 15 mM HEPES supplemented with streptomycin 1 μg/ml, 1 U/ml penicillin and 50 μg/ml neomycin, pH 7.6 (adjusted with NaOH) for 24 hours prior to micro injection of cRNA

2.5 Microinjection of cRNA

Needles for microinjection were prepared from Drummond glass capillaries (Sartorius, UK), which were pulled in one stage using a horizontal microelectrode puller (Campden Instruments–Model 753). Prior to use, the tip of a selected needle was broken using fine forceps to give a narrow tip length of approximately 3 mm with an external ranging from to 1.5 – 2.0 µm. The needle was back-filled with light mineral oil and loaded on to a Nanoject II microinjector (Drummond, USA). Wild type or mutant concatemeric receptor cRNA were injected into the oocyte cytoplasm (50.6 – **70.9** nl at 0.1 ng/nl) as illustrated in figure.2.1. Injected oocytes were transferred to 96 well sterile dish (one oocyte per well) containing modified Barth's solution and incubated at 18ºC

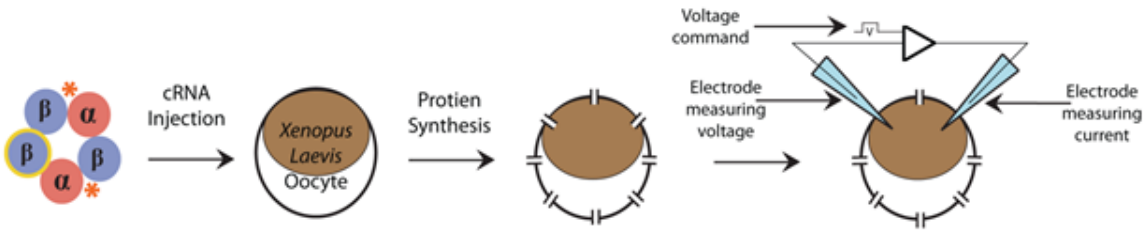

Figure. 2.1. Diagram showing β2_α4_β2_α4_α4 cRNA injection into oocytes. After 2-3 days post-injection currents were recorded using two-electrode voltage clamp technique.

2.6 Electrophysiological Recordings

After at least 3 days post-injection oocytes were selected for electrophysiological recordings according to their appearance. Only oocytes with integral membrane and no signs of degradation were chosen for electrophysiological recordings and dead cells were removed from the plate daily. Oocytes were placed in a 30µl recording chamber (Digitimer, UK) and bathed with a modified Ringer solution (in mM: NaCl 150, KCl 2.8, HEPES 10, $CaCl_2$ 1.8; pH 7.2, adjusted with NaOH). A gravity driven perfusion system was used for all the experiments. All solutions were freshly made prior to recordings. Oocytes were impaled by two electrodes connected to a Geneclamp 500B (Molecular Devices, USA) for standard voltage clamp recordings as illustrated in Fig. 2.1. Briefly, electrodes were made from borosilicate capillary glass (Harvard Apparatus, GC 150 TF) using a vertical two stage electrode puller (Narishige PP-83) to give a tip diameter of 1-2 µm. Prior to recordings electrodes were filled with 3 M KCl and only electrodes with a resistance between 0.5 and 2 M were used for voltage clamping. Oocytes were continually perfused with fresh Ringer solution at a rate of 10 ml/min and switching between different solutions occurred through manually activated valves.

2.7 Concentration response curves for agonists and antagonists

Concentration response curves (CRC's) for agonists were obtained by normalizing agonist-induced responses to the control responses induced by a near-maximum effective agonist concentration, as previously described (Moroni *et al*., 2006; Mazzaferro *et al*., 2011; Carbone *et al*., 2009). An interval of 5 min was allowed between agonist applications to ensure reproducible recordings. The agonist CRC data were first fitted to the one-component Hill equation with Prism v5 (GraphPad 5 software, GraphPad, CA, USA):

$$Y = Bottom + (Top – Bottom) / (1 +10^{((Log\ EC50 - X) * nH}$$

where *Bottom* is the Y value at the bottom plateau of the curve, *Top* is the Y value at the top plateau of the curve, EC_{50} represents the concentration of agonist inducing half of the maximal response (I_{max}), *X* is the agonist concentration and *nH* the Hill coefficient.

When agonists induced biphasic receptor activation, agonist CRC were fitted with the sum of two Hill equations a two-component Hill equation from Prism v 5 (GraphPad 5 software) :

$$Y=Bottom + (Top-Bottom) *Frac/(1+10^{((LogEC_{50}\_1-X)*nH1))} + Top-Bottom * (1-Frac)/(1+10^{((LogEC_{50}\_2-X)*nH2))}$$

where $LogEC_{50}\_1$ and $LogEC_{50}\_2$ are the concentrations that give half-maximal stimulatory and inhibitory effects in the same units as X. *nH1* and *nH2* are the a-dimensional values representing slope factors or Hill slopes. Frac is the proportion of

maximal response due to the more potent response phase due to the higher sensitivity component of receptor.

2.8 Substituted cysteine accessibility method (SCAM)

The substituted cysteine accessibility method (SCAM) was used to assess the impact of the agonist binding and non-agonist binding interfaces of the β2_α4_β2_α4_ β2 receptor on receptor activation and to determine movements within ACh binding sites at α4(+)/β2(-) and the β2(+)/β2(-) interface. SCAM was first applied to pLGIC to identify the amino acid residues lining the ion channel of the muscle nAChR (Karlin & Akabas, 1998). Since then, SCAM has become a powerful experimental strategy that has been successfully applied to gain invaluable insights into diverse aspects of pLGIC functional and structural such as amino acid residues contributing to competitive or allosteric ligands bindings, conformational changes induced by agonist or allosteric modulators, and secondary structure of functional domains (see for ex., Boileau *et al*., 1999; Holden & Czajkowski, 2002). SCAM involves the introduction of free cysteine residues, one at a time, into a protein region and the subsequent application of thiol specific reagents to the introduced cysteine residues to determine whether they are modified by the thiol reagent (Figure.2.2) (Karlin & Akabas, 1998). Modification of the introduced cysteine is monitored using electrophysiological or biochemical assays.

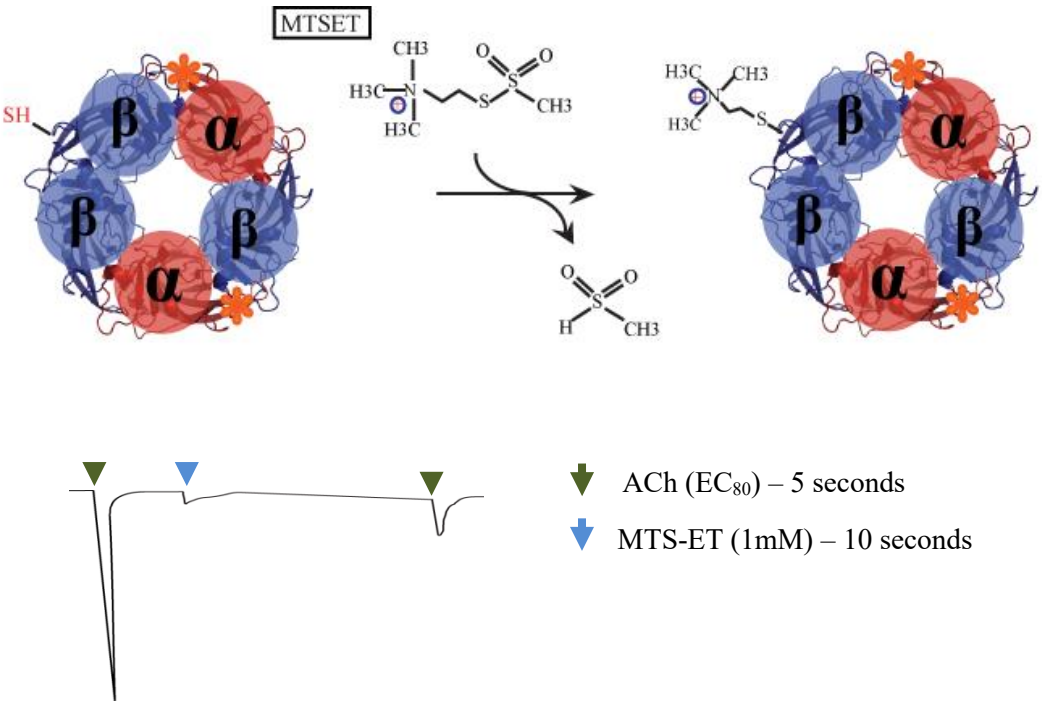

Figure 2.2. Covalent MTS modification of substituted cysteine in an identified subunit interface. **(A)** Using concatenated $(\alpha4\beta2)_2\beta2$ nAChRs it is possible to introduce single point mutations at identified subunit interfaces. The diagram shows the reaction of MTSET with the thiolic group of a cysteine introduced in the complementary face of the β2(+)/β2(-) interface. **(B)** Representative traces that shows max inhibition of ACh current (green arrows) after maximal MTSET concentration (1mM) treatment. MTSET is applied for 60 s (black arrow).

2.8.2 Modification of Interfaces Using Substituted Cystine Accessibility Method

MTSET was used to covalently modify a cysteine residue introduced at the L146 position on the complementary (-) face of agonist sites at α4(+)/β2(-) and β2(+)/β2(-) interfaces. Previous studies have shown that β2L146 in loop E is suited for cysteine substitution studies: β2L146C has little impact on receptor sensitivity but in the presence of MTS reagents produces a profound decrease in the responses of α4β2 receptors to ACh (Papke et al., 2011). The following concatemers were engineered for the SCAM studies: $\beta2^{L146C}$_α4_β2_α4_β2, β2_α4_$\beta2^{L146C}$_α4_β2 and β2_α4_β2_α4_$\beta2^{L146C}$ concatemers were constructed **(Figure 2.3)**. Mutant

concatemers were expressed in *Xenopus laevis* oocytes, and characterised using two electrode voltage clamping procedures, as described above.

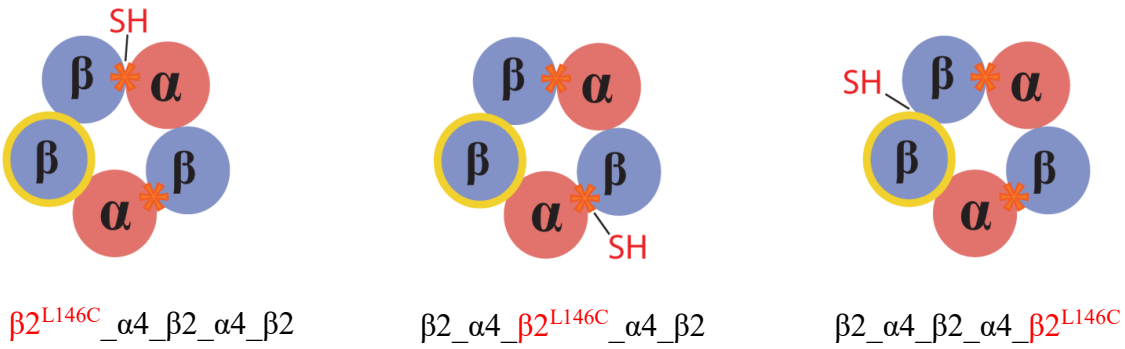

Figure 2.3. Location of introduced cystine residues in mutant β2_α4_β2_α4_β2 concatemers. B2L146C substitutions are on each complementary β2 subunit of the interfaces to produce receptors with free thiol groups able to react with MTS-ET within the α4(+)/β2(-) binding interfaces and β2(+)/β2(-) interface.

2.8.3 Maximum Effects of Covalent Modification of Introduced Cysteines by MTSET Reagent

The maximal effect of the MTSET reagent on agonist responses was assessed as shown in **Figure. 2.2**. Briefly, oocytes expressing receptors with a free cysteine or wild type receptors were first challenged with a control agonist (ACh, TC-2559) concentration (EC_{80}) every 6 min until a stable response (defined as <5% within 4 consecutive responses) was obtained. After a 2 min 10 sec wash period with Ringer's solution, oocytes were perfused with Ringer's solution containing MTSET (1 mM) or MTSES (10 mM) (maximal concentrations; Zhang & Karlin 1997) for 60 s (determined as maximal time by preliminary studies ensuring maximum effect after this time.) After this treatment the impaled cells were washed with Ringer's solution for 2min50sec. After washing, the agonist was applied again every 6 min until the

amplitude of the responses was constant (as previously described). The average of the current amplitudes prior to application of MTS was the control response current ($I_{initial}$), and the average of current amplitudes after rinsing was the average response after MTSET application ($I_{after\ MTS}$). The effect of the MTS reagents was estimated using the following equation:

$$\% \ Change = ((I_{after\ MTS}/I_{initial}) - 1) * 100$$

2.8.4 MTSET Reaction Rates of β2(+)/β2(-) and α4(+)/β2(-) Interfaces

To determine whether nicotinic ligands recognize the agonist site at the β2(+)/β2(-) interface, and distinguish differences between α4(+)/β2(-) sites, we assayed the effect of nicotinic ligands (termed 'protectant') on the rate of MTSET modification of the three β2(-)L146C residues **(Figure 2.3)**. If reversible ligands reduce MTSET reaction rates, it was initially considered that the reversible ligands bind the site, thus impeding, likely by steric hindrance, the modification of the introduced cysteine residue by MTSET **(Figure 2.4)**. The rate of MTSET covalent modification of introduced cysteines was determined by measuring the effect of sequential applications of sub-saturating concentrations of MTSET on I_{ACh} responses in the presence and absence of 'protectant'. These rates were then compared. The concentrations of MTSET reagent used were 10μM. Preliminary experiments established that these concentrations of MTSET were optimal to describe adequately the early and plateau phases of the MTSET reaction rate data. The rate of MTSET covalent modification of introduced cysteines was initially obtained in the absence of protectant ligand as control studies.

Because α4β2 nAChRs are highly prone to long-term desensitisation when

exposed to agonists, the protectant was applied in the control experiments prior to the MTS reagent to correct for any process of desensitisation that could develop during the protection assays, when the protectant is added together with the MTSET reagent**.** Responses to ACh prior to MTSET reagent application were first stabilised as follows:

1. ACh (EC_{80}) pulses were applied for 5 s
2. Step 1 was followed by a recovery time of 125 s
3. The protectant (EC_{20} or EC_{80}) was then applied for 10 s
4. Step 3 was followed by a washing period of 3 min and 40 s with ringer solution.

- The 6 min total cycle was repeated until the responses to ACh were stable (<5% on four successive applications of EC_{80} ACh).

MTS reagent was then applied using the following sequence of reactions:

1. At time = 0s, ACh (EC_{80}) was applied for 5 s
2. Step one was followed by a period of recovery of 95 s
3. MTSET was then applied for 10 s
4. Step 3 was then followed by a recovery period of 20 s.
5. Immediately after the recovery time, the protectant was applied for 10s
6. Cells were then washed with Ringer's solution for 3 min and 40s.

- The 6 min total cycle was repeated until MTSET applications produced less than 5% changes in I_{ACh} on four successive applications of EC_{80} ACh).

MTSET application was repeated 9 times to give a total cumulative application time of 90 s. To confirm that any observed decrease in I_{ACh} was due to the effects of MTSET and not to receptor desensitisation, ACh and protectant pulses (following the same scheme used to stabilize the ACh responses prior the MTSET application) were applied at the end of the protocol as illustrated in **Figure. 2.4.**

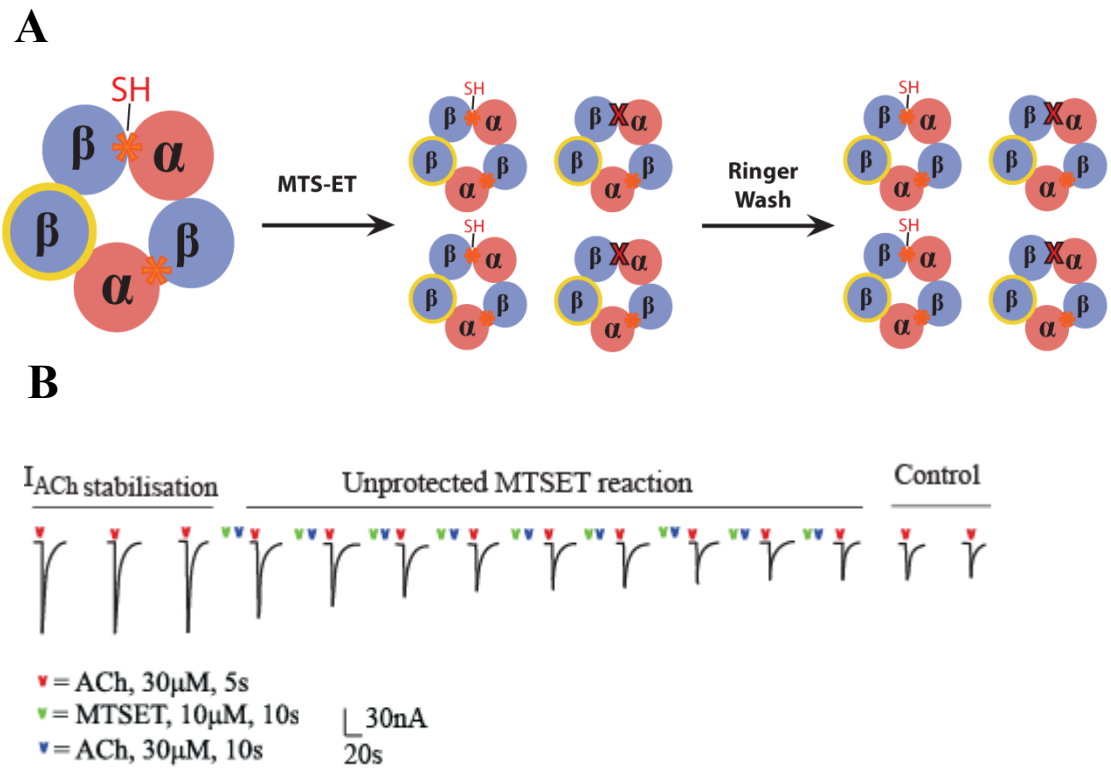

Figure 2.4. Exponential decay assay control experiment for ACh at a α4(+)/β2(-) interface of the β2L146C_α4_β2_α4_β2 mutant. (A) General scheme of the exponential decay assay control experiment. After short (10s) application of low concentration MTS-ET (10μM) a given population of receptors will be modified at the introduced cystine residue which remains after ringer wash time. The degree of this modification is then assessed by decrease of following ACh current output. **(B)** Representative traces of exponential decay assay protocol. Green dashed line shows ACh current stabilisation prior to MTS-ET applications. Black line shows duration of accumulative MTS-ET application and blue line shows receptor stabilisation after MTS-ET exposure and the reaction is complete. Agonist is applied prior to MTS-ET (red arrows) to ensure desensitisation does not effect current and results can be compared to those of protection assay protocol. The application duration is acumulative to determine the $k1$ for the exponential decay of IACh as a result of MTS-ET modification to give a rate of reaction with introduced cystine.

2.8.5 Protection Assays with Agonists

The effects of agonists and antagonists on the rate of MTSET modification were tested by co-applying MTSET with agonist (EC80). The protocol used was identical to the one used to determine the rate of MTSET reaction, except that the reversible ligand (protectant) was co-applied with MTSET reagent. The sequence of steps illustrated in **Figure 2.5** was as follows:

I_{ACh} was stabilised by:

1. Applying EC80 pulses of ACh for 5 s
2. Step 1 was followed by a 95s period of recovery
3. The protectant was then applied for 10s
4. Step 3 was followed by a recovery period of 4 min and 10s
5. This cycle was repeated until stability was achieved. (<5%change in IACh elicited by four successive applications of EC_{80} ACh).

The sequence of MTSET reactions was as follows:

1. At time 0, ACh (EC_{80}) was applied (5 s)
2. Step 1 was then followed by a brief period of recovery (95 s)
3. MTSET and the protectant were co-applied for 10 s
4. Step 3 was followed by a recovery period of 4 min and 10 s. This cycle was repeated until the application of MTSET produced no further changes in I_{ACh} (<5% on four successive applications of EC_{80} ACh).

To exclude receptor desensitisation as responsible for decreases in I_{ACh}, ACh and protectant pulses (following the same scheme used to stabilize the ACh responses prior the MTSET application) were applied at the end of the protocol as a control.

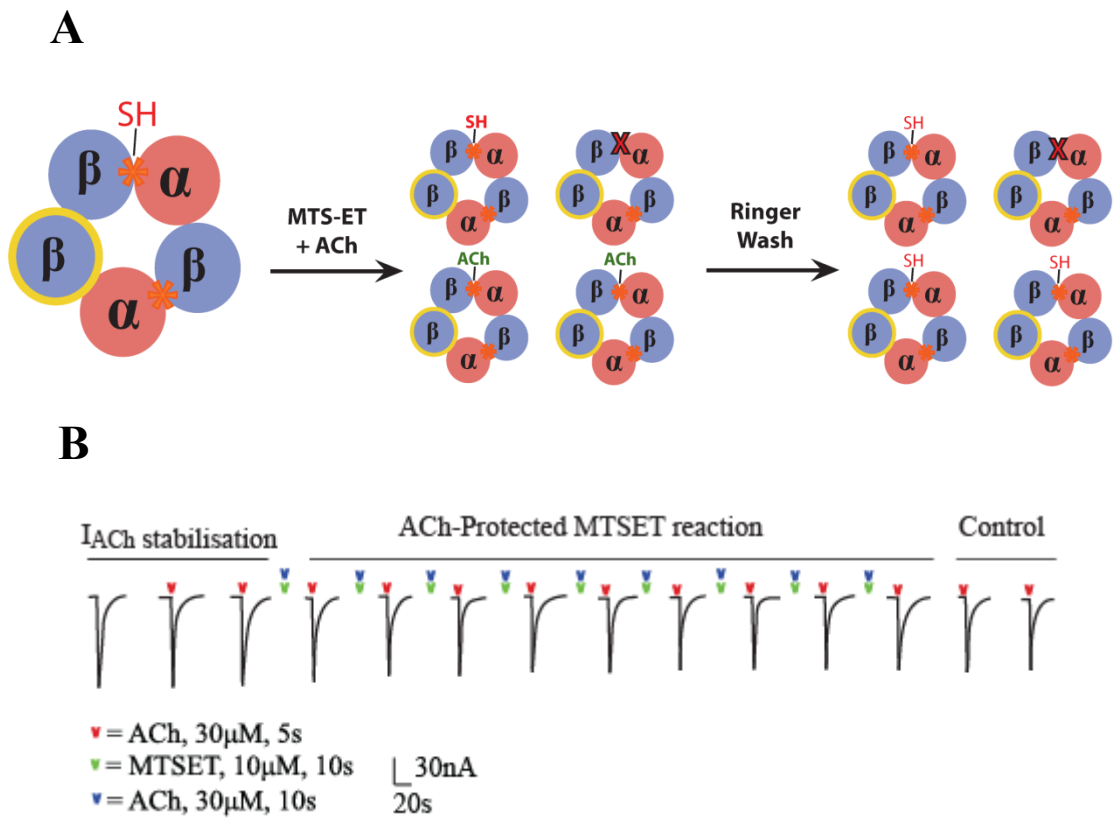

Figure 2.5. Protection assay experiment for ACh at a α4(+)/β2(-) interface of the β2L146C_α4_β2_α4_β2 mutant. (A) Schematic of protection assay experiment mechanism. When agonist (eg ACh) and MTS-ET are co-applied (protected reaction), the ligand competes with MTS-ET, impeding the MTS-ET reaction with the free cysteine introduced in the agonist site at the α4(+)/B2(-) interface, thus the reaction rate is slower. **(B)** Representative traces of protection assay protocol. Green dashed line shows ACh current stabilisation prior to MTS-ET applications. Black line shows duration of accumulative MTS-ET application and blue line shows receptor stabilisation after MTS-ET exposure and the reaction is complete. MTS-ET application duration is accumulative to determine the *k*1 for the exponential decay of IACh as a result of MTS-ET modification to give a rate of reaction with the introduced cysteine.

The change in current was plotted versus cumulative time of MTSET exposure. A pseudo–first-order rate constant was calculated from the change in I_{ACh}. Peak values at each time point were normalized to the initial peak at time 0 s, and a pseudo–first-order rate constant ($k1$) was determined by fitting the data with a single exponential decay equation:

$$Y = (Y0 - Plateau)*exp(-K*X) + Plateau$$

using Prism v.5.0 (GraphPad Software). Because the data are normalized to values at time 0, span *(Y0 - Plateau)* = 1 - plateau. Data analyses were performed using Graphpad-Prism software. Data were pooled from at least three different experiments.The second order rate constant ($k2$) for MTSET reaction was determined by dividing the calculated pseudo–first-order rate constant by the concentration of MTSET reagent used.

2.10 Statistical Analysis

For ligand CRC data, F-tests determined whether the one-site or biphasic model best fit the data; the simpler one-component model was preferred unless the extra sum-of-squares F test had a value of p less than 0.05. Log EC_{50} values for ligand responses changes in current amplitudes in response to mutations or MTS application were analysed using one-way ANOVA (analysis of variance) with Dunnett or Bonferroni post hoc corrections for the comparison of all mutated receptors to determine significance between wild type and mutant receptors. Significance levels between mutant receptors were determined using unpaired t tests. Data are plotted as mean ± Standard Error Mean (SEM) of n number of experiments. Parameter values are the best fitting values with the SEM values estimated from fit.

2.11 Structure Homology Modelling and Docking

Homology modelling and docking studies were kindly performed by Dr Maria Musgaard and Professor Philip C Biggin from the Department of Biochemistry, Oxford University. The following is a brief description of the approaches used to build the homology models and carry out the docking studies. Homology models of the α4β2 nAChRs were constructed using MODELLER 9.12 (Šali,. and Blundell, 1993) and were based on the murine 5-HT_3 receptor X-ray structure (PDB ID: 4PIR) at 3.5 Å resolution (Hassaine et al., 2014). The template X-ray structure comprises the ECD, the TMD and part of the intracellular domain. Four residues are missing in the extracellular M2-M3 loop, and more than 60 residues are missing in the intracellular linker between M3 and M4. Sequences of the human α4 and β2 nAChR subunits were obtained from the ExPASy proteomics server with accession numbers P43681 (α4) and P17787 (β2) and aligned to the 5-HT_3R subunits using the alignment function of MODELLER (align2d) and, for comparison, also using two different alignment tools from the European Bioinformatics Institute (EBI), EMBOSS Stretcher and EMBOSS Needle, respectively. The sequence identity is 25% and the sequence similarity is approximately 45%. The three alignments were compared and the final alignment constructed with manual changes in regions where the alignment algorithms were not optimal. Disulphide bonds were included and 50 models for each of $(\alpha4)_3(\beta2)_2$ (α4-β2-α4-β2-α4) and $(\alpha4)_2(\beta2)_3$ (α4-β2-α4-β2-β2) were constructed. The models mainly varied in regions where the template was missing, and the best models were chosen based on analysing the MODELLER scores (molpdf, DOPE and GA341). The 3-4 best models in terms of all of these scores were further assessed with

QMEAN (Benkert et al., 2010) and the best QMEAN scoring model from this process was chosen as the appropriate model for docking.

Protein and ligand models were prepared for docking using Autodock Tools (Morris et al., 2009) and docking calculations were performed with Autodock Vina (Trott and Olsen, 2010). A large box of 74x74x40 $Å^3$ centered in the extracellular half of the ion channel and covering a large part of the TMD of all five chains was used as the search space for docking calculations. 20 binding models were generated for each ligand docked into each protein model, i.e. 80 poses were generated in total. The binding models were analysed visually as the docking scores were all very similar (best score among 80 posed was -7.5 and the worst -6.2).

Chapter 3

Is there an agonist site at the β2(+)/β2(-) interface of the HS α4β2 nAChR

3.1 INTRODUCTION

Functional differences of the α4β2 nAChR stoichiometries have been shown to have strong structural basis (Grady 2010). Disentangling the structural mechanism underlying the functional differences between the alternate receptors is of general structural and functional interest and has the potential to aid the design of new drugs more rationally than can be done at present. In common with all members of the pLGIC, the functional properties of the α4β2 nAChRs are determined by subunit receptor composition.

Although the molecular mechanisms underpinning the dominant role of the α4(+)/α4(-) on the sensitivity to agonists have not been identified yet, studies of non-concatenated (Harpsoe et al., 2011) and concatenated (Mazzaferro et al., 2014) α4β2 nAChRs have highlighted the importance of non-conserved E loop residues on the complementary side of the α4(+)/α4(-) interface for both agonist potency and macroscopic efficacy. More recently, Lucero *et al*., (2016) using concatenated α4β2 nAChRs found that introducing non-conserved E residues on the β2(+)/α4(-) interface greatly decreased ACh EC_{50}, suggesting that all interfaces flanking agonist sites contribute to define the functional properties of the receptors.

The additional agonist site in the α4(+)/α4(-) interface forms because the α4 subunit conserves non-α agonist-binding aromatic residues such as W88 (Mazzaferro et al., 2011). In this respect, it is significant that key aromatic residues forming part of the primary side of canonical agonist sites in the α4β2 nAChR are conserved in the β2 subunit (i.e., W182 and Y126) **(Figure 3.1).** By analogy to the α4(+)/α4(-) interface, the conserved residues could contribute to agonist binding in the β2(+)/β2(-) interface, leading to unique HS $(\alpha4\beta2)_2\beta2$ functional properties. To

examine this possibility the effects of the cysteine-modifying sulphydryl reagent MTSET on concatenated HS receptors with a cysteine substituted β2(+)/β2(-) interface were examined.

The aim of the studies described in this Chapter was to determine whether there is an agonist binding site at the β2(+)/β2(-) interface of the HS α4β2 nAChR that could account for the pharmacological properties of this receptor, including high sensitivity to ACh. To circumvent ambiguities in data analysis brought about by expression of both forms of the α4β2 nAChR, the studies described here were carried out using fully concatenated HS α4β2 nAChR (β2_α4_β2_α4_β2 nAChRs). For clarity, in the concatenated HS α4β2 nAChR, the first subunit in the linear sequence of the concatemer (a β2 subunit) interfaces with the fifth subunit of the linear sequence of the concatemer (a β2 subunit) to give signature β2(+)/β2(-) interface **(Figure 3.1B).** The first subunit contributes the principal face, whilst the fifth subunit contributes the complementary interface **(Figure 3.1B).** Canonical agonist sites in the concatenated receptors are formed at the interface between the first subunit of the linear sequence of the concatmer and the second subunit (henceforth termed agonist binding site 1) and between the third and fourth subunits (hereafter termed agonist site 2) **(Figure 3.1B).** Note that the fifth subunit was often termed 'auxilliary' subunit, however, it is clear from studies of Cys loop receptors, including α4β2 nAChRs (Harpsoe et al., 2011; Mazzaferro et al., 2011; 2014), *Torpedo* nAChR (Unwin and Fujiyosi, 2012) and GABA-A receptors (Sigel and Steinmann, 2012), that the fifth subunit makes important contributions to the function of Cys loop receptors.

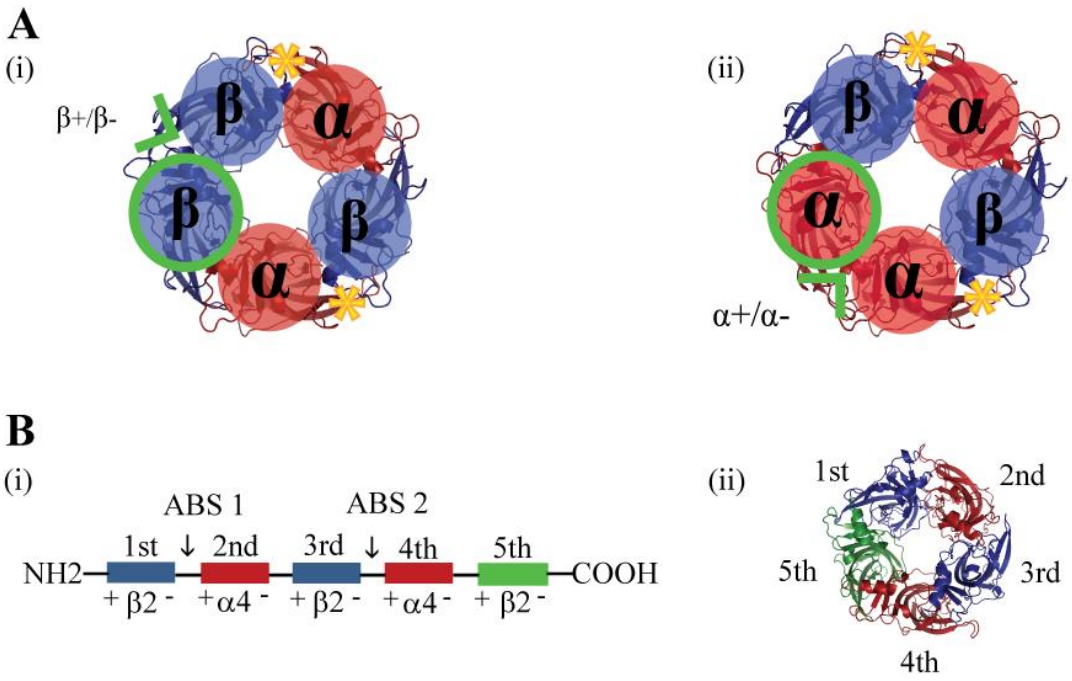

Figure 3.1. Subunit arrangement of two stoichiometries of α4β2 nAChRs . (A) Schematic representations of the high sensitivity (HS) (i) and low sensitivity (LS) (ii) stoichiometries of α4β2 nAChRs. β2-subunits are shown in blue and the α4 in red. Agonist binding sites at α4(+)/β2(-) interfaces are indicated by yellow asterisk. The fifth subunit is highlighted by a green circle. The stoichiometry specific subunit interfaces β2(+)/β2(-) and α4(+)/α4(-) are shown by a green arrow. **(B)** Cartoon depicting the linear sequence of the concatenated form of the HS α4β2 nAChR. The orientation of the principal and complementary side of the subunits is shown. The position of the canonical agonist binding sites (ABS) is shown by arrows.

3.2 RESULTS

3.2.1 – The ECD of the Fifth Subunit Subunit Confers α4β2 nAChR properties

Preliminary experiments were designed to determine if the fifth subunit in the HS α4β2 impacted the functional properties of this receptor type. This was carried out using concatenated receptors with chimeric fifth subunit subunits. These contained either the ECD of the α4 subunit and the remaining part (TM regions and C-terminus) of the β2 subunit (α4/β2), or the ECD of the β2 subunit and the remaining part of the α4 subunit (β2/α4) **(Figure 3.2A).**

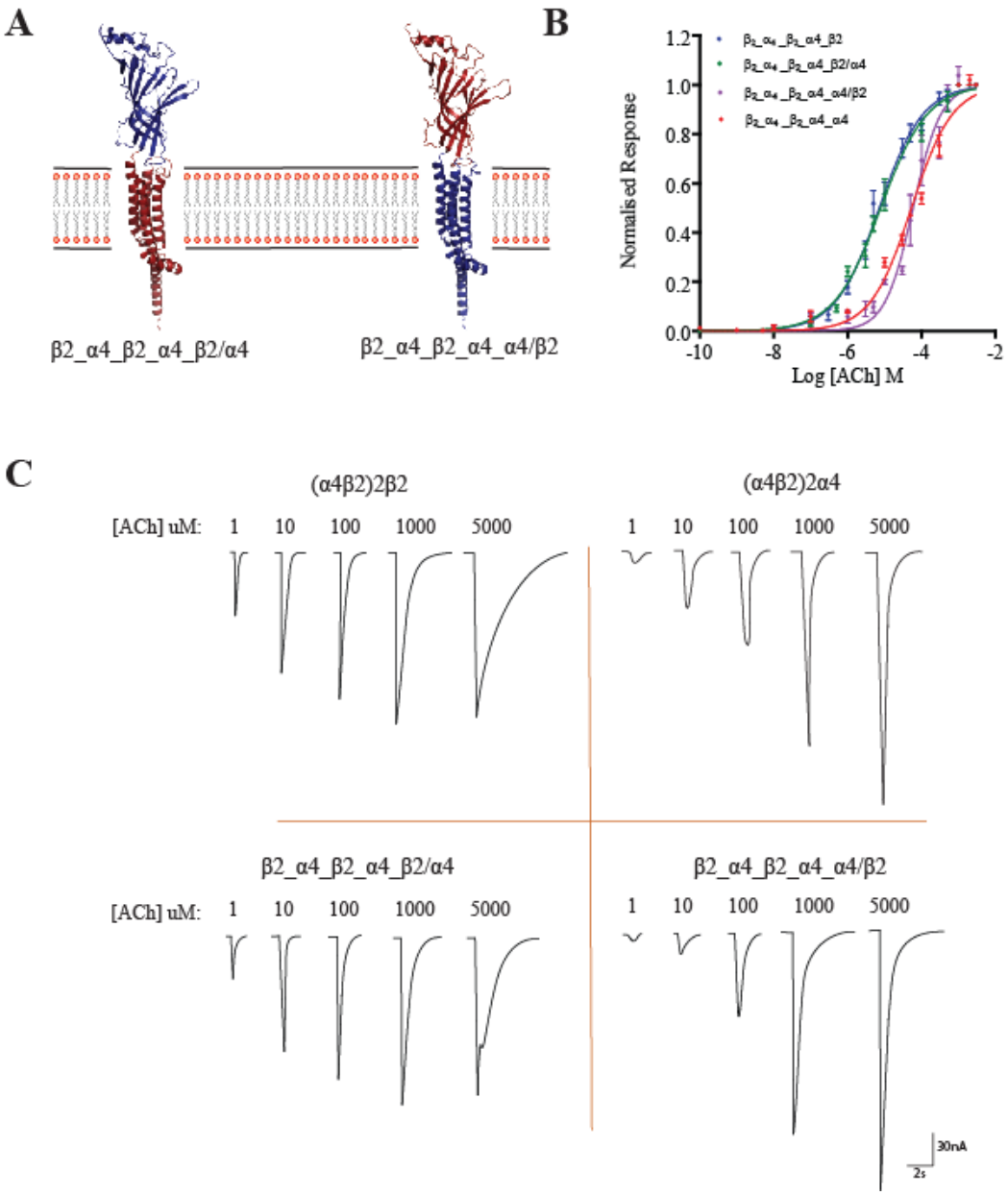

Figure 3.2. Chimeric fifth subunits confer functional changes to α4β2 nAChRs. (A) Homology models of the chimeric β2/α4 (left) and α4/β2 (right) subunits demonstrating regions of chimeric subunit comprised of α4 (red) and β2 (blue) nAChR subunits. **(B)** Concentration response curves of ACh at wild type and chimeric α4β2 nAChRs. Recordings were carried out as described in Materials and Methods. Data were analysed using non-linear regression with GraphPad 5 software. Each data point represents the mean ± SEM of at least 3 individual recordings. **(C)** Representative traces of the responses of wild type and chimeric receptors.

Concatemer	EC_{50} (uM)	nHill	I_{max}
β2_α4_β2_α4_β2	7.19 ± 1.5 ^^^	0.73 ± 0.08	1.01 ± 0.018^
β2_α4_β2_α4_β2/α4	8.03 ± 1.2 ^^^	0.67 ± 0.09	1.01 ± 0.05^
β2_α4_β2_α4_α4	53.79± 8.0 ***	0.77 ± 0.08	1.24 ± 0.06*
β2_α4_β2_α4_α4/β2	58.19± 12 ***	1.15 ± 0.25	1.19 ± 0.07*

Table 3.1. Concentration Response Data for ACh activation of concatemeric α4β2 HS nChRs with chimeric fifth subunit. Data are the mean ± SEM for all experiments from at least two different batches of oocytes. Statistical analysis was performed using One-way ANOVA with Bonferroni post-test (*** and ^^^, $p < 0.0001$; *).or ^, $p < 0.05$). * indicates values compared to β2_α4_β2_α4_β2, and ^ indicates values compared to β2_α4_β2_α4_α4. I_{max} values reported are normalised to responses elicited by 1mM ACh in order to demonstrate differences in receptor efficacies.

Figure 3.2B and C (see **Table 3.1** for estimated values of ACh sensitivity) show that the ACh sensitivity of receptors containing a chimeric α4/β2 subunit at the fifth position was statistically different from β2_α4_β2_α4_β2 (high sensitivity) nAChRs ($p < 0.001$) but not different from that of β2_α4_β2_α4_α4 (low sensitivity) nAChRs. In contrast, when the chimeric fifth subunit contained the extracellular N-terminal region of the β2 subunit (i.e., β2_α4_β2_α4_β2/α4 nAChRs), the sensitivity to ACh was comparable to that of β2_α4_β2_ α4_β2 nAChRs and was statistically different ($p < 0.001$) from that of β2_α4_β2_α4_α4. These findings indicate that the presence of the extracellular domain of the β2 subunit in the fifth subunit of α4β2 nAChRs brings about ACh sensitivity similar to that of β2_α4_β2_α4_β2 nAChRs, supporting the view that the fifth subunit plays a key role in determining the ACh sensitivity of the $(\alpha4\beta2)_2\beta2$ nAChR and further suggests that the N-terminal is the region contributing to the differences seen in responses to ACh from the two receptor stoichiometries.

3.2.2 – The β2(+)/β2(-)interface of HS α4β2 nAChRs contributes to Ach efficacy

Sequence alignment and examination of a homology model of the HS α4β2 nAChR suggested that the β2(+)/β2(-) interface in the HS α4β2 nAChR may house an agonist binding pocket contributed by conserved aromatic residues that line the agonist binding pocket in the α4(+)/β2(-) interfaces **(Figure 3.3A, B).** An additional operational agonist binding site has been identified in the α4(+)/α4(-) interface of the LS α4β2 nAChR (Harpsoe et al., 2011; Mazzaferro et al., 2011), and this site plays a dominant role in defining the apparent agonist affinity and maximal current responses of the LS receptor (Harpsoe et al, 2011; Mazzaferro et al., 2011; 2014). To test the possibility of an operational binding site at the β2(+)/β2(-) interface, a cysteine residue was introduced in lieu of β2 L146 (an E loop residue) on the complementary side of β2(+)/β2(-) interface to determine the functional consequences of modifying it with MTSET.

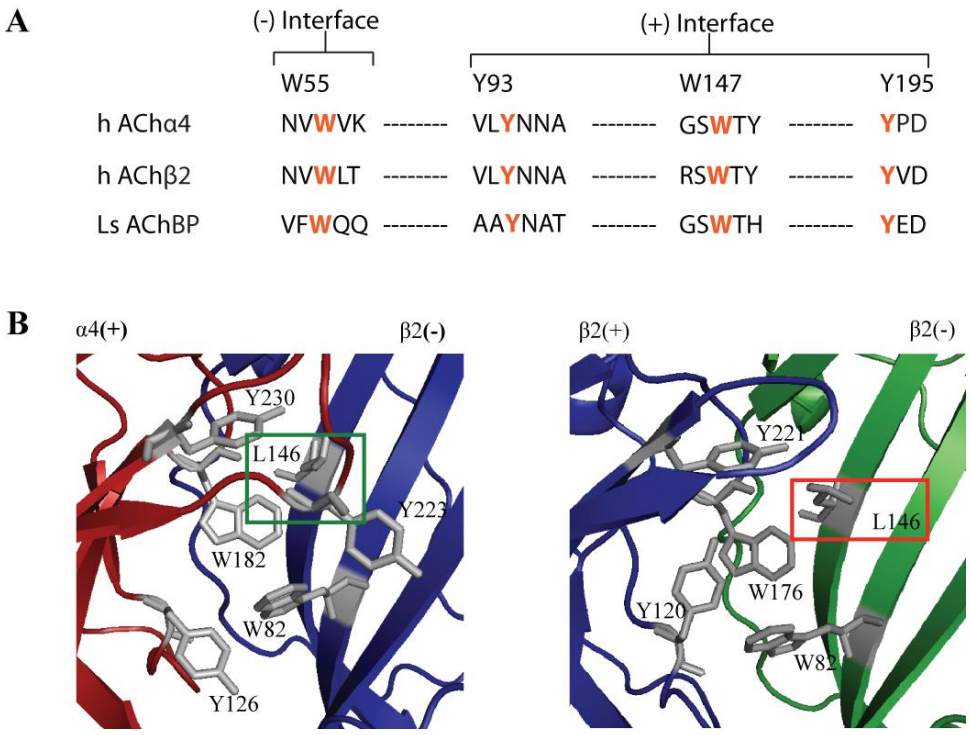

Figure 3.3. Conserved aromatic residues in the α4(+)/β2(-) and β2(+)/β2(-) subunit interfaces in HS α4β2 nACh and relative position of β2(-)L146C. (A) Sequence alignment of conserved aromatic residues lining the agonist binding pocket in α4(+)/β2(-) interface are conserved in the β2(+)/β2(-) interface). **(B)** Homology model of the α4(+)/β2(-) and β2(+)/β2(-) subunit interfaces in the HS α4β2 nAChRs

Following introduction of a free cysteine into a desired region of a protein, the MTS reagent MTSET reacts with the available sulphydryl group and covalently attaches a small positively charged moiety to that residue. When introduced to a putative ACh binding pocket, this modification can sterically or electrostatically block ACh access to the site, preventing agonist accessing the putative binding. The outcome of this upon receptor function and thus degree of binding perturbation can then be investigated (Karlin and Akabas, 1998; Mazzaferro et. al., 2011; 2014).

The residue β2L146 is within loop E on the complimentary face of the β2 subunit and structural homology modelling of the ECD of the β2(+)/β2(-) interface predicts L146 to reside within the putative agonist site in a position homologous to that occupied by β2L146 on the canonical agonist site in α4(+)/β2(-) interfaces

(Figure 3.3B). This position within both interface trypes is confirmed by x-ray crystallography of $(\alpha4\beta2)_2\beta2$ as just above and projecting into the conserved aromatic pocket (Morales-Perez et. al., 2016).

Importantly, previous studies have shown that derivatisation of β2(-)L146C in α4(+)/β2(-) interfaces by MTS reagents reduces agonist-driven current responses by reducing access to the agonist site (Papke et al., 2011; Mazzaferro et al., 2011; 2014).

HS α4β2 concatemers with this mutation in the 5th β2 subunit ($\beta2\_\alpha4\_\beta2\_\alpha4\_\beta2^{L146C}$) were thus engineered to investigate effects of MTS-ET modification at the β2(+)/β2(-) interface. As a measure of control and in order to gain insight to binding site differences, this substitution was also individually introduced to the α4(+)/β2(-) interfaces housing orthosteric ligand binding sites. Cysteine substitution of L146 on the 1st β2 subunit produces a $\beta2^{L146C}\_\alpha4\_\beta2\_\alpha4\_\beta2$ concatemer, and this construct can be used to study agonist binding site 1. Incorporation of L146C on the third position (a β2 subunit) of the concatenated HS receptor produced $\beta2\_\alpha4\_\beta2^{L146C}\_\alpha4\_\beta2$, which can be used to study agonist binding site 2.

Substitution of L146 for a free cysteine at these positions had no significant functional consequences on the sensitivity of the receptors to activation by ACh **(Figure 3.4, Table 3.2)**. This indicates that the L146C in any of the sites introduced is well tolerated. Importantly, it also suggests that any changes in receptor function following exposure to MTSET can be attributed to the covalent modification of the cysteine substituted concatenated nAChRs with MTS-ET.

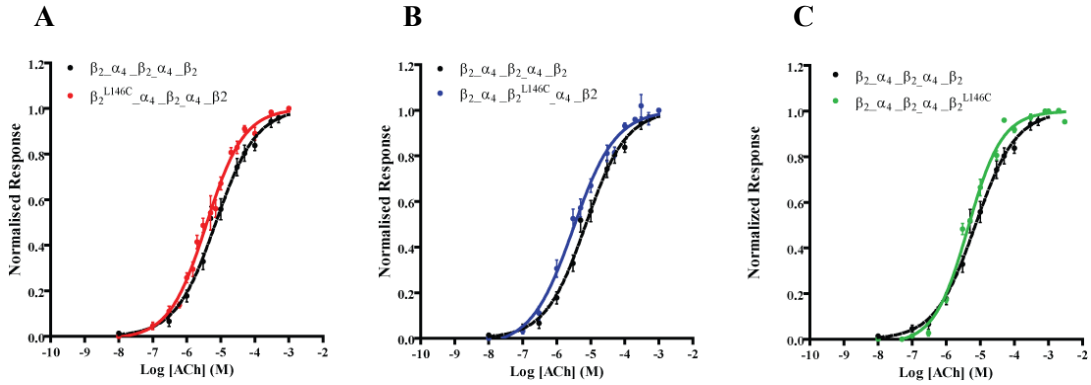

Figure 3.4. ACh concentration-response relationships for wild type and β2(-)L146C substituted concatemeric HS α4β2 nAChRs. The β2(-)L146 residue of each β2 subunit was individually substituted to cysteine in the α4(+)/β2(-) **(A and B)** and β2(+)/β2(-) **(C)** interfaces. The consequences of the mutations upon sensitivity to activation by ACh were examined using two-electrode voltage clamping, as described in Materials and Methods. Data points represent the mean ± SEM of at least three independent experiments. Data were fit by nonlinear regression, as described under Materials and Methods. Dashed lines are curve fits for wild type (WT) receptors. ACh EC_{50} and nHill coefficient values are summarised in **Table 3.2**.

Receptor	ACh EC_{50} (μM)	n	nHill	Remaining I_{Ach} Post MTS-ET (%)	n
β2_α4_β2_α4_β2	7.19 ± 1.5	14	0.7458 ± 0.12	85.67 ± 2.5	6
β2_α4_β2_α4_β2 L146C	3.71 ± 0.8	6	0.9348 ± 0.12	41.10 ± 2.9 ***	10
β2L146C_α4_β2_α4_β2	3.77 ± 1.3	6	0.8738 ± 0.16	34.77 ± 2.0 ***,++,^^^	11
β2_α4_β2 L146C _α4_β2	3.19 ± 1.4	6	0.6756 ± 0.09	23.36 ± 2.1 ***,++,^	13

Table 3.2. Effects of MTSET on the ACh responses of wild type and cysteine substituted concatenated HS α4β2 nAChRs. Ooocytes expressing wild type or cysteine substituted concatenated HS α4β2 nAChRs were exposed to 1 mM ACh prior and after a 1 min application of 1 mM MTSET. The percentage of remaining activation by 1 mM ACh after MTSET treatment was defined as ($I_{afterMTSET}/I_{initial}$) x 100. Data are the mean ± SEM of n number of experiments. Significant differences between mutant and wild type receptors (noted by *) or between β2_α4_β2_α4_β2^{L146C} and the β2^{L146C}_α4_β2_α4_β2 and β2_α4_β2 ^{L146C}_α4_β2 receptors were estimated using One-way ANOVA with Dunnett's post-test (***, $p < 0.0001$). ++ indicates that the values for β2^{L146C}_α4_β2_α4_β2 and β2_α4_β2^{L146C}_α4_β2 are statistically different from each other ($p < 0.001$). Statistical comparison of the values obtained for β2_α4_β2_α4_β2 ^{L146C} and β2^{L146C}_α4_β2_α4_β2 showed $p < 0.0001$ levels of significance (noted by ^^^), whilst comparisons between the % change obtained for β2_α4_β2_α4_β2^{L146C} and β2_α4_β2^{L146C}_α4_β2 receptors showed a $p < 0.05$ level of significance (noted by ^).

Following this, the accessibility of the substituted cysteines to MTS reagent MTSET was determined. This was achieved by exposing the receptors to a maximal MTSET concentration (1 mM) (Zhong and Karlin, 1997), as described in Materials and Methods. MTSET reduced ACh EC_{80}-evoked currents recorded from all cysteine substituted receptors, showing not only that the substituted cysteines are available to MTS-ET, but that covalent modification at the cysteine substituted β2(+)/β2(-) interface substantially reduces the efficacy of ACh (**Figure. 3.5**). Since agonist binding sites must be exposed to water for the agonist to access the site, the accessibility of the substituted cysteine to MTSET is consistent with the presence of an agonist site at the β2(+)/β2(-) interface. In accord with studies showing that canonical agonist sites in LS α4β2 (Mazzaferro et al., 2011; 2014) and HS (Lucero et al., 2016) α4β2 nAChRs contribute asymmetrically to receptor function, the extent of ACh EC_{80} current reduction by MTSET reaction was 1.2 fold greater for $\beta2^{L146C}$_α4_β2_α4_β2 than for β2_α4_$\beta2^{L146C}$_α4_β2 receptors ($p < 0.001$) **(Figure 3.5, Table 3.2)**. Significantly, reduction of β2_α4_β2_α4_β2 ^{L146C} function by MTSET was 1.3-fold ($p < 0.001$) and 1.1-fold ($p < 0.05$) lesser pronounced than on $\beta2^{L146C}$_α4_β2_α4_β2 receptors and β2_α4_$\beta2^{L146C}$_α4_β2 receptors, respectively **(Table 3.1)**. Overall, these findings show that L146 in the β2(+)/β2(-) is accessible to MTSET and while it does appear to be important for ACh macroscopic efficacy, canonical agonist sites play a dominant role in receptor function.

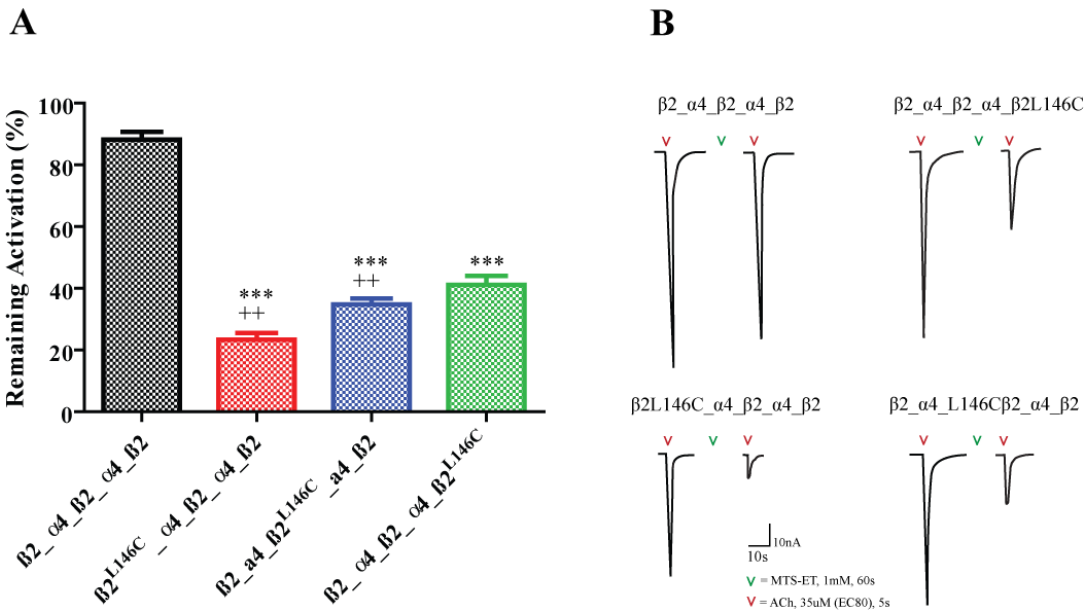

Figure. 3.5. Maximal effects of MTSET on ACh responses of wild type and mutant concatenated HS α4β2 nAChRs. **(A)** Bar graphs show the percentage of original current response to ACh EC_{80} remaining following MTSET modification. The percentage of remaining responses elicited by EC_{80} ACh after MTSET treatment was defined as (($I_{afterMTSET}/I_{initial}$) x 100). Data are the mean ± SEM of n number of experiments. Significant differences between mutant and wild type receptors or between β2_α4_β2_α4_β2 ^{L146C} and the β2^{L146C}_α4_β2_α4_β2 and β2_α4_β2 ^{L146C} _α4_β2 receptors were estimated using One-way ANOVA with Dunnett's post-test (***, $p < 0.0001$). ++ indicates that the values for β2^{L146C}_α4_β2_α4_β2 and β2_α4_β2 ^{L146C} _α4_β2 are statistically different from each other ($p < 0.001$). **(B)** Representative current traces from oocytes expressing mutant or cysteine substituted concatenated HS α4β2 nAChRs showing ACh EC_{80} current response prior and after a 1 min exposure to 1 mM MTSET. Arrows indicate the application of ACh (red) or MTSET (green).

3.2.3 - Rates of MTS-ET Reaction at α4(+)/β2(-) and β(+)/β(-) Interfaces in the Presence and Absence of ACh

This effect of MTS-ET at the β2(+)/β2(-) interface and the contribution of this region to receptor function was further investigated by measuring the rate of MTS-ET modification of β2_α4_β2_α4_$β2^{L146C}$ in the presence or absence of ACh. If ACh binds the putative agonist pocket in the β2(+)/β2(-) interface, ACh and MTS-ET co-application should impede MTS-ET modification of L146C in β2_α4_β2_α4_$β2^{L146C}$ receptors, thus slowing down the rate of the MTSET reaction. This effect can occur because the substituted cysteine is a contact point for ACh, steric hindrance, changes in electrostatic potentials or allosteric structural changes (Boileau et al., 2002; Mercado and Czajkowski, 2006; Mazzaferro et al., 2011; 2014).

Consistent with the role of the agonist sites in the α4(+)/β2(-) interfaces in receptor activation, presence of ACh significantly decreased the rate of MTSET modification of $β2^{L146C}$_α4_β2_α4_β2 and β2_α4_$β2^{L146C}$_α4_β2 receptors **(Figure 3.6; Table 3.3)**. ACh was more effective at protecting $β2^{L146C}$_α4_β2_α4_β2 from MTS-ET modification than β2_α4_$β2^{L146C}$_α4_β2 receptors (5.0 vs 1.5-fold decrease), further confirming the functional asymmetry of the canonical agonist sites in α4β2 nAChRs (Mazzaferro et al., 2011; 2014; Lucero et al., 2016). In accord with a role in receptor activation, the rate of MTSET reaction with β2(+)/β2(-) interface decreased in the presence of ACh **(Figure 3.6, Table 3.3).** Interestingly, although ACh was more effective at protecting $β2^{L146C}$_α4_β2_α4_β2 from MTSET modification than β2_α4_β2_α4_$β2^{L146C}$ (5.0-fold *versus* 3.9-fold), the rate of protection measured for β2_α4_$β2^{L146C}$_α4_β2 and β2_α4_β2_α4_$β2^{L146C}$ receptors was not (3.9 versus 1.5-fold decrease) **(Table 3.3).** When the protectant ACh

concentration was reduced to EC_{20}, the rate of MTSET reaction with β2_α4_β2_α4_$β2^{L146C}$ also decreased, however the impact of ACh on MTSET reaction rate diminished **(Table 3.4).**

Receptor	Control k_2 ($M^{-1}s^{-1}$)	n	+ ACh EC_{80} k_2 ($M^{-1}s^{-1}$)	n	k_2 /k_2 + ACh EC_{80}
β2_α4_β2_α4_β2 L146C	1864 ± 263+++	4	475.0 ± 131**	4	3.9
β2L146C_α4_β2_α4_β2	5639 ± 758+++	4	1134 ± 139***	5	5.0
β2_α4_β2 L146C _α4_β2	1022 ± 91+++	5	683.2 ± 46*	5	1.5

Table 3.3. Rates of MTSET modification of cysteine substituted concatemeric HS α4β2 nAChR in the absence or presence of ACh. Rates of MTSET reaction with introduced cysteine were measured, and second-order rate constant (k_2; $M^{-1}s^{-1}$) were calculated as described in the Materials and Method Chapter. Second order rate constants represent the mean ± SEM of n number of experiments. The rate of MTSET reaction of the three mutant receptors studied were significantly different (+++, $p < 0.0003$) (One-way ANOVA test with post-Dunnett's correction. Asterisks show levels of significance between rates of reaction in the presence and absence of ACh (*, $p < 0.05$; **,p <0.005 ***, $p < 0.0001$) (Student t-tests).

[ACh] (μM)	3.0 (EC_{80})	1.0 (EC_{20})
k_1 (s^{-1}) (decay)	0.019 ± 0.002	0.012 ± 0.002
k_1(s^{-1})(protection)	0.005 ± 0.001***	0.01 ± 0.002+++
k_2 ($M^{-1}s^{-1}$) (decay)	1864 ± 263	1208 ± 160
k_2 ($M^{-1}s^{-1}$) (protection)	475.0 ± 131***	1010 ± 233+++

Table 3.4. Rates of MTSET modification of β2_α4_β2_α4_$β2^{L146C}$ in the absence or presence of ACh. Rates of MTSET reaction with introduced cysteine were measured, and second-order rate constant (k_2; $M^{-1}s^{-1}$) were calculated as described in the Materials and Method Chapter. Second order rate constants represent the mean ± SEM of n number of experiments. The rate of MTSET reaction across the two conditions of ACh application were significantly different (+++, $p < 0.0001$) (Students t-test). Asterisks show levels of significance between rates of reaction in the presence and absence of ACh, ***, $p < 0.0001$).

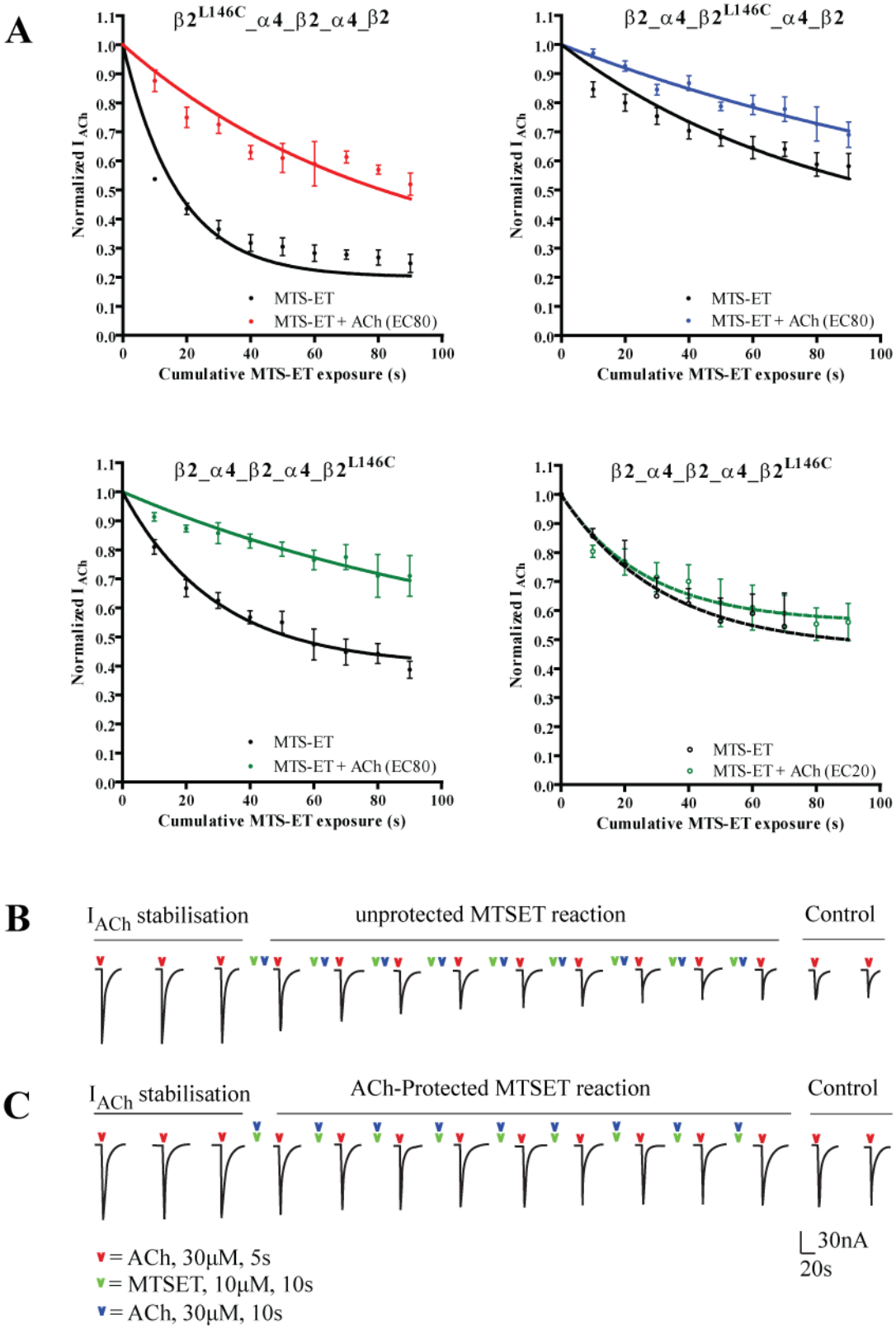

Figure 3.6. Effect of ACh on the rate of MTSET-modification of cysteine substituted α4(+)/β2(-) and β2(+)/β2(-) interfaces of concatemeric HS α4β2 nAChRs. (A) normalised ACh currents in the presence or absence of ACh were plotted versus cumulative time of exposure to MTSET and fit with a single exponential function, as described in Materials and

Methods. Data points were normalised to ACh currents at time 0 and represent the mean ± SEMs of at least three experiments. Second-order rate constants for MTSET modification of the cysteine substituted receptors are summarised in **Table 3.4**. **(B)** Representative ACh EC_{80} current responses of current of β2_α4_β2_α4_$β2^{L146C}$ receptors showing the protocol used to measure the rate of the derivatization of the cysteine substituted β2_α4_β2_α4_β2 receptors by a 2 min application of sub-maximal concentration of MTSET (10 μM) in the absence (B) or presence **(C)** of ACh. EC_{80} ACh was applied during the stabilisation of the responses to ACh in (B) and (C) to correct for any receptor desensitisation that could developduring the experiment. For the measurement of the rate of reaction in the presence of ACh, the agonist was co-applied with MTSET.

3.2.4 - Is There an ACh Binding Site in the β2(+)/β2(-) Interface?

The discovery that ACh prevents MTS-ET modification of β2(+)/β2(-)^{L146C}, and furthermore that MTS-ET modification of β2(+)/β2(-)^{L146C} perturbs receptor function, supported the hypothesis that the conserved agonist-binding aromatic residues may form an operational agonist binding site in the β2(+)/β2(-) interface. This hypothesis was further examined by mutating the conserved aromatic residues to alanine, a small inert residue that does not interact with ACh. Previous work has shown that impairment of individual agonist sites by alanine substitution yields biphasic ACh concentration response curves, comprising a high-affinity and a low-affinity component (Mazzaferro *et a*l., 2011; 2014; Lucero *et al*., 2016). The high-sensitivity component of the bi-phasic curves is contributed mostly by intact agonist sites whereas the low-sensitivity component is contributed by both intact and mutated agonist sites (Mazzaferro et al., 2011; 2014).

3.2.4.1 – Alanine substitutions of β2(+)/β2(-)

Individual or simultaneous alanine substitution of Y120, W175 and Y221 on the (+) face of the β2(+)/β2(-) interface and W82 on the (–) face, which are equivalent to α4Y126, α4W182, α4Y223 and α4W88 **(Figure. 3.3)**, had no effect on sensitivity to ACh, compared to wild type **(Figure 3.8; Table 3.5)**. Further analysis

of the homology modelling of the β2(+)/β2(-) interface suggested that two aspartic acid residues on the (+) face present in the middle of the putative agonist binding pocket, (D217 and D218), and a phenylalanine on the (-) face juxtaposed to the L146 side chain (F144) could interact with ACh, forming part of the cavity proposed to house an agonist site **(Figure. 3.7).** Positions of these amino acid side-chains were confirmed withint the x-ray crystaolgraphy data of $(\alpha4\beta2)_2\beta2$ nAChRs (Morales-Perez et. al., 2016. Alanine substitution on these residues had no effect on the sensitivity of β2_α4_β2_α4_β2 nAChRs to ACh **(Table 3.5)**. Thus, overall, the results strongly suggest that none of the residues tested are contact-points for ACh on the β2(+)/β2(-) interface to form a functional binding site.

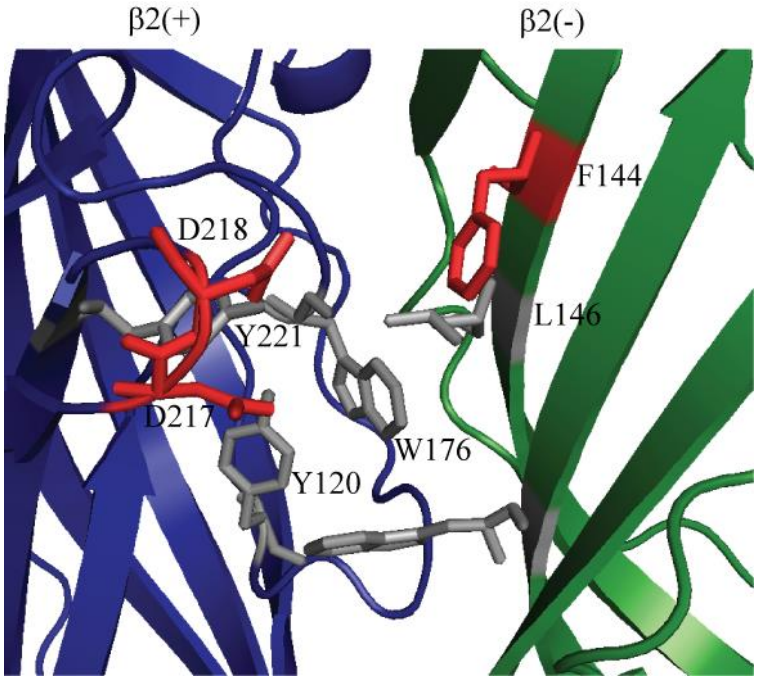

Fig. 3.7. Homology model of the β2(+)/β2(-) interface of the HS α4β2 nAChR. α-aromatic residues conserved in β2 are shown in gray sticks. Additional residues that could contribute to agonist binding due to the orientation of their side chain towards the putative agonist binding pocket are shown as red sticks.

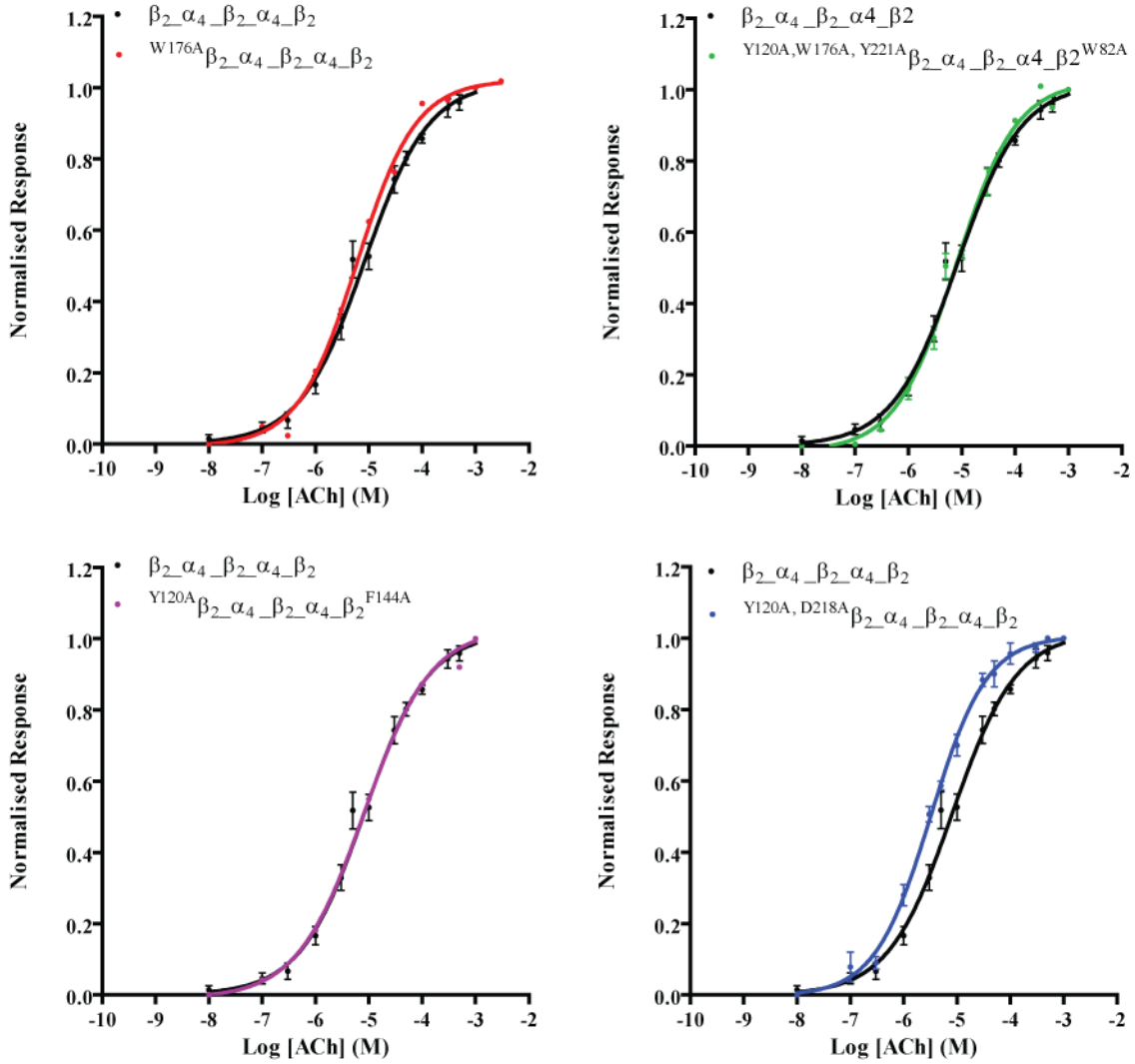

Figure 3.8. ACh Concentration-response relationships for wild type and β2(+)/β2(-) interface alanine substituted concatemeric HS α4β2 nAChRs. Conserved aromatic residues that interact with agonists in canonical agonist sites in nAChRs were mutated to alanine in the β2(+)/β2(-) interface , and the consequences of the mutations for sensitivity to activation by ACh were examined using two-electrode voltage clamping, as described in Materials and Methods. Data points represent the mean ± SEM of at least three independent experiments. Data were fit by nonlinear regression, as described under Materials and Methods. Dashed lines are curve fits for wild type (WT) receptors. ACh EC50 and nHill coefficient values are summarised in Table 3.3.

Receptor	ACh EC_{50} ± SEM (μM)	nHill ± SEM	mut/wt	n
β2_α4_β2_α4_β2	7.19 ±1.6	0.89±0.22	1	20
Y120Aβ2_α4_β2_α4_β2	10.74 ±5.4	0.94±0.24	1.5	6
Y221Aβ2_α4_β2_α4_β2	8.62 ±2.1	0.90±0.1	1.2	3
W176Aβ2_α4_β2_α4_β2	7.15 ±0.93	0.93±0.17	0.99	5
β2_α4_β2_α4_β2W82A	7.79 ±2.3	0.82±0.19	1.08	10
Y120A,Y221Aβ2_α4_β2_α4_β2	3.89 ±0.35	0.97±0.21	0.54	5
Y120Aβ2_α4_β2_α4_β2W82A	4.64 ±2.2	0.85±0.14	0.65	4
Y120A,W176A, Y221Aβ2_α4_β2_α4_β2W82A	7.56±2.4	0.83±0.34	1.05	5
Y120Aβ2_α4_β2_α4_β2F144A	5.9 ±3.4	0.76±0.25	0.82	6
Y120A,D217Aβ2_α4_β2_α4_β2	3.17 ±1.8	0.82±0.5	0.44	3
Y120A,D218Aβ2_α4_β2_α4_β2	3.10 ±0.9	0.84±0.15	0.43	3

Table 3.5. Concentration Response Data for ACh activation on concatemeric α4β2 HS nChRs with alanine substituted β2(+)/β2(-) interface. Data are the mean ± SEM for no experiments from at least two different batches of oocytes. Mutant/wild type (mut/wt) were calculated. None of the mutant EC_{50} values were significantly different from wild type (One-way Anova with Dunnett's post-test).

3.2.4.2 - MTS-ET Modification of β2_α4_β2_α4_β2L146C in the presence and absence of Competitive antagonist dihydro-β-erythroidine (DhβE)

As alanine mutations in the β2(+)/β2(-) interface did not affect receptor function, to further test for the presence of an operational agonist binding site in the β2(+)/β2(-), the rate of MTSET modification was measured in the absence or presence of the α4β2 nAChR competitive antagonist dihydro-β-erythroidine DhβE. Outcomes of "protection" seen with both classes of ligand (agonist and antagonist) are regarded as affirmative of presence of a binding site in region probed (Liapkis, 2001). Functional studies of alanine-mutated agonist binding sites (Iturriaga-Vásquez et al., 2010) as well as crystal structures of *Lymnea* AChBP bound with

DhβE (Shahsavar et al., 2012) show that as a competitive antagonist it interacts with the same residues as ACh in the agonist binding pocket. However, unlike ACh, DhβE stabilises the receptor in a closed state. This means that during co-application with MTSET, if binding sites are occupied by DhβE the receptor will remain in the closed conformation, and not undergo the structural changes induced by ACh binding. If there is a difference in k_1 values between applications of MTS-ET alone and when co-applied with DhβE, it can be concluded that the protection seen with co-application with ACh is not due to alteration in exposure of introduced cysteine to MTSET due to movement of this residue during receptor activation following agonist binding. Therefore the site is being protected from MTS-ET by the competitive antagonist, signifying a binding site as the competitive antagonist and binds in same nature as ACh.

As shown in **Figure 3.9 (Table 3.6)**, when the rate of MTSET reaction was measured in the presence of DhβE IC_{80}, there was little if any shift in the rate of reaction (13.-fold difference). Importantly, decreasing the concentration of DhβE had no impact on the rate of reaction **(Table 3.6).** If DhβE competes with MTSET for access to the putative agonist site, the rate of MTSET reaction should be perturbed in the presence of DhβE. Thus, this finding, together with the lack of functional effects of alanine substituted β2(+)/β2(-) interface do not support the presence of an operational agonist site in the β2(+)/β2(-) interface.

As ligand occupation of putative binding site eliciting no conformational change does not alter the MTSET modification of substituted β(+)/β(-) L146C, it is more than likely that disparity rates in ACh studies is not due to functional binding site at the β(+)/β(-) interface, but reveals important movements of the substituted residue following agonist binding at orthosteric sites and subsequent receptor

activation.

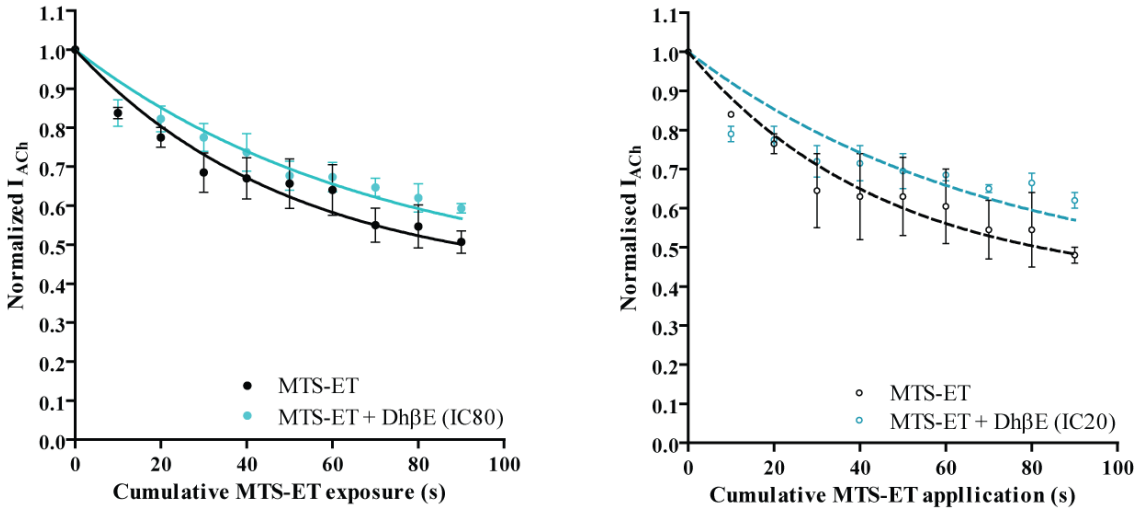

Figure 3.9. Effects of the competitor antagonist DhβE on the rate of MTSET modification of the β2(+)/β2^{L146C}(-) interface of the HS α4β2 nAChR. Rates experiments were carried out as described in Materials and Methods. Normalised EC80 current responses were plotted *versus* cumulative time of MTSET exposure in the absence or presence of DhβE IC_{80} or IC_{20}. Data were were fit to a single-phase exponential decay as described in Materials and Methods. Each data point represents the mean ± SEM of at least three independent experiments.

Reaction Conditions	k_2 ($M^{-1}s^{-1}$)	
	DhβE IC_{80}	DhβE IC_{20}
- DhβE	1340 ± 323	1398 ± 498
+ DhβE	985 ± 208	1134 ± 526

Table 3.6. Rates of MTSET modification of the β2(+)/β2(-)^{L146C} interface in the presence or absence of the competitive nicotinic inhibitor DhβE. Rates of MTSET reaction with the introduced cysteine were measured, and second-order rate constants (k_2, $M^{-1}s^{-1}$) were calculated as described under Materials and Methods. Second-order rate constants are the mean ± SEM of at least three independent experiments. Rates were measured using two different concentrations of DhβE (IC_{80} and IC_{20}) but none of these conditions perturbed the rate of MTET reaction as suggested by lack of significant differences shown by students t-tests.

3.2.5 – Effect of Modification of β(+)/β(-) Interface upon Macroscopic Properties of the (α4β2)$_2$β2 nAChR

The discovery that ACh, but not DhβE, affects derivatisation of β2_α4_β2_α4_β2^{L146C} receptors with MTSET further suggests the absence of an operational agonist site at the β2(+)/β2(-) interface. However, since modification of L146C at β2(+)/β2^{L146C}(-) impedes receptor function and ACh slows down the rate of MTSET modification, it may be that L146C or a neighbouring residue on the (-) side of the fifth subunit is a macroscopic efficacy element, whose accessibility is affected by binding of agonists to the canonical agonist sites on the α4(+)/β2(-) interfaces. To test this possibility, the full ACh CRC of β2_α4_β2_α4_β2 ^{L146C} was determined before and after a 2 min of application of 1 mM MTSET. If MTSET modification of β2(+)β2^{L146C}(-) perturbs an agonist efficacy mechanisms encoded by the fifth subunit or the β2(+)β2(-) interface, the maximal macroscopic maximal ACh responses should decrease with no significant changes in ACh EC_{50}. Alternatively, if modification affects agonist binding or agonist-binding and gating, the ACh CRC after the reaction should be characterised by a decrease in ACh maximal currents and a shift in the value of ACh EC_{50}. As shown in **Figure 3.10 (Table 3.10)**, MTSET modification of β2(+)/β2(-) resulted in decreased maximal currents for ACh without changes in the ACh EC_{50} (EC_{50} before MTSET = 6.1 ± 1.7 μM; EC_{50} after MTSET = 6.03 ± 1.0 μM).

In combination, the outcomes of studies outlined above suggest that the fifth subunit in HS α4β2 nAChRs modulates response to ACh efficacy, but not through the presence of an operational agonist site at the β2(+)/β2(-) interface.

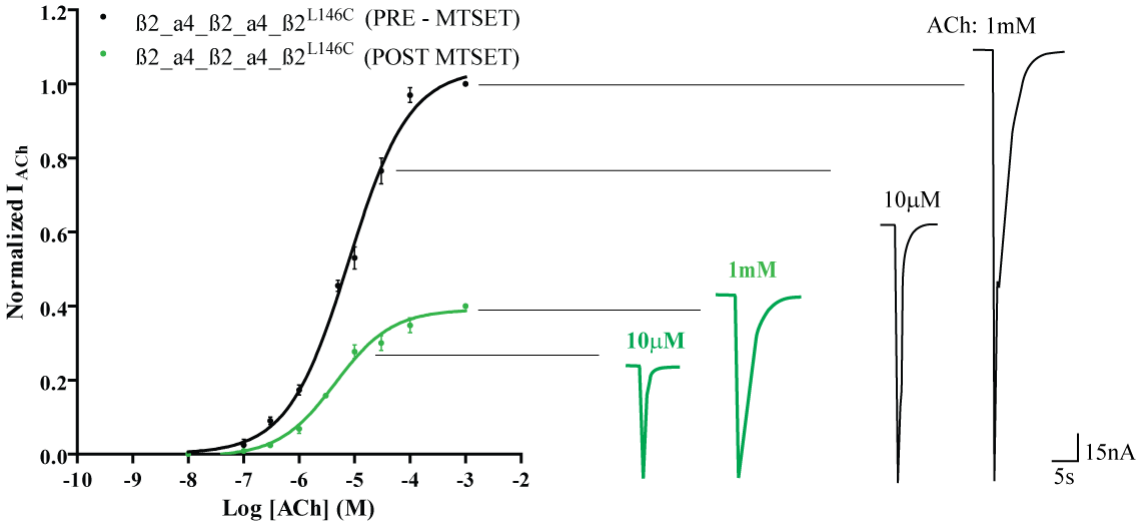

Figure 3.10. Effects of MTSET reaction on the ACh concentration-response curve of β2_α4_β2_α4_β2^{L146C} receptors. The full ACh concentration response curve for β2_α4_β2_α4_β2^{L146C} receptors was determined prior and after 2 min exposure to 1 mM MTSET. After application of MTSET the cells were washed with Ringer until the response to ACh EC80 were stable (less than 5% change), after which time the ACh concentration-response curve was determined again. The concentration response data were fit by nonlinear regression, as described under Materials and Methods.

Condition	EC_{50}	nHill	Top
β2_α4_β2_α4_β2^{L146C} Pre MTSET	6.1 ± 1.7	0.7 ± 0.05	1 ± 0.04
β2_α4_β2_α4_$β_2^{L146C}$ Post MTSET	6.03 ± 1.0	0.69 ± 0.1	0.41 ± 0.01***

Table 3.7. Effects of maximum blockage of β2(+)/β2 interface on concentration response relationships of ACh. Concentration dependent responses to ACh were measured and responses stablised prior to MTSET application. 1mM MTSET was then applied to oocytes to achieve saturating levels and full modification of receptors. The same concentration response measurement protocol was then carried out with responses normalised to responses achieved during stabilisation period. No significant difference of sensitivity parameters (EC_{50}) was observed, but as previously seen, students t-test showed difference in maximal efficacy following MTSET treatment (***,p<0.0001).

3.3 DISCUSSION

The fifth subunit in the two stoichiometries of α4β2 nAChR differs, thus producing two structurally distinct subunit interfaces within the alternate $(\alpha4\beta2)_2\beta2$ and $(\alpha4\beta2)_2\alpha4$ receptors. One of which, α4(+)/α4(-) in $(\alpha4\beta2)_2\alpha4$, contains an ACh-binding site that plays a dominant role in defining the pharmacology (Harpsoe et al, 2011; Mazaferro et al., 211; Absalom et al., 2013; Olsen et al., 2013; Mazzaferro et al., 2014) and desensitisation (marks etal., 2010; Benallegue et. al., 2013) of the $(\alpha4\beta2)_2\alpha4$ stoichiometry.

Here, by combining voltage-clamp electrophysiological recordings in *Xenopus* oocytes, site-directed mutagenesis, homology modelling, along with SCAM approaches, it is shown for the first time that the fifth subunit in the $(\alpha4\beta2)_2\beta2$ receptor makes a significant contribution to agonist-driven receptor activation. In contrast to the $(\alpha4\beta2)_2\alpha4$ stoichiometry, this effect is not through occupation of an agonist site at the β2(+)/β2(-) interface contributed by the fifth subunit, but likely through conformational changes in the fifth subunit brought about by agonist occupation of the agonist binding sites in the α4(+)/β2(+) interfaces. This is the first time that it is shown functionally that the fifth subunit subunit in a pLGIC plays a role in receptor gating. In addition to residues that directly contact the agonists or that facilitate occupancy of the site, there are residues in the agonist-binding α(+)/β(-) interfaces that communicate the agonist binding event down to the ECD/TM interface and ultimately to the channel gate. These include residues in the β1-β2 and Cys loops, M2-M3 linker and TM residues in M1, M3 and M4 (reviewed in Miller and Smart, 2010). However, recent structural studies of the *Torpedo* nAChR have suggested that asymmetric motions of the receptor subunits brought

about by agonist binding to the canonical agonist sites induces conformational transitions in the fifth subunit subunit (a β1subunit), which plays the key role in transmitting gating signals from adjacent agonist sites to the ion channel g ate (Unwin and Fujiyoshi, 2012).

Several lines of evidence support the conclusion that the fifth subunit is an important element of the gating pathways of the $(\alpha4\beta2)_2\beta2$ receptor. First, MTSET modification of L146C in the fifth subunit decreased the maximal ACh current in a manner consistent with removal by MTSET derivatisation of a gating element. Second, although ACh slowed covalent modification of L146C in the fifth subunit, the competitive antagonist DhβE did not. If there was an agonist binding site in the β2(+)/β2(+) interface, one would expect both ACh and DhβE to slow down the derivatisation of L146C. Available DhβE-bound crystal structures of *Lymnaean* AChBP (Shasavara et al., 2012), together with mutagenesis studies (Iturriaga-Vásquez et al., 2010), have established that DhβE and ACh contact the same conserved aromatic residues in the agonist sites in α4(+)/β2(-) interfaces. Additionally, although homology models of the $(\alpha4\beta2)_2\beta2$ receptor suggested conserved aromatic residues line a pocket in the β2(+)/β2(-) interface homologous to the canonical agonist sites in α4(+)/β2(-), individual or multiple alanine substitution of those residues did not perturb receptor function. Third, MTS-ET modification of the fifth subunit did not perturb the apparent affinity of the receptor for ACh but reduced the maximal ACh responses, indicating that MTSET-derivatisation removes a gating element only. If MTS-ET reduced the ACh responses by preventing agonist access to a binding site or changing the electrostatic environment of agonist contact points in the site, the ACh EC_{50} should be affected.

Despite being structurally equivalent, the agonist sites in the $(\alpha4\beta2)_2\beta2$ nAChR contribute asymmetrically to receptor function, as suggested by the differential effects of MTSET modification of individually cysteine substituted agonist sites in the presence and absence of ACh. These findings therefore add to the increasing body of evidence indicating that structurally equivalent agonist sites in heteromeric Cys-loop LGICs function asymmetrically (Baumann et al., 2003; Mazzaferro et al., 2011; Lucero et al., 2016). Functional asymmetry in structurally equivalent agonist sites likely results from the nature of the subunit flanking the agonist binding subunit pairs. Subunits flanking the agonist sites could alter the conformation of the sites through the action of modulatory sites (e.g., the benzodiazepine site on the α/γ interface of the $GABA_A\gamma$ receptors), additional agonist sites (e.g., the LS α4β2 nAChRs) or inter-subunit interactions, as suggested by the findings of previous studies (Lucero et al., 2016) and the findings reported in this Chapter. Significantly, the most recent structures of the *Torpedo* nAChR suggest that the outward movement of the β1 subunit, suggested to open the gate, is driven primarily by the agonist site on the α/γ interface (Unwin and Fujiyoshi, 2012). In this respect, the findings reported in this Chapter raise the question of whether the fifth subunit subunit is functionally coupled to the agonist sites and whether coupling is asymmetrical. These issues are examined in the next Chapter.

Chapter 4

Long-Range Coupling Between Agonist Sites and the β2(+)/β2(-) Interface

4.1 INTRODUCTION

When looking at alosteric mechanism of cys-loop receptor activation, attention has primarily focused on understanding the gating movements of the interfacial loops (β1-β2 loop, the Cys and M2-M3 linker), which form the primary allosteric pathway connecting the agonist sites to the ion channel gate (Xiu et al., 2005; Lee and Sine 2005; Lee et al., 2009; Grutter et al., 2005; Bouzat et al., 2008; Andersen et al., 2011), as reviewed by Bouzat (2012). However, studies of the TMD have suggested that other pathways not involved in the primary coupling path such as interactions between α helix M4 and membrane lipids and inter-helical interactions between M4 and M1 and M3 also modulate channel function (Carswell et al., 2015).

Structurally, gating involves a large re-organisation of the ion channel mediated by a global twisting and blooming of the whole ECD (Calimet et al., 2013, Cecchini and Changeux, 2015), which suggest that all subunits, thus interfaces, including non- agonist-binding ones may contribute to gating, directly or indirectly. Indeed, the most recent cryo-structures of *Torpedo* nAChR in closed and open conformations have suggested a key role for the fifth subunit subunit (β1) in gating (Unwin and Fujijoshi, 2012). In this respect, the findings described in the previous chapter are highly relevant. Does the effect of the fifth subunit on efficacy of ACh on the HS α4β2 nAChR represent an additional agonist-binding coupling pathway? And if this is the case, how is the agonist binding signal transmitted to the fifth subunit? This chapter examines possible functional links between the agonist sites and the fifth subunit by using subunit-targeted single point mutations and MTS-ET derivatisation of substituted cysteines.

4.2. RESULTS

The discovery that the fifth subunit has an effect on ACh maximal current responses in the presence of agonist suggests that binding of ACh to the canonical agonist binding sites may induce conformational changes in the fifth subunit that alters access to the substituted cysteine of β(+)/β(-)L146C. To initially probe any functional link between the fifth subunit and the agonist sites, double mutant concatemers were engineered to introduce the L146C on the fifth subunit alongside alanine substitutions of α4W182 on the agonist sites on α4(+)/β2(-)binding sites. As the α4W182A mutation is known to perturb agonist binding (Mazzaferro et al., 2011), the degree to which mutated agonist sites may affect MTS-ET modification of the cysteine substituted fifth subunit may provide insight into possible functional coupling between agonist sites and the fifth subunit.

4.2.1 - Alanine Substitution of Conserved Residues in α4(+)/β2(-) Interfaces

α4W182, one of the conserved aromatic residues contributing to the binding pocket in Cys loop receptors, establishes a direct cation-π interaction with the quaternary amine group of ACh in nAChRs (Zhong et al., 1998) and is responsible for the high-affinity of nicotine for α4β2 nAChRs (Xiu et al., 2009). It has also been implicated in the initiation of the gating isomerisation, rendering it a highly important feature of receptor function. Modification of this residue in the structurally identical binding sites can highlight any functional differences between the two regions.

Introduction of W182A into the agonist sites on the α4(+)/β2(-) interfaces

affected receptor sensitivity to activation by ACh and MTS-ET modification of the cysteine substituted fifth subunit, dependent on which site W182A was incorporated. When incorporated into agonist binding site 1 (i.e., β2_^{W182A}α4_β2_α4_β2), W182A caused a biphasic ACh sensitivity profile **(Figure 4.1, Table 7).** The higher sensitivity component comprises about half (55%) of the curve, and has an ACh EC_{50} (EC_{50}_1) similar to wild type **(Table 4.1)**. As previously published (Mazzaferro et al., 2011), biphasic agonist concentration response curves in concatenated α4β2 nAChRs represent the contribution of wild type agonist sites (high-sensitivity component) and mutant and wild type sites (low-sensitivity component).The low sensitivity component, with an EC_{50} (EC_{50}_2) tenfold higher than wild type **(Table 4.1)**, therefore reflects mostly the altered activity of the mutated binding site, as seen by the very uncharacteristically high gradient of the slope and corresponding nHill coefficient **(Table 4.1)**. In contrast, incorporation of W182A into agonist site 2 (i.e., β2_α4_β2_^{W182A}α4_β2) did not perturb the sensitivity to activation by ACh, compared to wild type **(Figure 4.1; Table 4.1).** When the α4W182A was introduced simultaneously on both agonist sites (i.e., β2_^{W182A}α4_β2_^{W182A}α4_β2), the concentration response curved was biphasic. As of these two substitutions one produces a shift from monophasic to a biphasic curve and the other does not appear to affect sensitivity, this is expected from the presence of the mutation on both sites (Mazzaferro et al., 2011). The potency of ACh decreased by 20-fold **(Figure 4.1, Table 4.1)** highlighting an allosteric connection between two binding interfaces. Taken together, the findings so far are in accord with previous findings that suggest that the agonist sites contribute asymmetrically to the function of α4β2 nAChRs (Mazzaferro et al., 2011; Lucero et al., 2016). Interestingly, the findings also suggest that agonist site 1 plays a dominant role in the function of HS α4β2 nAChRs.

The asymmetric effects of W182A may be residue-specific due to the key role that W182 plays in binding agonists in the α4β2 nAChR (Williams et al., 2009; Xiu et al., 2009) or may reflect overall functional differences between the sites. To examine these possibilities, further binding residues **(highlighted in Figure 3.2)** were alanine substituted and the functional consequences of the substitutions were examined using two-electrode voltage-clamping. α4Y126A from loop A produced biphasic ACh responses when introduced in agonist site 1 (Figure 4.1; Table 4.1). In contrast, when introduced in site 2, it produced monophasic ACh concentration response curves, albeit with increased EC_{50} **(Figure 4.1; Table 4.1)**. Y230A, from the loop C, did not yield functional expression when incorporated in agonist site 1, but in agonist site 2 produced biphasic ACh concentration response curves with increased ACh EC_{50} **(Figure 4.1; Table 4.1).** No functional expression was seen when β2W82A was introduced to either agonist site, implying high importance of this residue in receptor function. This finding is in agreement with previous studies that have shown that the W82 position does not tolerate structural changes, probably due to a role of this residue in gating (Williams et al., 2009). Overall, the findings suggest that the agonist sites bind the agonist in a site-specific manner, which is in accord with the findings of Mazzaferro et al., (2011) and Lucero et al. (2016).

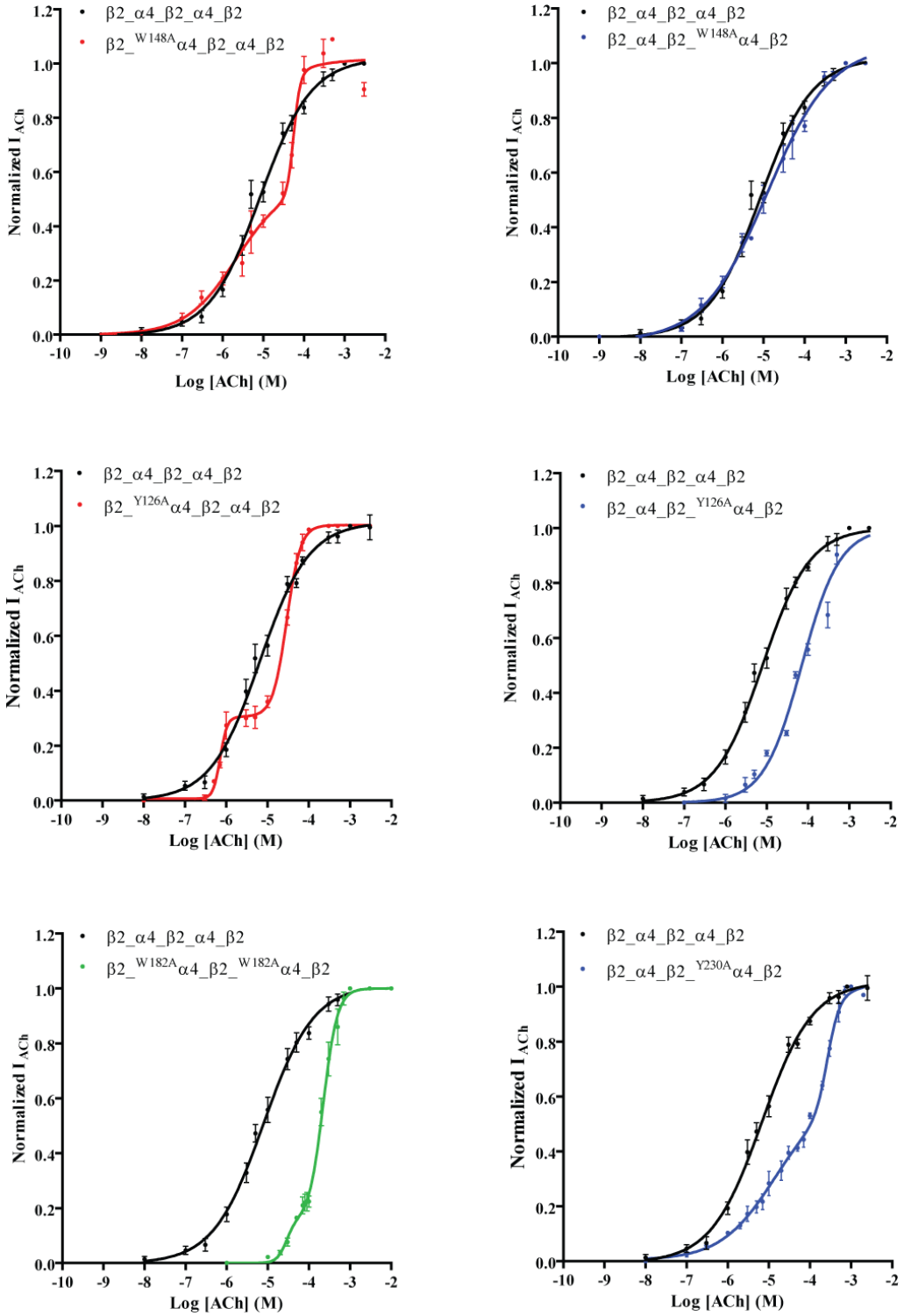

Figure. 4.1. Effect of alanine substitutions of conserved residues of binding pockets subunit on the ACh sensitivity of β2_α4_β2_α4_ β2 nAChR. ACh concentration response relationships were obtained, producing a range of mono and biphasic curves and altered ACh sensitivity. EC50 and Hill coefficient values are summarised in **Table 4.1**. In order to detect biphasic relationships, a wide range and many intermediate concentrations were utilised. Data was then fit by non-linear regression in Graph-Pad Prism 5, as outlined in Materials and Methods.

Concatemer	EC_{50}_1 (μM)	nHill_1	EC_{50}_2 (μM)	nHill_2	HFrac
β2_α4_β2_α4_β2	7.58 ± 2.6	0.74 ± 0.12	---	---	---
β2_^{W182A}α4_β2_α4_β2	2.2 ± 0.3	0.64 ± 0.21	62.0 ± 3.01	5.35 ± 1.1	0.55 ± 0.14
β2_α4_β2_^{W182A}α4_β2	11.5 ± 2.1	0.67 ± 0.018	---	---	---
β2_^{W182A}α4_β2_^{W182A}α4_β2	221 ± 19	3.2 ± 0.5	31.9 ± 8.1	5.14 ± 0.49	0.13 ± 0.07
β2_α4_β2_^{Y230A}α4_β2	14 ± 0.32	0.66 ± 0.17	270 ± 32.0	2.97 ± 0.89	0.58 ± 0.13
β2_^{Y126A}α4_β2_α4_β2	0.71 ± 0.03	4.06 ± 0.07	30.0 ± 0.04	2.30 ± 0.35	0.28 ± 0.03
β2_α4_β2_^{Y126A}α4_β2	86.8 ± 3.9***	0.72 ± 0.05	---	---	---

Table 4.1. Summary of ACh effects on wild type and β2_α4_β2_α4_ β2 nAChRs containg alanine substituted binding sites. Data was analysed with non-linear regression asare the mean ± SEM for at least 3 experiments. ACh EC_{50} values, Hill coefficients and where applicable high sensitivity fractions (HFrac) are reported. Where the data is monophasic only one of each is reported (EC_{50}_1 and nHill_1), whereas bi-phasic relationships are denoted by two of each parameter (EC_{50}_1 and nHill_1+ EC_{50}_2 nHill_2). Bi-phasic data is taken as significantly different to wild type. Significant differences of monophasic data in comparison to wild type are denoted by asterix (***,$p<0.0001$).

In these results, agonist binding sites of $(\alpha4\beta2)_2\beta2$ nAChRs are shown to be functionally diverse but alosterically linked. This raises questions of linkage between other interfaces - it is known that alosteric modulators can exert their effects via interaction at the β2(+)/α4(-), and it may be that the β2(+)/β2(-), modulates receptor activation in a similar manner. As subunit environment is suggested to underlie functional differences of binding sites, any functional linkage with the fith subunit of $(\alpha4\beta2)_2\beta2$ may give insight to this.

4.2.2 – Effects of W182A on MTS-ET Modification Of Cysteine Substituted Fifth Subunit

To probe effects of agonist sites on the fifth subunit, MTS-ET modification of the cysteine substituted fifth subunit was measured on β2_^{W182A}α4_β2_α4_β2^{L146C} and β2_α4_β2_^{W182A}α4_β2^{L146C} receptors.

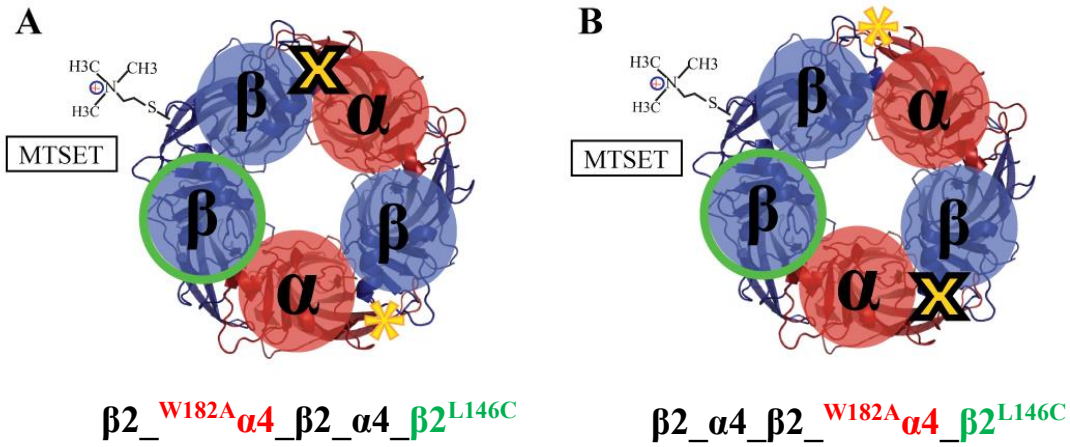

Figure 4.2. Schematic diagrams of $(\alpha4\beta2)_2\beta2$ demonstrating which α4(+)/β2(-) binding interface will be individually modified and blocked in each double mutant, highlighting differences in proximity to the β2(+)/β2(-) interface. Intact binding sites are shown by presence of yellow asterix, interfaces hosting the α4(+)W182 modification are shown by black and yellow X and molecular structure of MTSET is shown linked to β(+)/β(-) where it will be present following covalent modification of β(-)L146C here. **(A)** shows β2_^{W182A}α4_β2_α4_β2^{L146C} in which site 1 will be modified, **(B)** represents β2_α4_β2_^{W182A}α4_β2^{L146C} - in which site 2 hosts the alanine.

In the first instance, β2_^{W182A}α4_β2_α4_β2^{L146C} and β2_α4_β2_^{W182A}α4_β2^{L146C} ACh concentration responses were analysed against their non-cysteine substituted counterparts. β2_^{W182A}α4_β2_α4_β2^{L146C} ACh responses were biphasic, with a small non-significant reduction of the high sensitivity component, compared to β2_^{W182A}α4_β2_α4_β2 receptors, suggesting that incorporation of L146C does not significantly alter the function of β2_^{W182A}α4_β2_α4_β2 receptors **(Figure 4.2, Table 4.2)**. Incorporation of L146C into β2_α4_β2_^{W182A}α4_β2 did not alter the monophasic nature of the ACh concentration, although L146C significantly increased, ACh potency **(Figure 4.2, Table 4.2)**. This is particularly interesting considering that individually neither mutation has any effect on ACh responses. This suggests functional connections between binding sites and the fifth subunit.

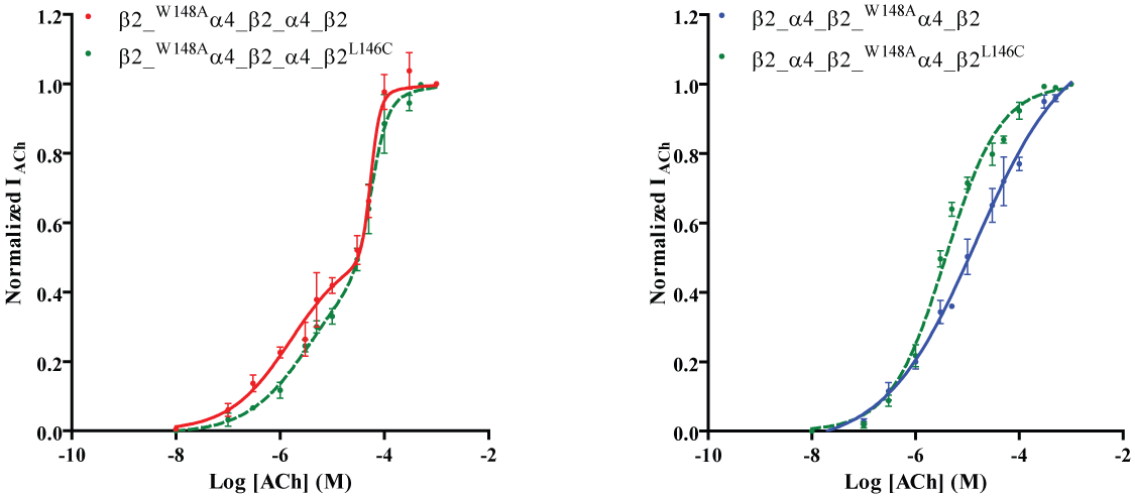

Figure 4.3. ACh concentration response relationships of concatemers in which binding impairment is introduced alongside cysteine substituted fifth subunit. Data are plotted alongside single point mutations of α4W182A in individual binding sites and changes of double substitution are seen. As can be seen in the case of β2_^{W182A}α4_β2_α4_β2^{L146C}this is only small, whereas the leftward shift of β2_α4_β2_^{W182A}α4_β2^{L146C} can be seen more prominently. This is reflected in data summarised in **Table 4.2** analysed by non-linear regression, as outlined in Chapter 2.

Concatemer	EC_{50}_1 (μM)	nHill_1	EC_{50}_2 (μM)	nHill_2	HFrac
$\beta2\_\alpha4\_\ \beta2\_\alpha4\_\ \beta2^{L146C}$	3.710 ± 0.8	0.93 ± 0.12	---	---	---
$\beta2\_^{W182A}\alpha4\_\ \beta2\_\alpha4\_\ \beta2^{L146C}$	320 ± 5.6	1.02 ± 0.21	76 ± 0.32	3.32 ± 1.18	0.50 ±0.09
$\beta2\_\alpha4\_\ \beta2\_^{W182A}\alpha4\_\ \beta2^{L146C}$	2.92 ± 0.62*, ++	0.69 ± 0.08	---	---	---
$\beta2\_\alpha4\_\ \beta2\_^{Y230A}\alpha4\_\ \beta2^{L146C}$	43.2 ± 8.15***	0.68 ± 0.07	---	---	---

Table 4.2. Summary of ACh concentration-response relationship parameters at concatenated HS $(\alpha4\beta2)_2\beta2$ nAChR containing the β(+)/β(-)^{L146C}and alanine substitutions of binding sites. Data was analysed with non-linear regression and are the mean ± SEM for at least 3 experiments. ACh EC_{50} values, Hill coefficients and where applicable high sensitivity fractions (HFrac) are reported. Where the data is monophasic only one of each is reported (EC_{50}_1 and nHill_1), whereas bi-phasic relationships are denoted by two of each parameter (EC_{50}_1 and nHill_1+ EC_{50}_2 nHill_2). Differences between monophasic and biphasic relationships of curves are concluded as a significant difference (such as in the case of β2_α4_ β2_^{Y230A}α4_ β2^{L146C} vs β2_α4_ β2_^{Y230A}α4_ β2). Statistical deviation from equivalent concatemer without L146C substitution is shown by ++,p=0.05 and Statistical differences from wild type are shown by asterix (*,p=0.03; ***,p<0.0001), as determined by student t-tests.

The accessibility of the cysteine substituted fifth subunit to the MTS-ET reagent was then determined in receptors with the mutated agonist site. As shown in **Table 4.3**, the accessibility of L146C did not change with incorporation of W182A into any of the two agonist sites or the presence of Y230A in site 2. Thus, when the cysteine substituted fifth subunit is derivatised by MTS-ET in the absence of ACh, the accessibility of the introduced cysteine is not perturbed.

Concatemer	Remaining I_{Ach} Post MTS-ET (%)
β2_α4_ β2_α4_ $\beta2^{L146C}$	41.1 ± 2.92
$\beta2_{}^{W182A}\alpha4$_ β2_α4_ $\beta2^{L146C}$	50.3 ± 2.34
β2_α4_ $\beta2_{}^{W182A}\alpha4$_ $\beta2^{L146C}$	38.3 ± 2.72
β2_α4_ $\beta2_{}^{Y230A}\alpha4$_ $\beta2^{L146C}$	40.1 ± 1.68

Table 4.3. Effects of maximal application of MTSET on β2_α4_ β2_α4_ β2 with L146C substitutions within the β(+)/β(-) interface and individual alanine substitutions of conserved binding residues in α(+)/β(-) interfaces. β2_α4_ β2_α4_ $\beta2^{L146C}$ data included to demonstrate additional binding site substitution does not alter maximum effect of MTSET application and modification of β(+)/β(-)^{L146C}. No significant difference is seen following ANOVA analysis with Dunnet's corrections.

4.2.2.1 - Rates of MTSET modification of β2_α4_β2_^{W182A}α4_$\beta2^{L146C}$ and β2_^{W182A}α4_β2_α4_$\beta2^{L146C}$.

To probe possible coupling of the agonist sites with the fifth subunit, the rate of reaction of MTS-ET with cysteine substituted fifth subunit on alanine substituted receptors was measured in the presence and absence of ACh. If the agonist sites couple functionally to the fifth subunit, the rate of reaction should be affected in the presence of ACh, i.e., when the binding site is engaged by the agonist. Thus, when α(+)/β(-) dependent receptor activation is modified by α(+)W182A, if the fifth subunit is coupled to the agonist sites, impairment of ACh binding to the sites by alanine substitution of α4(+)W182 should perturb coupling, altering the effects of bound agonist sites on MTSET derivatisation of L146C.

Incorporation of W182A in agonist site 2 did not affect the rate of modification of cysteine substituted fifth subunit in the presence of ACh **(Figure 4.4; Table 4.4)**. However, when incorporated in site 1, W182A markedly perturbed the rate of reaction. First, the presence of W182A decreased the rate of MTSET reaction with receptors in the closed state, in comparison to β2_α4_β2_α4_$\beta2^{L146C}$ receptors

(Figure 4.4; Table 4.4). In the presence of ACh the rate of reaction was accelerated **(Figure 4.4; Table 4.4)**. Although the mechanism of this cannot be elucidated via these experimental approaches, such outcomes provide very strong evidence of functional connections between agonist site 1 and the fifth subunit.

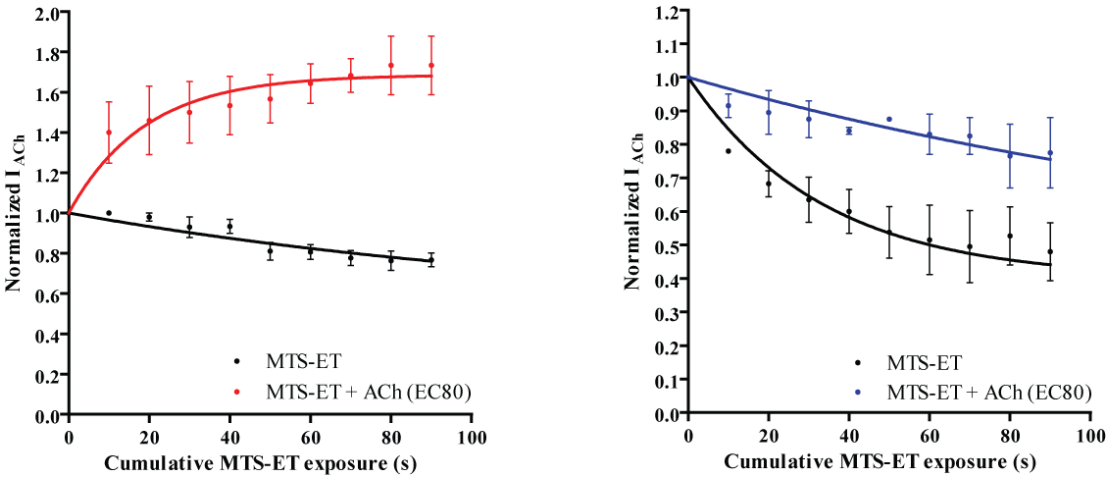

Figure 4.4. Rates of MTS-ET modification of β2_^{W182A}α4_β2_α4_β2^{L146C} and β2_α4_β2_^{W182A}α4_β2^{L146C} nAChRs. Experiments were carried out with MTS-ET in the absence (black) and presence (red and blue) of EC_{80} concentrations of ACh. Data were fit to a single-phase exponential decay as described in Materials and Methods.

	k_1 Values		k_2 Values	
Concatemer	**MTSET (control)**	**MTSET + ACh**	**MTSET (control)**	**MTSET + ACh**
β2_α4_ β2_α4_ β2^{L146C}	0.019 ± 0.002	0.005 ± 0.001	1864 ± 263	475.0 ± 131^{++}
β2_^{W182A}α4_ β2_α4_ β2^{L146C}	0.009 ± 0.001	0.029 ± 0.007	883 ± 139*	2860 ± 682**,$^{+}$
β2_α4_ β2_^{W182A}α4_ β2^{L146C}	0.021 ± 0.003	0.006 ± 0.001	2110 ± 303	593 ± 117^{++}
β2_α4_ β2_^{Y230A}α4_ β2^{L146C}	0.016 ± 0.003	0.007 ± 0.001	1604 ± 317	690 ± 101^{+}

Table 4.4. First and second order rates of MTS-ET modification of β(+)/β2(-)^{L146C} when substitutions of binding residues to alanine are present in HS α4β2nAChR concatemers. The only concatemer exhibiting differences to β2_α4_ β2_α4_ β2^{L146C} was β2_^{W182A}α4_ β2_α4_ β2^{L146C}, statistical differences shown by asterix (*,p = 0.02' **,p = 0.007). In all concatemers a significant difference was seen between conditions (+,p = 0.02; ++, p<0.005)

As introducing W182 to agonist site 2 did not affect MTS-ET-modification of the fifth subunit, the rate of modification of the fifth subunit was measured on β2_α4_β2_^{Y230}Aα4_β2^{L146C} receptors. Unlike W182A, introducing Y230A to agonist site 2 affected receptor function, as reflected by sensitivity to activation by ACh. As shown in **Figure 4.5 (Table 4.3)**, β2_α4_β2_^{Y230A}α4_β2^{L146C} receptors display monophasic ACh concentration response curves. When compared to the biphasic CRC of β2_α4_β2_^{Y230A}α4_β2 receptors, this suggests functional links between agonist site and the fifth subunit. However, the rate of MTS-ET reaction with the cysteine substituted fifth subunit is not significantly altered in the presence of ACh (**Figure 4.5; Table 4.4).** The findings also show no significant differences between the rate of reaction in the absence of ACh measured for β2_α4_β2_α4_β2^{L146C} and β2_α4_β2_^{Y230A}α4_β2^{L146C} receptors **(Figure 4.5; Table 4.4)**.

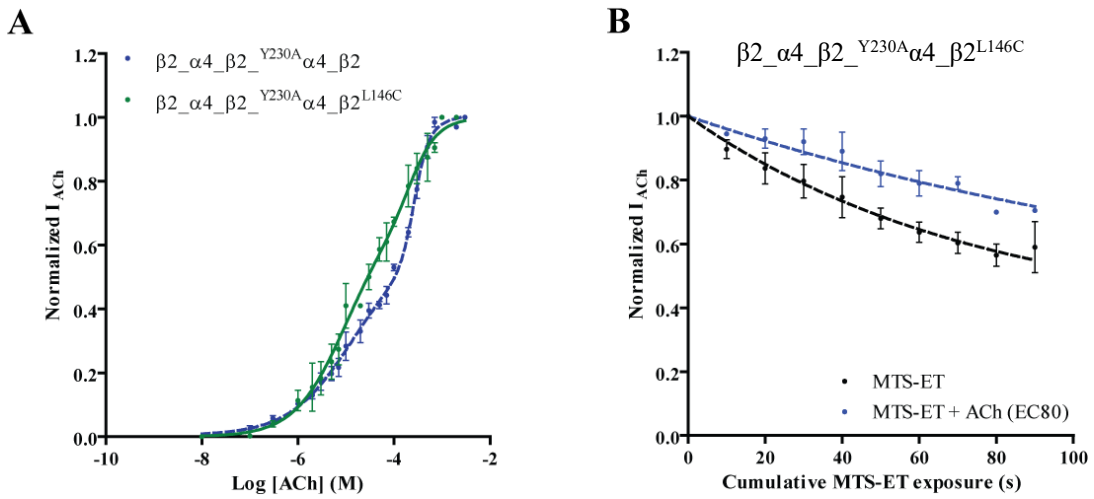

Figure 4.5.. Studies performed with β2_α4_β2_^{Y230A}α4_β2^{L146C} in order to investigate functional connection between agonist site 2 and the fifth subunit of (α4β2)$_2$β2 nAChRs. (A) ACh Concentration response curves of bi-phasic β2_α4_β2_^{Y230A}α4_β2 and monophasic β2_α4_β2_^{Y230A}α4_β2^{L146C}. Data fit with non-linear regression as outlined in Chapter 2. **(B)** One phase decay fit data of rates of β2_α4_β2_^{Y230A}α4_β2^{L146C} with MTSET in the presence and absence of ACh. It can be seen here that presence of α4Y230A at ABS2 does not modify the effect of MTSET at β(+)/β(-)^{L146C} or its rate of reaction with this cysteine in either condition.

4.2.3 - The β2(+)/β2(-) interface is central to functional coupling of agonist ABS 1 and the 5th subunit of (α4β2)$_2$β2 nAChRs

The findings so far suggest that agonist site 1, but not 2, functionally links to te fifth subunit in the presence of ACh, when the site is occupied by the agonist. This possibility implies a linking path between the agonist site and the fifth subunit. In order to identify potential contributors to the pathway, the homology model of the HS α4β2 receptor was examined. As shown in **Figure 4.6**, the (+) side of the β2 subunit contributing the complementary side of agonist site 1 interfaces with the fifth subunit. As leucine and tryptophan are hydrophobic residues, W176 and L146 could engage in hydrophobic interactions, which could in turn underlie the changes in the rate of L146C modification in the presence of ACh.

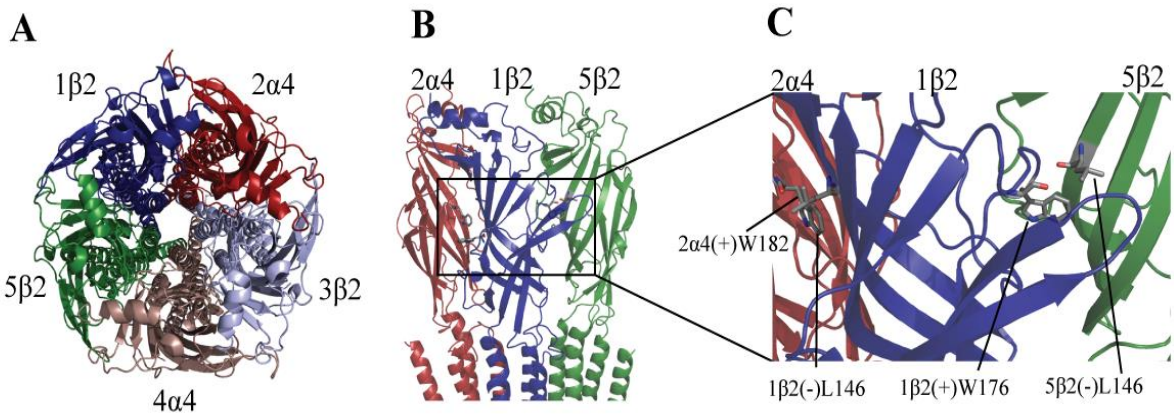

Figure 4.6. Homology model of $(\alpha4\beta2)_2\beta2$ nAChR highlighting 1β2 and flanking 5β2 and 2α4 subunits. (A) Areal view of pentamer with three subunits of the ABS1 and β(+)/β(-) interfaces highlighted in red (2α4), blue (1β2) and green (5β2). (B) Side view of $(\alpha4\beta2)_2\beta2$ showing these three subunits only. 2α4(+)W182, 1β2(+)W176C and 5β2(-)L146C are shown as grey sticks. (C) Close up of interfaces within this triad of subunits, showing 2α4(+)W182, 1β2(+)W176C and 5β2(-)L146C as grey sticks.

To probe functional coupling between β2(+)W176 and β2(-)L146 in the β2(+)/β2(-) interface, W176A was introduced in the first subunit of β2_α4_β2_α4_$\beta2^{L146C}$ to engineer ^{W176A}β2_α4_β2_α4_$\beta2^{L146C}$ receptors. If interactions between W176 and L146 are part of a coupling pathway between agonist site 1 and the fifth subunit, the rate of reaction of ^{W176A}β2_α4_β2_α4_$\beta2^{L146C}$ in the presence of ACh should be comparable to that measured in the absence of the agonist, or at least differ to β2_α4_β2_α4_$\beta2^{L146C}$. The same effect should also be seen for ^{W176C}β2_α4_β2_α4_$\beta2^{L146A}$ receptors. Furthermore, the effects of MTS-ET in the absence or presence of ACh on ^{W176C}β2_α4_β2_α4_β2 receptors should be comparable to those on β2_α4_β2_α4_$\beta2^{L146C}$ receptors.

All three receptors displayed no alterations to ACh sensitivity **(Table 4.5)**, indicating that HS α4β2 nAChRs tolerate well the presence of W175A on its own or together with L146C and this putative interaction does not have implications in agonist potency.

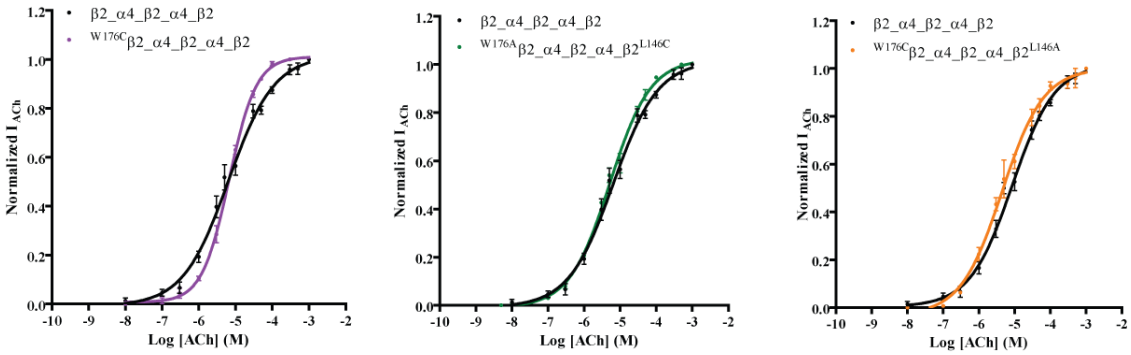

Figure 4.7. Concentration response relationships of β2_α4_β2_α4_β2 hotsting cysteine and alanine substitutions in the putatively functionally connected β2(+)W175 and β2(-)L146 residues of the β2(+)/β2(-) interface. Data were fit using non-linear regression as outlined in Chapter 2 – no changes to wild type were observed.

Concatemer	EC50 (μM)	nHill	Remaining I_{Ach} Post MTS-ET (%)
β2_α4_ β2_α4_ β2^{L146C}	3.71 ± 0.80	0.93 ± 0.12	41.1 ± 2.92
^{W176C}β2_α4_ β2_α4_ β2	6.74 ± 0.56	1.18 ± 0.06	45.7 ± 2.67
^{W176A}β2_α4_ β2_α4_ β2^{L146C}	5.40 ± 0.66	0.78 ± 0.04	52.3 ± 2.6
^{W176C}β2_α4_ β2_α4_ β2^{L146A}	4.64 ± 0.83	0.84 ± 0.05	55.7 ± 2.5

Table 4.5. ACh sensitivity parameters and maximal effect of MTSET on ACh activation of β2_α4_β2_α4_β2 hotsting cysteine and alanine substitutions in the putatively functionally connected β2(+)W175 and β2(-)L146 residues of the β2(+)/β2(-) interface. No significant change in sensitivity is seen in these mutants compared to wild type or β2_α4_ β2_α4_ $β2^{L146C}$ and although small and similar change seen in maximal MTSET effects of ^{W175A}β2_α4_β2_α4_$β2^{L146C}$ and ^{W175C}β2_α4_β2_α4_$β2^{L146A}$, this is not significant.

ACh EC_{80} current responses of ^{W176A}β2_α4_β2_α4_β2^{L146C} receptors were inhibited by 1 mM MTSET, showing that accessibility of L146C to MTSET was not perturbed compared to β2_α4_β2_α4_β2^{L146C} receptors **(Table 4.5)**. In contrast, the rate of MTSET modification in ^{W176A}β2_α4_β2_α4_β2^{L146C} was six-fold slower than in β2_α4_β2_α4_β2^{L146C} receptors, a significant difference expected to occur if W176 and L146 were functionally coupled in the β2(+)/β2(-) interface **(Figure 4.8; Table 4.6)**. As shown in **Figure 4.8** and **Table 4.6,** the rate of MTSET modification of ^{W176C}β2_α4_β2_α4_β2 receptors in the presence or absence of ACh was no different from that measured for β2_α4_β2_α4_β2^{L146C}, showing a similar effect regardless of which of these two residues is mutated to cysteine. Furthermore, when L146A was introduced in the fifth subunit of ^{W176C}β2_α4_β2_α4_β2 receptors, the rate of MTSET reaction was comparable to that measured in ^{W176A}β2_α4_β2_α4_β2^{L146C} receptors **(Table 4.6),** and in the presence of ACh modification by MTSET was almost abolished, as it was observed for ^{W176A}β2_α4_β2_α4_β2^{L146C} receptors **(Table 4.6).**

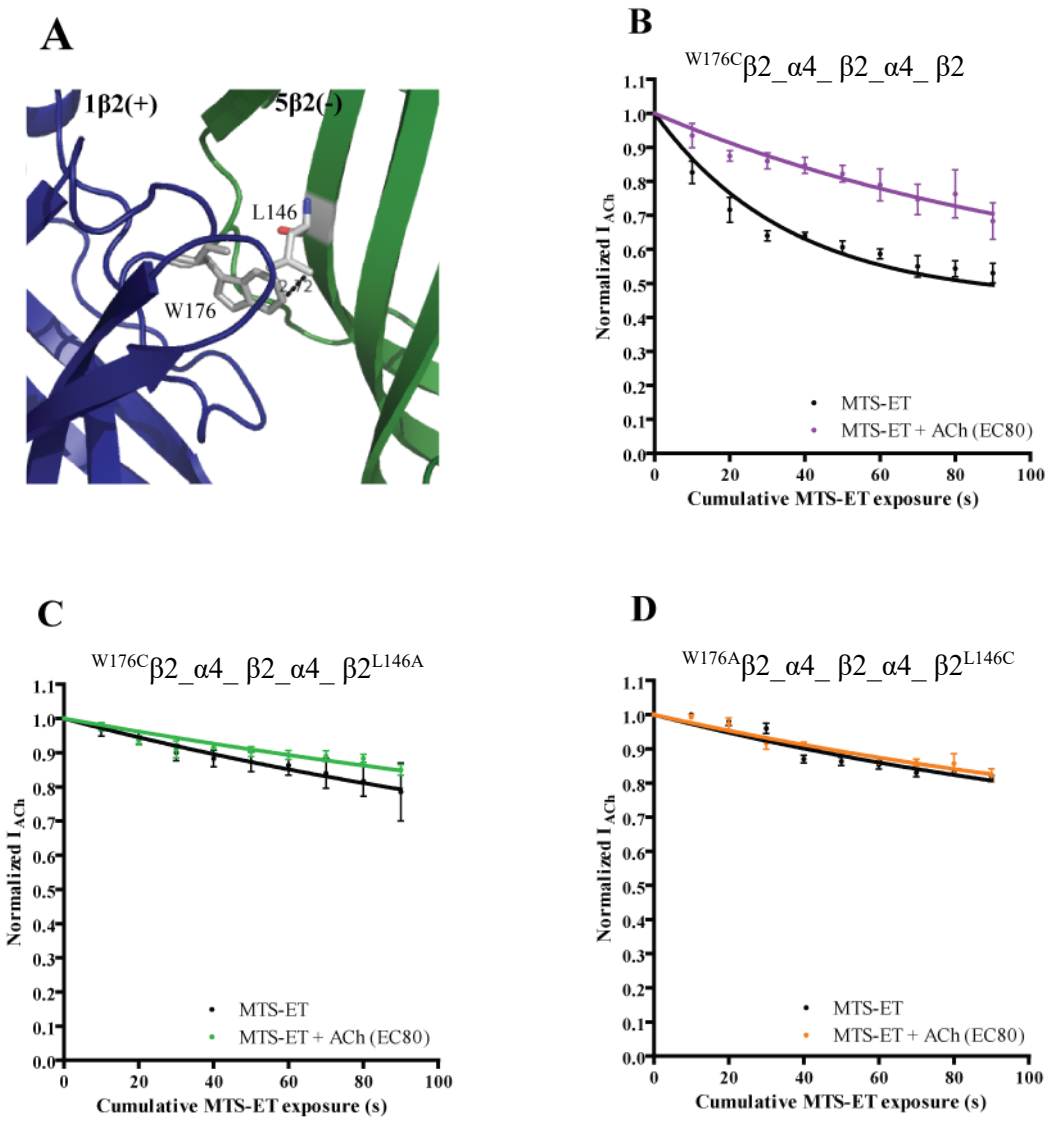

Figure 4.8. Rates of MTSET modification of residues of β2(+)/β2(-) of HS α4β2 nAChR showing functional link between two subunits. (A) Homology model of β2(+)/β2(-) interface showing residues with putative functional interaction sa grey sticks. **(B)** One phase decay plots of MTSET modification of α4β2 nAChR concatemers with residue β2(+)W176 (proposed to interact with β2(-)L146 at β2(+)/β2(-) interface) in the presence and absence of EC_{80} ACh and **(C-D)** plots when one functional group of putatively interacting pair is removed by substitution to alanine.

	k_1 Values		k_2 Values	
Concatemer	**MTSET (control)**	**MTSET +ACh**	**MTSET (control)**	**MTSET +ACh**
β2_α4_ β2_α4_ β2^{L146C}	0.018 ± 0.002	0.005 ± 0.001^{++}	1864 ± 236	475 ± 131 $^{++}$
^{W175C}β2_α4_ β2_α4_ β2	0.028 ± 0.006	0.007 ± 0.0007 $^{++}$	2850 ± 368.0	690.2 ± 77.1 $^{++}$
^{W175A}β2_α4_ β2_α4_ β2^{L146C}	0.006 ± 0.0004***	0.003 ± 0.0005	591.1 ± 42.6 ***	330.2 ± 46.4
^{W175C}β2_α4_ β2_α4_ β2^{L146A}	0.006 ± 0.0004 ***	0.005 ± 0.0006	623.3 ± 40.9 ***	547.5 ± 68.6

Table 4.6. Rates of MTS-ET reactions in HS α4β2 nAChR with cysteine substitution of putatively coupled residues of β2(+)/β2(-) interface. The rate of reaction of the substituted cysteines were measured in the presence and absence of ACh, as described in detail in Materials and Methods. The data points represent the mean ± SEM of at least three experiments carried out on different batches of oocytes. The data were fit to a one-exponential decay equation using GraphPad software 5, as described in Materials and Methods. First and second order rates were then calculated as described in Materials and Methods and values analysed by ANOVA with Bonferroni post corrections. Statistical differences between conditions within receptor shown as ++, $p<0.005$. Compariston of receptors to their non-alanine substituted counterparts within the same conditions shown by ***, $p<0.0001$.

4.3 DISCUSSION

The findings presented in this Chapter strongly suggest that agonist site 1 and the fifth subunit in HS α4β2 nAChRs functionally couple to impact receptor activation. This is the first time that long-range coupling between an agonist site and the fifth subunit has been described. Significantly, recent cryo-structures of *Torpedo* nAChRs suggest that agonist binding induces asymmetric motions of the different subunits, which are transmitted primarily to the channel gate through the β subunit (Unwin and Fujiyoshi, 2012). Additionally, recent structures of the human Glycine receptor bound to glycine have confirmed that interactions between the β1-β2 loop and the Cys loop of the principal subunit, together with the β8-β9 and pre-M1/M1 of the complementary subunit, interact with the M2-M3 loop of the principal subunit (Du et al., 2015) to gate the ion channel. These interactions have been suggested by previous structural studies (Unwin, 2005) and by extensive mutagenesis and functional studies (Andersen et al., 2011; Bouzat et al., 2004; 2008; Grutter et al., 2005;Jha et al., 2007; Lee et al., 2009; Lee and Sine, 2005).

If interactions of primary and complementary subunits in the ECD/TMD interface are critical gating elements, what may be the role of functional coupling between the fifth subunit and agonist site 1? On the basis of the impact of the fifth subunit on macroscopic maximal ACh currents, it may be that gating signals transmitted through interactions between the agonist sites and fifth subunit subunit are needed for maximally efficacious gating. In the case of the LS α4β2 receptor maximal gating is achieved through the contribution of the additional agonist site at the α4/α4 interface (Harpsoe et al., 2011; Mazzaferro et al., 2011). However, in

comparison to the LS α4β2 nAChR, the gating interactions that occur within the β2(+)/β2(-) interface do not include agonist binding.

The overall outcome of the studies presented here suggests that agonist site 1 has a stronger connection to the fifth subunit than agonist site 2. Since the two agonist sites responded differently to single-point alanine mutations and to MTSET derivatisation, it is clear that the agonist sites are functionally different. Thus, the findings are in accord with the findings of Mazaferro et al (2011) and Lucero et al. (2016) that have previously shown functional differences between the agonist sites housed by the α(+)/β(-) interfaces. Although the binding sites are structurally equivalent, subtle differences in the conformation, hydrophobicity or electrostatic environment brought about by different flanking subunits may differentiate them. The fifth subunit is different in the alternate forms of the α4β2 nAChR, which in turn differentiate the canonical agonist sites. It is interesting that in the HS α4β2 nAChR, it is coupling to agonist site 1 that has a greater impact on receptor activation. This could be because agonist site 1 probably communicates with the fifth subunit via the interface that the fifth subunit establishes with the complementary subunit of agonist site 1. It is widely recognised that the complementary subunit is an important efficacy element in the Cys loop receptors (Nys et al., 2013).

The interaction of the fifth subunit with agonist site 1 resembles that of the γ2 subunit of the benzodiazepine binding site with the complementary subunit (an α1 subunit) of an agonist binding site of benzodiazepine-sensitive GABA-A receptors. In this receptor type, binding of benzodiazepines to the α(+)/γ(-) interface potentiates the agonist responses of the receptor (Prichett et al., 1989; Smith and Olsen, 1995)

and, critically, induces structural re-arrangements of the adjacent GABA binding site (Kloda and Czajkowski, 2007). The binding sites are located at β(+)/α(-) interfaces (the β subunit is the principal subunit in the GABA-A) and, the γ2 subunit, besides contributing key determinants for benzodiazepine binding (for review, see Sigel, 2002), is the fifth subunit. Thus, coupling of agonist sites to the fifth subunit appears to be conserved among the Cys loop receptors.

Regardless of the asymmetrical coupling to the fifth subunit, the agonist sites are functionally different. They respond differently to single-point mutations, substituted cysteines show different degrees of accessibility to MTS-ET derivatisation in the presence or absence of ACh. These findings suggest important structural differences, yet it is difficult to visualise the underlying structural mechanisms that sustain the observed functional differences. Could interactions between the (+) side of the complementary subunit of agonist site 1 and the (-) side of the fifth subunit be sufficient to account for the differences between the agonist sites? Work published by Lucero et al. (2016) supports such possibility. These authors found that the E loop, in agonist binding and non-agonist binding, impacted receptor signature properties, which is in accord with the view presented in this Chapter that interactions between the agonist sites and the fifth subunit differentiate the agonist sites. It is interesting that in the muscle nAChR, the most recently evolved nAChR (Ortells and Lunt, 1995), the agonist sites are different due to the complementary subunit being different (ε/γ and δ).

In summary, the findings of this chapter strongly suggest coupling of agonist site 1 to the fifth subunit subunit and that this coupling increases the efficacy of agonist-driven gating. Does this mechanism underlie the super-agonism of compounds such as TC-2559 on HS α4β2 nAChRs? Chapter 4 examines this possibility using the same experimental strategies used in this Chapter and Chapter 3.

Chapter 5

Does the β2(+)/β2(-) Interface Account for TC-2559 Super-Agonism at HS α4β2 nAChRs?

5.1 INTRODUCTION

The nicotinic agonist TC-2559 exhibits strikingly different efficacy at the HS and LS α4β2 nAChRs. At the LS α4β2 nAChR, it acts as a partial agonist (Moroni et al., 2006; Carbone et al., 2009), which is accounted for by the inability of this compound to enter the agonist site at the α4/α4 interface of the LS receptor (Mazzaferro et al., 2014). In the case of the high sensitivity α4β2 receptor, TC-2559 displays 4-fold greater efficacy than ACh, thus behaving as a super-agonist. Since HS α4β2 nAChRs possess agonist sites only at the α4(+)/β2(-) interfaces, it is reasonable to suggest that the super-agonism of TC-2559 on HS α4β2 nAChRs may be encoded, at least partly, by structural elements in fifth subunit and the β2(+)/β2(-) interface it establishes with the β2 subunit of agonist site 1.

Agonist efficacy and the structural and molecular mechanisms that modulate it are a central preoccupation in the field of Cys loop receptor pharmacology. Seven years ago, a breakthrough on the understanding of the molecular mechanisms underlying agonist efficacy was made using kinetic analysis of microscopic currents. This showed that partial agonist and agonist open the gates similarly but what differentiates them is the ability to transit to closed states immediately preceding the open state (Lape et al., 2009). Intermediary closed states have been observed in glycine receptors using cysteine cross-bridging but it is not clear whether these states precede gating or represent desensitised states (Prevost et al., 2013). Despite these insights, the structural determinants of agonist efficacy remain unknown. As expected from the critical role of the primary component of the agonist site in agonist binding and gating, electrophysiological studies suggest the principal side of

agonist sites as a key determinant of efficacy (Chavez-Noriega et al., 1997; Mukhtasimova et al., 2009). Consistently with this view, crystal structures of AChBP in complex with ligands have shown that partial agonists, but not full agonists, induce incomplete capping of loop C around the agonist site, which may decrease gating efficacy (Hibbs and Gouaux, 2011; Brams et al., 2011; Kletke et; al., 2013). However, although an attractive possibility in its simplicity, the degree of loop C contraction is not an accurate predictor of agonist efficacy as some partial agonists cause full capping of loop C (Hibbs and Gouaux, 2011) and competitive antagonists such as DhβE induce agonist-like capping of loop C (Shasavara et al., 2012). Studies of AChBP crystal structures in complex with partial agonists of nAChRs have noted that partial agonist, but not full agonists, establish water-mediated hydrogen-bonds between their hydrogen-bond acceptor moiety and the backbone atoms of hydrophobic residues on the complementary face, which could lead to reduced gating efficacy (Hibbs and Gouaux, 2011; Rohde et al., 2012). Significantly, studies of the interactions between agonists and α4β2 nAChRs by unnatural amino acid mutagenesis have shown hydrogen-bonds between the complementary face and the H-bond acceptor moieties of agonists, although not necessarily mediated by a water molecule (Harpsoe et al., 2012; Tavarez et al, 2012).

Given the discovery that the fifth subunit, through functional coupling with agonist sites, modulates ACh efficacy, it may be that TC-2559 efficacy on HS α4β2 nAChRs can be accounted for by coupling between the agonist sites and the fifth subunit. In this Chapter, using SCAM, mutagenesis and two-electrode voltage-clamping, the contribution of the fifth subunit to TC-2559 efficacy was examined

5.2 RESULTS

5.2.1 - Chimeric Fifth Subunit Effects on Macroscopic Efficacy

In order to determine whether the fifth subunit encodes efficacy elements for TC-2559, the chimeric receptors described in Chapter 3 were assayed for their sensitivity and maximal response to this compound. These receptors were characterised by analysis of TC-2559 concentration response relationships normalised to maximal (1 mM) ACh. These assays revealed that β2_α4_β2_α4_α4/β2 receptors behaved as LS (α4β2)2α4 nAChR, in respect of sensitivity to TC-2559 (**Figure 5.1; Table 5.1**). In contrast, β2_α4_β2_α4_β2/α4 receptors responded to TC-2559 in a fashion that was comparable to that of wild type HS receptors (**Figure 5.1; Table 5.1**). These findings suggest the N-terminal domain of the fifth subunit in HS α4β2 receptors as a key determinant of TC-2559 efficacy, as it is for ACh.

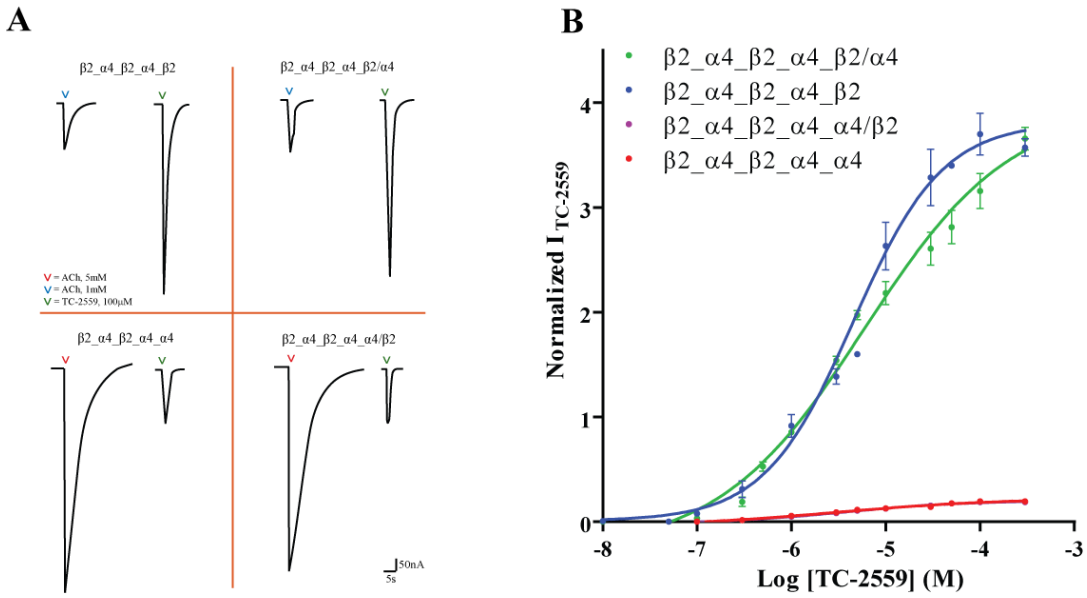

Figure 5.1. Effects of TC-2559 on wild type and chimeric concatenated α4β2 nAChRs. **(A)** Representative traces of the current responses elicited by TC-2559 on wild type and chimeric α4β2 nAChRs. Chimeric receptors were engineered as described in Materials and Methods. **(B)** Concentration responses curves for the effects of TC-2559 on wild type and chimeric receptors. The concentration response curves were fit to the Hill equation using non-linear regression, as described in materials and Methods. EC50 values, nHill coefficient and relative maximal responses of TC-2559 are shown in **Table 5.1**.

Receptor	EC_{50} (μM)	nHill	Imax TC2559/Imax ACh
β2_α4_β2_ α4_β2	1.84 ± 0.1	0.86 ± 0.19	3.81 ± 0.39
β2_α4_β2_ α4_β2/α4	2.74 ± 0.44	0.65 ± 0.07	3.43 ± 0.03
β2_α4_β2_ α4_α4	5.67 ± 1.95	0.64 ± 0.07	0.23 ± 0.01***
β2_α4_β2_ α4_ α4/β2	4.85 ± 1.43	0.73 ± 0.15	0.21 ± 0.03***

Table 5.1. Effects of TC-2559 on wild type and chimeric concatenated α4β2 nAChRs. Data are the mean ± SEM from at least 4 independent experiments from at least two different batches of oocytes. Concentration response data were analysed by non-linear regression, as described in Materials and Methods. Statistical differences between wild type HS α4β2 nAChR and LS and chimeric receptors were determined by One-way Anova with Bonferoni post-test. ***, $p < 0.0001$.

5.2.2 - MTS-ET modification of the β2(+)/β2(-) Interface Affects TC-2559 Efficacy

To assess whether the fifth subunit contributes to the efficacy of TC-2559 in a manner comparable to its contribution to ACh efficacy, the rate of MTS-ET derivatisation of β2_α4_β2_α4_$β2^{L146C}$ concatemeric receptors was measured in the presence or absence of TC-2559. Prior to the rate measurements, the concentration effects of TC-2559 on β2_α4_β2_α4_$β2^{L146C}$ were determined. For comparative purposes, the concentration effects of TC-2559 on individually cysteine substituted receptors (i.e., $β2^{L146C}$_α4_β2_α4_β2 and β2_α4_$β2^{L146C}$_α4_β2) were also determined. Comparison of concentration response curves for TC-2559 on the three mutant receptors showed interesting differences. First, TC-2559 EC_{50} was decreased only when the L1456C mutations was introduced into agonist site 1 and 2, in accord with these two regions contributing to TC-2559 binding. **(Figure 5.2; Table 5.2).** Efficacy decreased significantly when L146C was in the fifth subunit or in the complementary side of site 1 **(Figure 5.2; Table 5.2)** and the decrease was comparable (approx.1.8-fold) **(Table 5.2).** In contrast, cysteine substituted agonist site 2 (i.e., β2_α4_$β2^{L146C}$_α4_β2 receptors) had no impact on TC-2559 efficacy **(Figure 5.2, Table 5.2).** These findings further confirm both the importance of the fifth subunit as an element of agonist efficacy and the asymmetric contribution to receptor gating of the agonist sites in HS α4β2 nAChRs.

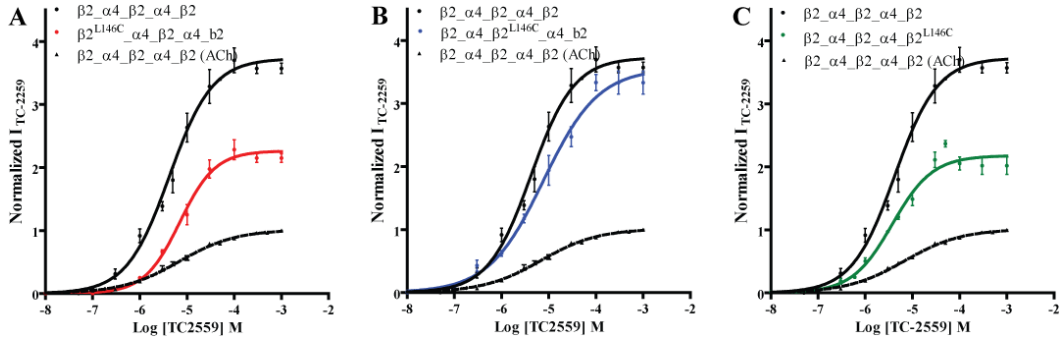

Figure 5.2. Concentration response curves for TC-2559 on β2(-)L146C substituted HS α4β2 nAChRs. L146C was substituted individually on agonist sites and the β2(+)/β2(-) interface and the consequences of the substitution on TC-2559 EC50 and relative efficacy were determined, as described in Materials and Methods. Concentration response curves were obtained by non-linear regression analysis, as described in Materials and Methods. Parameters estimated from the curve are shown in Table 5.2. β2_α4_β2_α4_β2^{L146C}.

Receptor	EC_{50} (μM)	nHill	Imax TC2559/Imax ACh
β2_α4_β2_ α4_β2	1.84 ± 0.1	0.86 ± 0.19	3.81 ± 0.39
β2_α4_β2_ α4_β2^{L146C}	4.11 ±0.49	0.94 ± 0.21	2.19 ± 0.21***
β2 ^{L146C}_α4_β2_ α4_ β2	9.80 ± 1.86**	0.96 ± 0.12	2.63 ± 0.26 ** ++
β2_α4_β2 ^{L146C}_ α4_ β2	7.17 ± 1.21**	0.71 ± 0.11	3.73 ± 0.21

Table 5.2. Concentration-response effects of TC-2559 on β2(-)L146C substituted concatenated HS α2β2 nAChRs. Current responses elicited by a range of concentrations of TC-2559 were normalised to ACh EC_{100} (1 mM). Concentration-response data were fit with non-linear regression, as described in Materialas and Methods. Statistical differences between mutant and wild type receptors are shown by asterisks: **, $p < 0.001$; ***, $p < 0.0001$ (One-way Anova tests with Dunnett's post-test). Statistical differences between binding sites are shown by +: $^{++}$, $p < 0.001$ (One-way Anova tests with Dunnett's post-test).

5.2.2.1 - Maximal effects of MTS-ET modification of β2L146C on TC-2559 efficacy

As expected, maximal modification of the cysteine substituted receptors following responses to TC-2559 was comparable to the pattern observed when ACh was used to monitor the accessibility of the substituted cysteines. Thus, agonist site 1 (i.e., $\beta2^{L146C}$_α4_β2_α4_β2) showed the largest reduction in TC-2559 induced activation following MTSET modification (64%), followed by site 2 (58%) and the fifth subunit (57%), although these differences were not statistically different **(Table 5.3)**.

Concatemer	$I_{TC-2559}$ after MTS-ET Exposure (%)
β2_α4_β2_ α4_β2	0.88 ± 0.07
β2_α4_β2_ α4_β2^{L146C}	0.43 ± 0.07**
β2^{L146C}_α4_β2_ α4_ β2	0.36 ± 0.06**
β2_α4_β2^{L146C}_ α4_ β2	0.42 ± 0.06**

Table 5.3. Cysteine accessibility in β2(-)L146C substituted concatenated HS α4β2 nAChRs. Ooocytes expressing mutant or cysteine substituted concatenated HS α4β2 nAChRs were exposed to EC_{80} TC-2559 prior and after a 2 min application of 1 mM MTSET. The percentage change in the responses elicited by TC-2559 ACh after MTSET treatment was defined as $((I_{afterMTSET}/I_{initial}) -1) \times 100]$. Data are the mean ± SEM of at least three independent experiments. Significant differences between mutant and wild type receptors (noted by asterisks) were estimated using One-way ANOVA with Dunnett's post-test. **, $p < 0.001$

5.2.2.2 - Rates of MTS-ET modification of cysteine substituted fifth subunit

To assess whether TC-2559 activation of HS α4β2 nAChRs protected cysteine substituted fifth subunit from modification by MTS-ET, the rate of modification of β2_α4_β2_α4_$\beta2^{L146C}$ receptors in the presence or absence of TC-2559 was measured. As expected, TC-2559 decreased the rate of reaction (k_1 in the absence of TC-2559: 0.025 ±0.005 s^{-1} *vs* k_1 in the presence of TC-2559, 0.012 ± 0.002 s^{-1}). However, comparison of the rate constants measured in the presence of ACh or TC-2559 showed that ACh was approximately 2-fold more efficacious than TC-2559 at protecting the substituted fifth subunit from MTS-ET modification **(Figure 5.3**, **Table 5.4)**. If the fifth subunit were solely responsible for TC-2559 super-agonism, the decrease in the rate of MTS-ET reaction in the presence of TC-2559 should have been greater than in the presence of ACh. This also suggests that movements of the 5^{th} β2 are agonist specific.

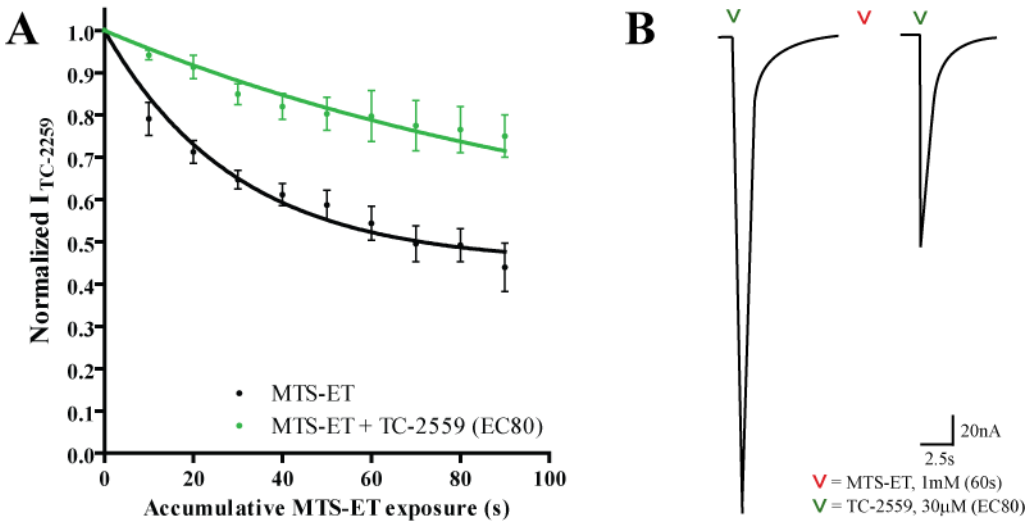

Figure 5.3. MTSET studies of TC-2259 activation of β2_α4_β2_α4_β2^{L146C}. (A) Rate of modification of β2_α4_β2_α4_β2^{L146C} by MTS-ET. The rate of reaction of MTS-ET with β2_α4_β2_α4_β2^{L146C} was measured in the presence and absence of EC80 TC-2559. The rate data were fit to a single exponential equation, as detailed on Materials and Methods. Each data point represents the mean ± SEM of three-four independent experiments. Estimated rate constants are shown in **Table 5.4**. **(B)** Representitive traces of maximal TC-2559 responses of β2_α4_β2_α4_β2^{L146C} before and after MTSET exposure.

	k_1 Values		**k_2 Values**	
Agonist	**MTSET (control)**	**MTSET + ACh**	**MTSET (control)**	**MTSET + ACh**
ACh	0.018 ± 0.002	0.005 ± 0.001 **,^	1864 ± 236^	474.8 ± 130**,^
TC-2559	0.026 ± 0.002	0.012 ± 0.002 ***,^	2600 ± 191^	1150 ± 202***,^

Table 5.4. Rates of MTS-ET reaction in absence or presence of ACh or TC-2559 on β2_α4_β2_ α4_β2^{L146C} receptors. The rate of modification of L146C on the β2(+)/β2(-) interface was measured in the absence or presence of TC-2559 EC_{80}. Data from three experiments were fit to a single exponential rate equation, as described in Materials and Methods. k_2 values were calculated by dividing k_1 values by the concentration of MTS-ET used in the experiments. Data analysed using unpaired t-tests. *** depicts significant differences between MTSET application condition using the same agonist (*** $p < 0.0007$, **$p < 0.003$). ^ depicts significant differences between agonist tested in same conditions ($p < 0.05$)

5.2.3 – Effect of Alanine Substitution of Canonical Agonist sites on TC-2559 Activation of $(\alpha4\beta2)_2\beta2$

Given that the fifth subunit does not account for the super-agonism of TC-2559 at HS α4β2 nAChRs, it was examined whether canonical agonist sites encode defining efficacy elements for TC-2559. Docking on homology models of the HS α4β2 nAChR suggested that α4W182, α4E224 and β2S63 contact TC-2559 **(Figure 5.4)**.

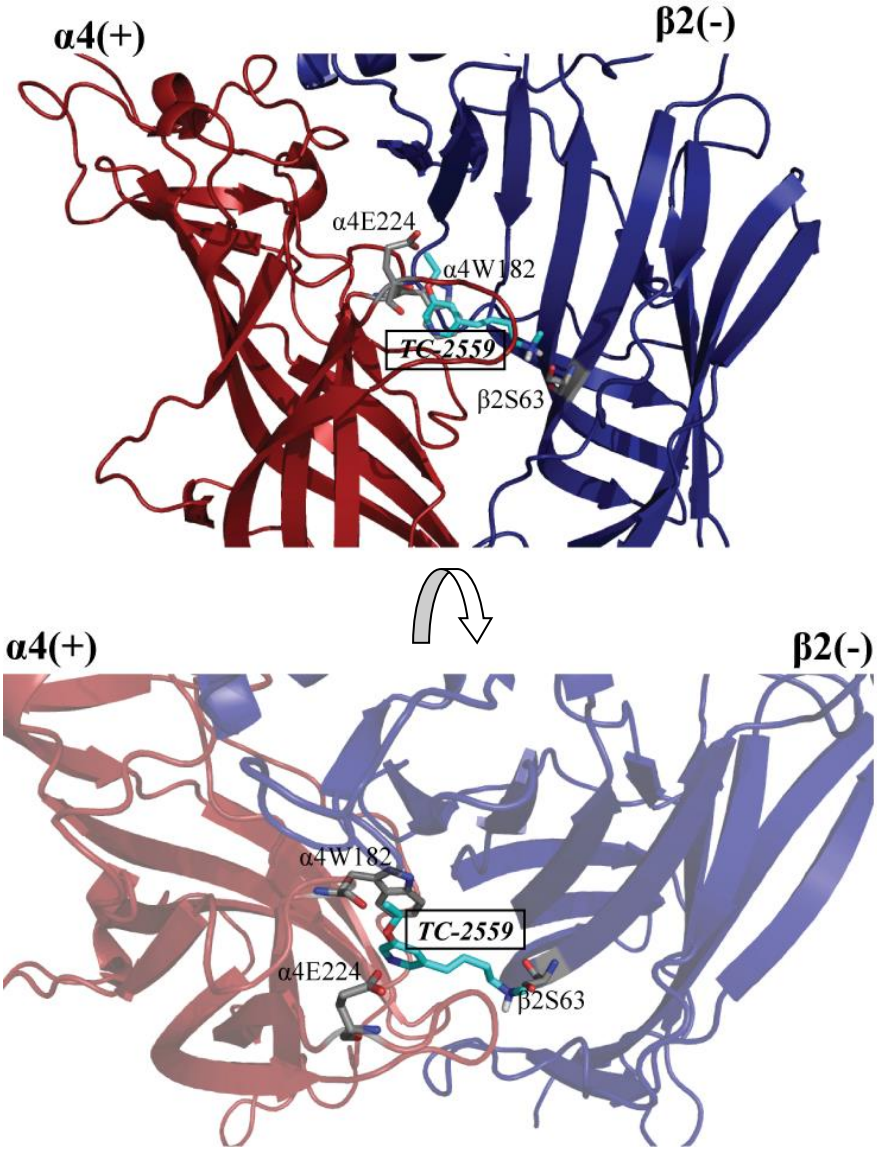

Figure 5.4. Docking of TC-2559 on a homology model of α4(+)/β2(-) interface. TC-2559 is predicted to make contacts with W182, E224 and S63. **(A)** is view from the membrane bi-layer, **(B)** is arial view of receptor

To determine if these residues affect the efficacy of TC-2559, they were alanine substituted and the consequences of the substitutions were assayed by two-electrode voltage clamp electrophysiology. Efficacy of TC-2559 decreased by approximately half when W182A was introduced individually in either binding site **(Figure 5.5A; Table 5.5)**. When W182A was simultaneously present in both agonist sites, TC-2559 did not evoke responses **(Figure 5.5B)**. To determine whether TC-2559 was still able to bind the agonist sites but unable to evoke responses, ACh EC_{80} responses were measured alone or in the presence of either 1μM, 10μM or 100μM TC-2559 and the two conditions compared. As seen by representative traces in **Figure 5.5E**, the level of impairment of ACh response was TC-2559 concentration dependent. To test if TC-2559 behave as a competitive antagonist at β2_^{W182A}α4_β2_^{W182A}α4_β2 receptors, the concentration response curve for ACh was obtained in the presence or absence of EC_{50} TC-2559. If TC-2559 behaves as a competitive inhibitor on β2_^{W182A}α4_β2_^{W182A}α4_β2 receptors, the ACh concentration response should be shifted to the right in the presence of TC-2559, compared to wild type. As shown in **Figure 5.5.C**, TC-2559 co-application induced a rightward displacement in the ACh concentration response curve.

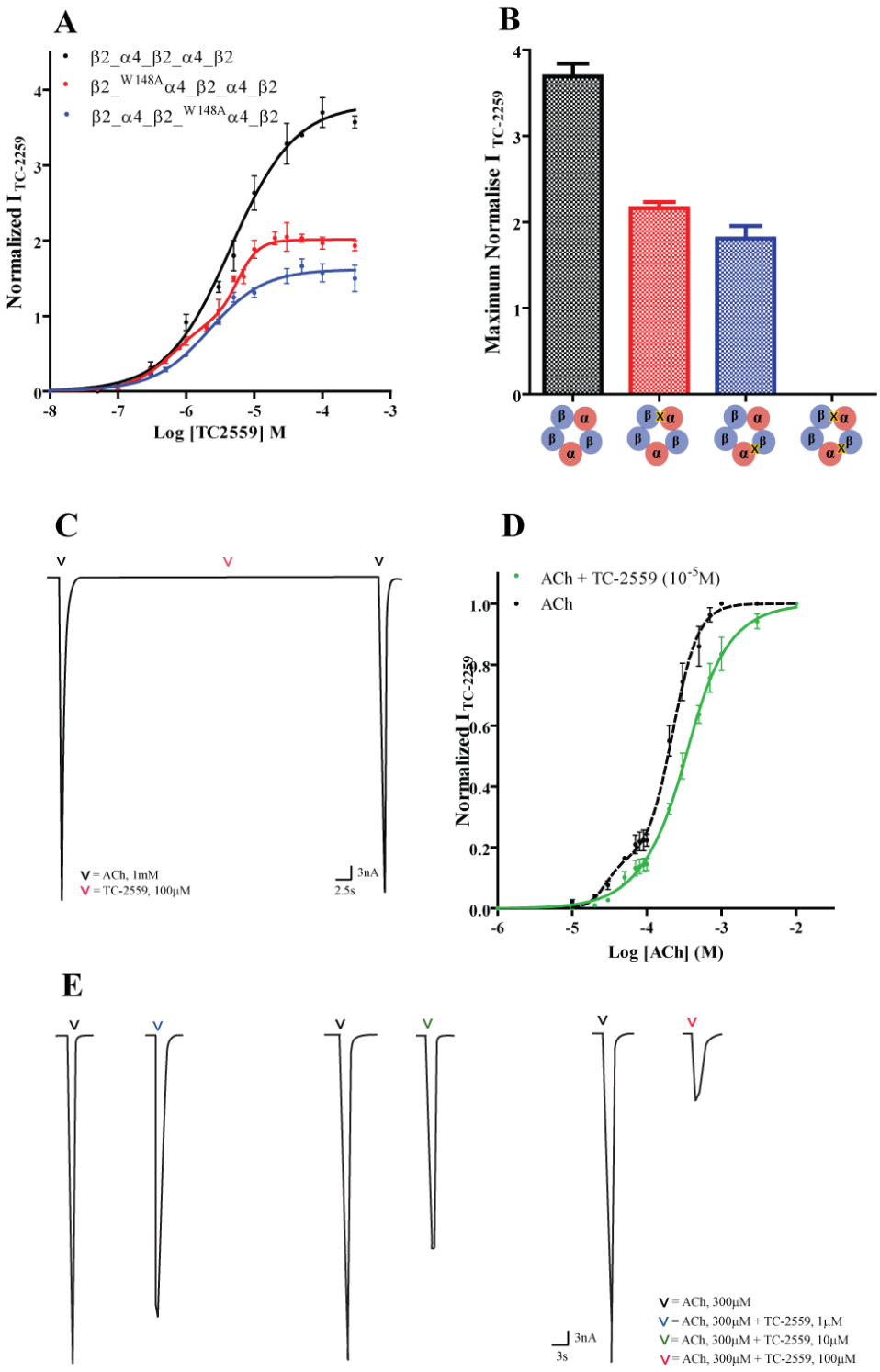

Figure 5.5. Concentration response effects of TC-2559 on the HS α4β2 nAChRs containing W182A agonist sites. W182A was introduced individually or simultaneously in the agonist sites of concatenated HS α4β2 nAChRs. **(A)** The concentration-response curves for TC-2559 on the mutated receptors were obtained as described in Materials and Methods. EC50 and relative efficacy determined from the fit curves are shown in Table 5.5.**(B)** Representative traces showing that ACh responses are inhibited in the presence of TC-2559. **(C)** Concentration response curve for ACh on β2_^{W182A}α4_β2_^{W182A}α4_β2 in the absence and presence of TC-2559. EC50 and relative efficacy values are shown in Table 5.5.

Concatemer	EC_{50} (μM)	nHill	Maximum $I_{TC-2559}$/ I_{ACh}
β2_α4_β2_ α4_β2	5.73 ± 1.89	0.86 ± 0.19	3.81 ± 0.39
β2_^{W182A}α4_β2_ α4_ β2	3.04 ± 0.72	0.82 ± 0.11	2.01 ± 0.1**8
β2_α4_β2_^{W182A}α4_ β2	6.31 ± 0.99	0.98 ± 0.014	1.81 ± 0.14 (***)
β2_^{W182A}α4_β2_^{W182A}α4_ β2	N/A	N/A	0
β2^{S63A}_α4_^{S63A}β2_ α4_β2	3.77 ± 0.54	0.92 ± 0.06	3.47 ± 0.43
β2_^{E224A}α4_β2_^{E224A}α4_β2	2.45 ± 1.10	0.65 ±0.10	1.41 ± 0.20(***)
β2_^{E224A}α4_β2_α4_β2	2.67 ± 1.19	0.99 ± 0.12	2.76 ± 0.29(*)
β2_α4_β2_^{E224A}α4_β2	1.84 ± .026	0.82 ± 0.05	3.43 ± 0.22

Table 5.5. Concentration-response effects of alanine substituted agonist sites on TC-2559 effects on HS α4β2 nAChRs. Responses elicited by a range of TC-2559 concentrations were normalised to ACh EC_{100} peak responses and the data were then analysed by non-linea regression, as described in Materials and Methods. Data points represent the mean ± SErM of at least three independent experiments. Statistical differences between mutant and wild type receptors were carried out by One-Way Anova with Dunnett's post-test. *, $p < 0.05$; ***, $p < 0.0001$. NA, no agonist effects.

Double mutant β2_^{E224A}α4_β2_^{E224A}α4_β2 and β2^{S63A}_α4_β2^{S63}A_α4_β2 were then tested. The β2S63A substitutions did not have significant effects on TC-2559 or efficacy effect on the responses of TC-2559 **(Figure 5.6; Table 5.5)**, hence the β2S63 mutation was not further analysed. In contrast, simultaneous incorporation of E224A on both agonist sites decreased efficacy by 2.7-fold, indicating this residue as an important component of for TC-2559 efficacy. The sensitivity of β2_^{E224A}α4_β2_^{E224A}α4_β2 receptors to activation by TC-2559 was comparable to wild type, indicating that E224 is likely to impact gating rather than agonist binding. Significantly, when E224A was introduced only in agonist site 1, efficacy was reduced by 2.8-fold, but when introduced in site 2 only, efficacy was not perturbed compared to wild type. Thus, as for ACh agonist site 2 appears to make a lesser contribution to receptor function than binding site 1.

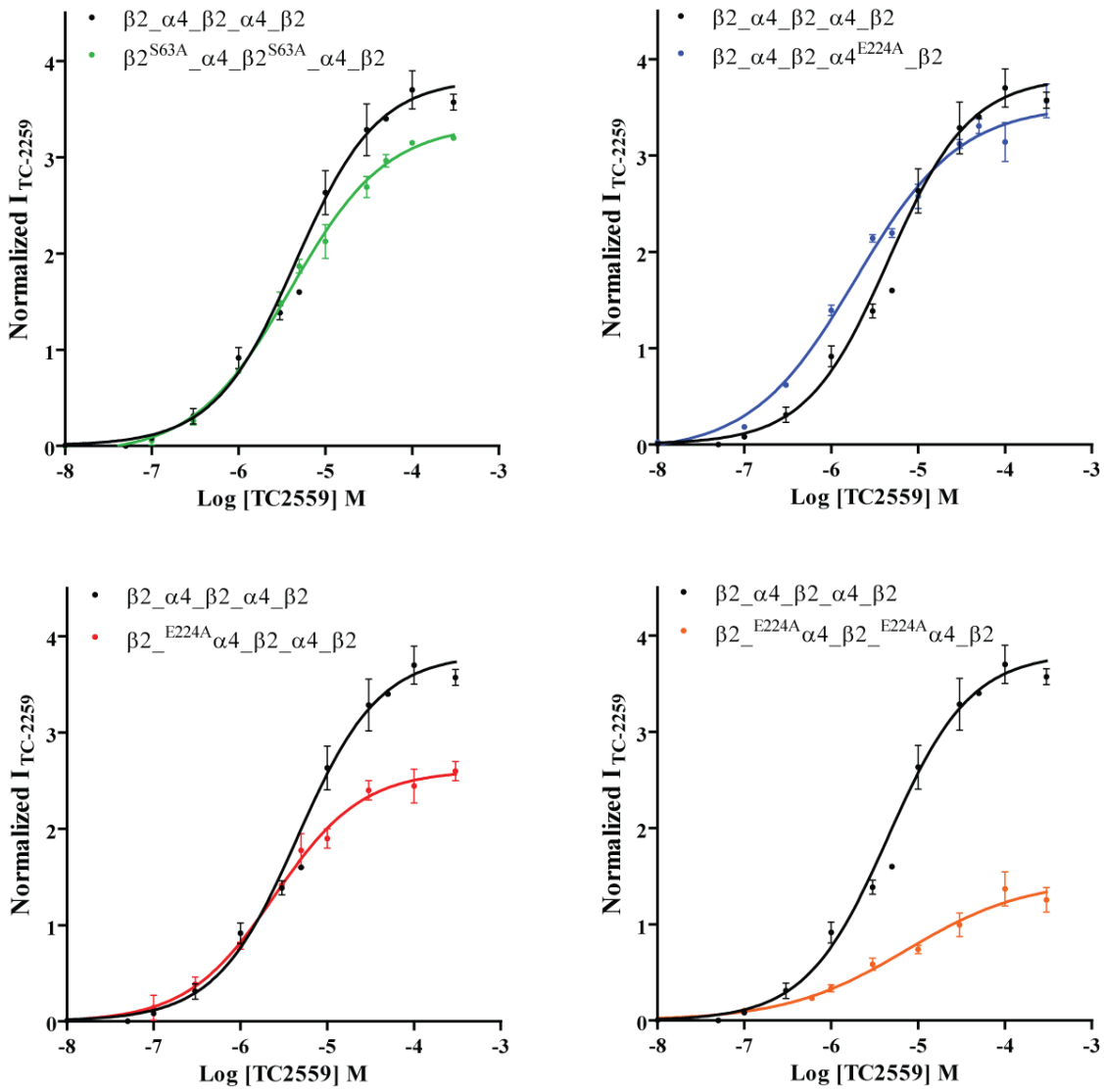

Figure 5.6. Concentration effects of TC-2559 on E224A or S63A substituted HS α4β2 nAChRs. E224A or S63A were individually or simultaneously introduced in the agonist binding sites. The concentration effects of TC-2559 on the mutant receptors were determined as described in Materials and Methods. Dta points represent the mean ± SEM of at least thre independent experiments. Estimated EC50 and relative efficacy are shown in **Table 5.5.**

5.2.4 - Functional Link of α4(+)/β(-) Binding Interfaces to 5β2 subunit and β(+)/β(-) interface

Lucero et al. (2016) have recently shown that E loop residues in β2 and α4 subunits can modulate α4β2 nAChR function at all receptor interfaces. L146 is an E loop residue, and taken with studies with ACh above, a role of L146 in efficacy was considered. This was first tested in terms of functional connection with β(+)/β(-).

Double mutant concatemers with substitutions in the biding sites alongside the L146C substitution within the β2(+)/β2(-) were assayed for maximum efficacy in order to gain insight to connections of these functional regions. An additive effect of two substitutions would imply mechanisms of efficacy reduction employed by these regions would be different. As double mutants (β2_^{W182A}α4_β2_α4_β2^{L146C} and β2_α4_β2_^{W182A}α4_β2^{L146C}) did not display additive effect compared to single substitutions, a functional connection between each binding site and the β2(+)/β2(-) is assumed **(Figure 5.7, Table 5.6).**

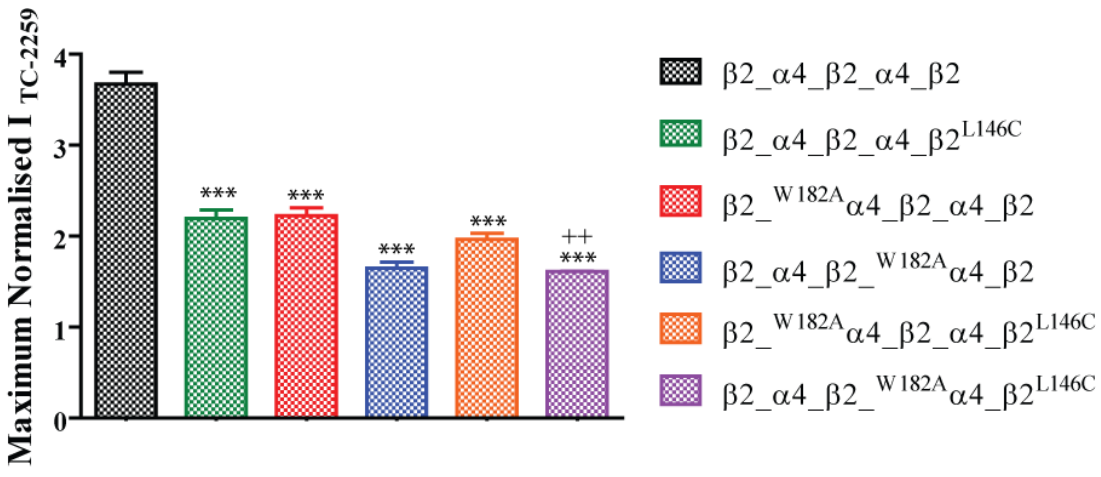

Figure 5.7. Histogram of effects of maximal TC-2559 efficacy of HS α4β2 nAChRs with substitutions of binding and β2(+)/β2(-) interfaces. Binding site W182A and β2(+)/β2(-)L146C substitutions shown for clarity. All differed from wild type significantly (***p<0.0001). Only one small but significant difference was seen in double substitutions between β2_α4_β2_^{W182A}α4_β2^{L146C} and β2_α4_β2_α4_β2^{L146C} ($^{++}$, p=0.003)

Concatemer	Maximum $I_{TC-2559}$/ I_{ACh}
β2_α4_β2_ α4_β2	3.81 ± 0.39
*β2_*^{W182A}*α4_β2_ α4_ β2*^{L146C}	1.97 ± 0.05***
*β2_α4_β2_*^{W182A}*α4_ β2*^{L146C}	1.61 ± 0.006***,++

Table 5.6. maximal TC-2559 efficacy of HS α4β2 nAChRs witth substitutions of binding and β2(+)/β2(-) interfaces. Binding site W182A and β2(+)/β2(-)L146C substitutions shown for clarity. All differed from wild type significantly (***p<0.0001). Only one small but significant difference was seen in double substitutions between β2_α4_β2_^{W182A}α4_β2^{L146C} and β2_α4_β2_α4_β2^{L146C} ($^{++}$, p=0.003)

Following this it was considered that other E loop residues may affect TC-2559 efficacy. The residues substituted were as follows (shown in **Figure 5.8**):

- β2(-)V135 - equivalent to α4(-)H142, a determinant of TC-2559 low efficacy on LS α4β2 nAChRs (Mazzaferro et al., 2014)
- β2(-)F144 - equivalent to α4(-)Q150
- β2(-)L146 - shown here to be important for agonist efficacy in HS α4β2 nAChRs and equivalent to α4(-)T152

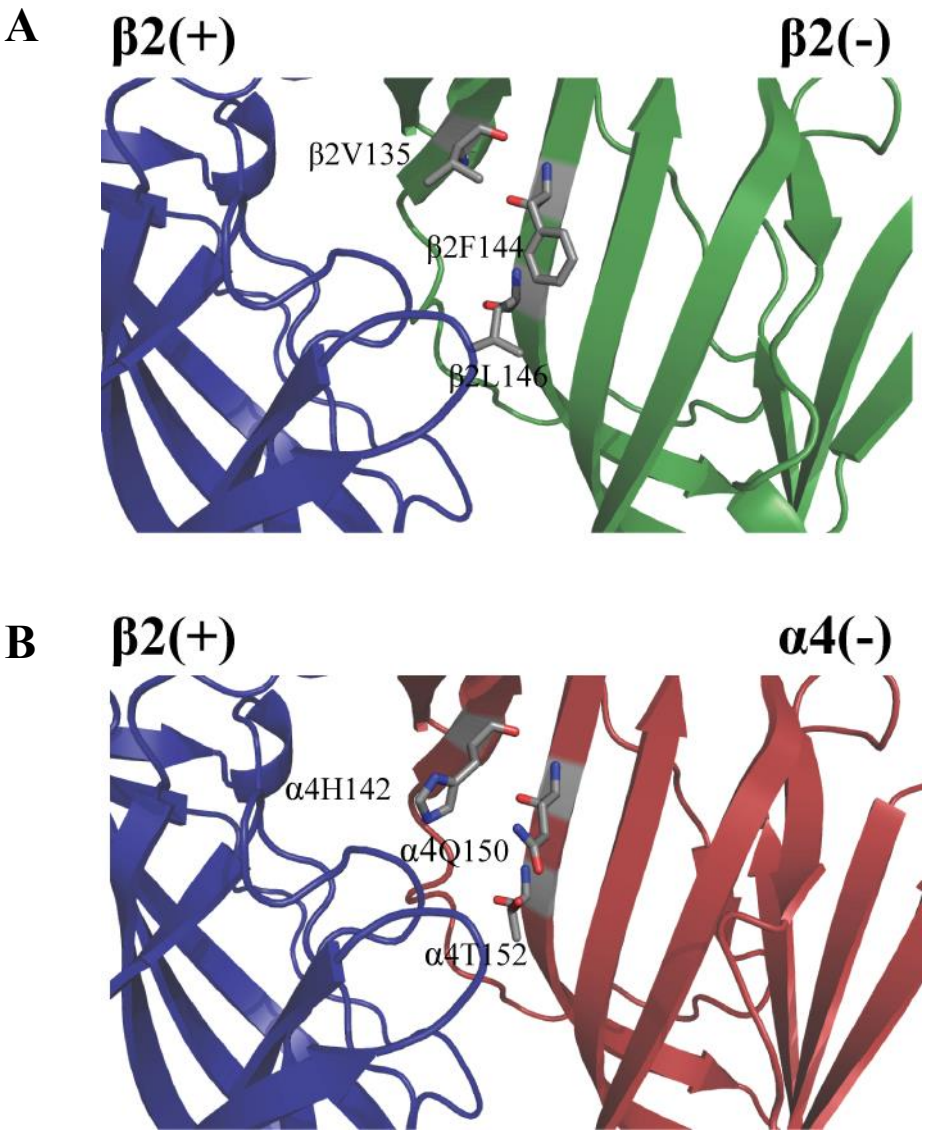

Figure 5.8. Homology model of the E loop shown within β(+)/β(-) (A) and α(+)/β(-) interfaces (B). Residues considered to be implicated in receptor function are shown in grey sticks.

Some of these residues are in close proximity, suggesting they may interact with each other **(Figure 5.7; Table 5.6)**. Each of the identified E-loop residues were individually substituted to alanine or to their equivalent α4 residues in the β(+)/β(-) interface to construct the following:

- β2_α4_β2_α4_β2^{V135A}
- β2_α4_β2_α4_β2^{F144A}
- β2_α4_β2_α4_β2^{L146A}
- β2_α4_β2_α4_β2^{V135H}
- β2_α4_β2_α4_β2^{L146Q}
- β2_α4_β2_α4_β2^{F144T}

These mutants were assayed for their sensitivity to activation by TC-2559 using two-electrode voltage-clamp electrophysiology, as described in Materials and Methods (Chapter 2). The concentration-response parameters obtained by non-linear regression analysis of the data are summarised in **Table 5.7**. None of the mutants tested affected TC-2559 potency **(Table 5.7)**. TC-2559 efficacy was not affected by β2V135A or β2V135H **(Table 5.7)**. As expected, the βL146A mutant decreased TC-2559 efficacy to the same level obtained by introducing L146C in the β2(+)/β2(-) interface **(Figure 5.8; Table 5.7)**. A novel revelation of this work is the reduction in overall function following the F144 side chain removal, a structural alteration that renders TC-2559 efficacy 2.4 times that of ACh **(Figure 5.8; Table 5.7)**. This puts forward another component of the E-loop as partaking in determination of ligand efficacy at the HS α4β2 nAChR. Interestingly, when mutants of F144 and L146 were simultaneously present in the β2(+)/β2(-) interface, the reduction in efficacy was not multiplicative. Efficacy was reduced to the same level obtained with the individual

alanine substitutions, suggesting that F144 and L146 may be functionally coupled **(Figure 5.8; Table 5.7)**. Thus, overall the findings indicate that at least two residues of the E loop, F144 and L146, are important for the contribution of the fifth subunit to agonist-driven recptor function.

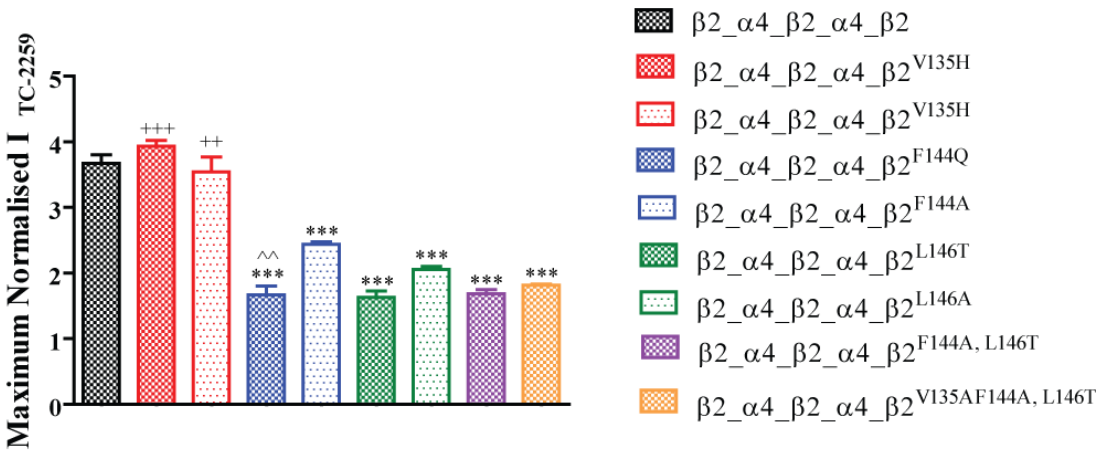

Figure 5.9. Histogram showing variation in TC-5229 efficacy with E loop substitutions to alanine or α4-subunit equivalent . The relative efficacy of TC-2559 was calculated by dividing the peak TC-2559 current responses by the peak current elicited by ACh EC_{100} (1 mM). Statistical differences between wild type and mutant receptors were estimated using one-way Anova with Dunnett's post-tests (***, $p<0.0001$) ANOVA with Bonferroni corrections were performed to assess variances between residues withinin alanine or α-subunit equivalent substitutions ($^{+++}$,$p<0.0001$' $^{++}$,$p < 0.0005$). Only one difference of residues between alanine and α equivalent substitutions as determined by students t-test (^^,$p=0.005$). Concentration response parameters EC_{50} and relative efficacy are shown in Table 5.7.

Receptor	EC_{50} (μM)	$Imax_{TC2559}/Imax_{ACh}$
β2_α4_β2_α4_β2	1.84 ± 0.1	3.81 ± 0.39
β2_α4_β2_ α4_β2^{V135A}	2.98±0.98	3.55 ± 0.22
β2_α4_β2_ α4_β2^{F144A}	2.01±0.84	2.44 ± 0.04 ***
β2_α4_β2_ α4_β2^{L146A}	3.7±0.7	2.06 ± 0.04 ***
β2_α4_β2_ α4_β2^{V135H}	3.0±1	3.91±0.01
β2_α4_β2_ α4_β2^{F144Q}	2.84±0.98	1.67 ± 0.06 ***
β2_α4_β2_ α4_β2^{L146T}	3.05±	1.63 ± 0.09 ***
β2_α4_β2_ α4_β2$^{F144Q, L146T}$	3.6±1.1	1.68 ± 0.06 ***
β2_α4_β2_ α4_β2$^{V135H, F144Q, L146T}$	3.87±1	1.81±0.1***
β2_α4_β2_^{H142A}α4_β2	3.21 ± 0.82	3.81 ± 0.39
β2_α4_β2_^{Q150A}α4_β2	2.65 ± 2.21	3.45 ± 0.36
β2_α4_β2_^{T152A}α4_ β2	3.1 ± 1.34	3.88 ± 0.24
β2_^{H142A}α4_β2_α4_β2	2.97 ± 0.82	3.85 ± 0.05
β2_^{Q150A}α4_β2_α4_β2	2.78 ± 2.21	3.7±0.01
β2_^{T152A}α4_β2_α4_ β2	3.00 ± 1.34	3.2±0.1

Table 5.7. Effects of E loop residues on TC-2559 effects on concatenated HS α4β2 nAChRs. Loop E residues were mutated to alanine or their equivalents on their interfacing subunit. The concentration effects on the responses of the mutants to TC-5299 were analysed by non-linera regression, as described on Materials and Methods. Statistical differences between mutant and wild type receptors were determined by One-way Anova with Dunnett's post-test. ***, $p < 0.0001$.

5.2.5 - Functional links in β2(+)/β2(-) Implicated in TC-2559 Efficacy

Examination of the homology model of the β2(+)/β2(-) interface suggest that residues that could couple functionally include β2(-)L146 and β2(-)F144 on the complementary side of the β2(+)/β2(-) interface and β2(+)W176, β2(+)T177, and1β2(+)Y178 on the principal side of the β2(+)/β2(-) interface. As shown in **Table 5.8**, these residues are in close proximity and could engage in hydrophobic or π stacking interactions, depending on the nature of the residues involved. Of the residues mentioned above, β2(+)W176 has already been suggested as being couple to β2(-)L146 to contribute to ACh efficacy (Chapter 4). The additional two residues suggested by this approach (1β2T177 and 1β2Y178) were individually substituted by alanine to produce ^{T177A}β2_α4_β2_α4_β2 and ^{Y178A}β2_α4_β2_α4_β2 concatemers, and the TC-2559 concentration response relationships of each were analysed. Removal of the Y178 had no effect upon TC-2559 potency or efficacy **(Table 5.9).** In contrast, β2T177 reduced TC-2559 efficacy 2.2 times, compared to wild type **(Table 5.9).**

To determine whether β2(-)L146 and the β2(+)W176 and β2(+)T177 of the β(+)/β(-) interface are coupled, the effect of double substitutions here upon TC-2559 efficacy was examined. If these residues are not coupled functionally, then the effect on efficacy of the double mutants and single mutants should be multiplicative. Neither of these mutants displayed EC_{50} values different from wild type, but, compared to wild type, TC-2559 efficacy was reduced to the same level obtained with the individual substitutions **(Table 5.9)**.

Taken together, all data concerning β2(+)/β2(-) residues strongly suggest presence of inter-subunit interactions between the fifth subunit and the neighbouring β2, and the importance of these interactions in determination of receptor efficacy.

1β2 (+)	5β2 (+)	Distance (Å)	Possible Nature of Interaction
W176	*V135*	9.85	Hydrophobic
T177	*V135*	3.40	Hydrophobic
Y178	*V135*	3.20	Hydrophobic
W176	*F144*	6.83	π Stacking
T177	*F144*	5.04	π Stacking
Y178	*F144*	6.10 (backbone)	π Stacking
W176	*L146*	3.20	Hydrophobic
T177	*L146*	4.83	Hydrophobic
Y178	*L146*	4.46	Hydrophobic

Table 5.8. Possible inter-residue interactions in the β2(+)/β2(-) interface. Homology models of the β2(+)/β2(-) interface predict several residues in loop A and loop E to be in close proximity to be able to engage in inter-facial interactions.

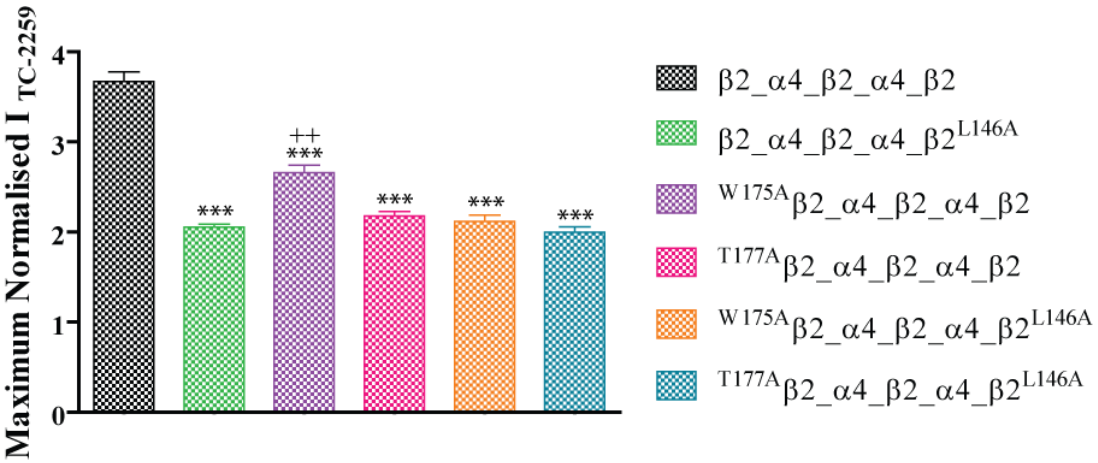

Figure 5.10. Histogram of effects of TC-2559 efficacy following removal of putatively linked residues in β2(+)/β2(-) interface. Maximal responses of single and double substitutions shown for clarity. All are significantly different to wild type receptors as measuresd by ANOVA with Dunnets corrections (***,p<0.0001). As determined by ANOVA with Bonferroni correction, only ^{W176A}β2_α4_β2_α4_β2 was significantly different from its double mutant counterpart (++,p=0.01), but reduction following L146A substitution was not additive.

.

Receptor	EC_{50} (μM)	$Imax_{TC2559}/Imax_{ACh}$
β2_α4_β2_ α4_β2^{L146A}	3.7±0.7	2.06 ± 0.04 ***
^{W176A}β2_α4_β2_α4_β2	4.36 ± 1.09	2.66 ± 0.16 ***
^{T177A}β2_α4_β2_α4_β2	2.96±1.1	2.18 ± 0.06 ***
^{Y178A}β2_α4_β2_α4_β2	2.45±0.67	3.29 ± 0.11
^{W176A}β2_α4_β2_α4_β2^{L146A}	4.19 ± 0.22	2.12 ± 0.09
^{T177A}β2_α4_β2_α4_β2^{L146A}	3.04 ± 0.51	1.99 ± 0.06

Table 5.9. Effects of β2(+)/β2(-) interface residues on TC-2559 effects on concatenated HS α4β2 nAChRs. Loop A or B residues were mutated to alanine or their equivalents on their interfacing subunit. The concentration effects on the responses of the mutants to TC-5299 were analysed by non-linear regression, as described on Materials and Methods. All are significantly different to wild type receptors as measuresd by ANOVA with Dunnets corrections (***,p<0.0001). As determined by ANOVA with Bonferroni correction, only ^{W176A}β2_α4_β2_α4_β2 was significantly different from its double mutant counterpart (++,p=0.01), but reduction following L146A substitution was not additive

5.3 DISCUSSION

The findings of this study confirm the findings of Chapter 3 and 4 that the fifth subunit contributes to receptor activation through functionally linking to the agonist sites of the HS receptor. The importance of interaction between the β2(+)/β2(-) and α4(+)/β2(-) interfaces in maximum activation and ligand specific response is highlighted, while suggesting that the α4(+)/β2(-) site coupling to the fifth subunit through the β2(+)/β2(-) interface may be a gating mechanisms additional to the pathway linking the agonist site to the ECD/TMD interface and M2. Thus, the findings further support the most recent cryo-structures of Torpedo nAChRs showing a key role for the fifth subunit in channel gating (Unwin and Fujiyoshi, 2012).

The most novel of findings concerning TC-2559 activation of HS α4β2 nAChRs are those pertaining to the α4(+)/β2(-) binding interfaces. Taken together, the double mutant concatemers β2_^{W182A}α4_β2_W^{182A}α4_β2 and β2_^{E224A}α4_β2_^{E224A}α4_β2 suggest that ACh and TC-2559 bind the agonist sites with different poses, Such differences were also suggested by docking stimulations. This implies different energy release profiles following the interaction of these two agonists at binding site that will then lead to unique activities throughout the pentamer during activation events leading to opening of the channel (Taly et al., 2013). Binding interactions are thus shown to be the initial and major determinant of receptor response to particular agonists. Because the double mutants led to almost (E224A) or complete (W182A) ablation of the super-agonism of TC2559, which was not obtained with mutants β2(+)/β2(-)-containing receptors, it is clear that binding of the agonist to the agonist sites is the dominant determinant of agonist efficacy. \this

is in accord with studies that show that agonist binding site residues, wheather in the principal or complementary side of the agonist site are key determinants of efficacy (Chavez-Noriega et al., 1997; Mukhtasimova et al., 2009; Hibbs and Gouaux, 2011; Brams et al., 2011; Harpsoe et al., 2012 Rohde et al., 2012; Tavarez et al, 2012; Kletke et; al., 2013).

As shown in ACh studies, the binding site characteristics contribute largely to the unique functional features of the α4β2 nAChRs, primarily via their individual modes of action and the dominance of site 1, closest to the β(+)/β(-) interface. In respect of TC-2559 activation, this is shown here to also be the case. When introducing single mutants of binding residues in the α4 subunits (α4(+)W182A or α4(+)E224A), the reduction of TC-2559 responses are significantly different between the two binding sites. In the case of α4E224A, the additional TC-2559 binding residue identified by this work, the usual pattern of site 1 alteration having the largest effect is witnessed. In contrast, alanine substitution of the well-established conserved binding residue α4W182 resulted in larger perturbation of receptor function when introduced in site 2. This is not seen in any other studies, including those of ACh effects at receptors with this substitution in individual sites and shows that site 1 is not strictly dominant in all aspects of activation. Sensitivity effects as a result of this substitution are constant between ACh and TC-2559, supporting the findings of no effect to the ACh EC50 in site 2, while site 1 produced bi-phasic CRC.

The studies reported here demonstrate that binding sites also work together to determine efficacy as well as potency of agonists, most evident in comparison of the three mutants containing α4E224A substitutions. This glutamate is suggested to be

important in TC-2559 binding at site 1, by reduction in activation following removal of its side chain. However, receptor activation by TC-2559 is not affected by the α4E224A substitution in site 2 alone, and its binding interaction with the E224 at this interface doesn't appear to be central to the maximum response elicited. As the effects of this alanine substitution in site 2 does have an impact on receptor response to TC-2559 when the E224 binding is interrupted at site 1 (double mutant significantly perturbed compared to β2_^{E224A}α4_β2_α4_β2), it appears that altered binding at site 1 will in turn alter activity of site 2. This suggests that specific binding profiles will initiate different conformational changes throughout the pentamer, in turn impacting conformational changes and any additional binding that follows this and consequentially channel gating and activation. This process has previously been outlined in ACh activation, but these studies are only able to highlight the effects of agonist potency and the action of conserved binding residues. The data with additional non-conserved binding residues suggests that this may be a consequence of interfaces moving as a whole as opposed to specific residues. Thus, it may be an effect of global conformational changes throughout the receptor (reviewed by Cecchini and Changeux, 2015). Thus, the involvement of agonist-binding and non-binding interfaces is consistent with the current view of gating in the Cys loop receptors (Cecchini and Changeux, 2015). Agonist binding appears to close the loop C, promoting a concerted anti-clockwise rotation around the pore axis of all five subunits and pushing the fifth subunit outwardly (Unwin anf Fujiyoshi, 2012; Du et al., 2015). Thus, the whole protein undergoes extensive rearrangements, which are likely to involve inter and intra-interactions between residues.

An important observation of this collection of studies is that none of the mutations studies decreased the efficacy of TC-2559 to the level seen for LS α4β2 nAChR

(Moroni et al., 2006; Carbone et al., 2009; Mazzaferro et al., 2014). LS α4β2-like efficacy is only achieved when the complete ECD of the fifth subunit is replaced with the ECD of an α4 subunit. Thus, it may be possible that the α4(+)/α4(-) interface impairs efficacy of TC-2559. This ligand does not bind the α4(+)/α4(-) interface (Mazzaferro et al., 2014), but it may be that communicating pathways between the agonist sites on α4(+)/β2(-) and the α4(+)/α4(-) interface regulate agonist efficacy in the same fashion the equivalent pathway does in the HS receptor.

Overall the findings highlights well the importance of information transmission between subunits and in turn the inter-subunit interactions governing this. Knowing from ACh studies the role that the E-loop of the fifth subunit β2 plays in these events; TC-2559 data here has supported the importance of this region and allowed identification of specific amino acids conducting the interface specific interactions. From work by others (Harpsoe et al., 2011 and most recently Whiteaker et. al., 2016) and ourselves (Mazzaferro et al., 2011; 2014), it is known that the E-loop, situated on the complementary face of subunit interfaces is important in α4β2 nAChR function. The findings of this thesis shows the E loop within the β2(+)/β2(-) interface as an important efficacy element. Alongside chimera studies, MTS-ET modification of residues at this location revealed its importance in levels of ACh activation, as well as intersubunit connections central to this mechanism. Considering this, and the findings of Whiteaker et. al. (2016) that all subunit interfaces contribute to receptor activation in distinct manners, it seems that gating of Cys loop receptors is more complex than previously thought (reviewed by Miller and Smart, 2010), even considering recent structural studies of nAChRs (Unwin and Fujiyoshi, 2012). The challenge for the future is to determine how all these various

pathways combine to achieve efficacious gating.

This Chapter confirms the link of agonist site 1 to the fifth subunit and the asymmetrical function of the agonist sites. As discussed in previous chapters, it seems that asymmetrical function of agonist sites may be the norm in heteromeric Cys loop receptors (Baumann et al., 2005; Price et al., 2002). This is not surprising, the Cys loop receptors and its prokaryotic homologs are asymmetric proteins and their gating, even when considered purely from the subunits binding agonist is highly asymmetric (Cecchinni and Changeux, 2015). It is in this asymmetric function that offers the possibility of developing highly specific drugs. So far, drug discovery projects have not being highly fructiferous in developing stoichiometry-specific α4β2 nAChR-drugs (Bruce et al., 2005; Olsen et al., 2013), but the identification of receptor unique gating pathways may provide a new impetus and focus to drug discovery programs.

Chapter 6

-Final Discussion-

Through extraordinary advances in a multitude of experimental approaches that have been applied to studies of the atomic structure and function of pLGICs, our understanding of how these allosteric proteins couple agonist binding to ion channel gating has been increased to a level that we could not even imagine fifteen years ago, when the crystal structure of the AChBP, the homolog of the ECD of the nAChR, was resolved (Brejc et al., 2001). The last three years have had a tremendous impact on our understanding of the pLGICs. The resolution of the crystal structures of prokaryotic (Hilf and Dutzler, 2008, 2009; Bocquet et al., 2009; Sauguet et al., 2014; and eukaryotic pLGICs in resting, open and desensitised states (Hibbs and Gouaux, 2011; Nury et al., 2010; Calimet et al., 2013; Miller and Aricescu, 2014; 5-HT3; Hassaine et al., 2014; Althoff et al., 2014), cryo-EM structures (Unwin, 2005; Unwin and Fujiyosi, 2012; Du et al., 2015), molecular dynamics analysis of the gating of pLGICs (Nury et al., 2010; Calimet et al., 2013) as well as REFER studies of the microscopic kinetics of these ion channels (Purohit et al., 2007) have insight how these channels transit energetically and structurally from the resting (unbound close) to the open (bound) and then desensitised (close bound) states. This thesis builds upon these achievements, demonstrating that gating involves all subunits, including those not directly involved in agonist binding. The most important finding of this study is that the fifth subunit (previously considered an auxiliary or structural subunit) participates in gating, albeit by functionally linking to one the agonist sites on α4/β2. This link is asymmetrical; it takes place only with the agonist site whose complementary subunit interfaces with the fifth subunit (agonist binding site 1 in the concatemer HS α4β2).

The widely accepted mechanism of channel gating, known as the principal pathway, constitutes transmission of ligand binding energies through the structure of the receptor downwards to the distally located gate via a series of conformational changes. This signal propagates from the binding site to the region known as the coupling region at the interface between the extracellular domain and the pore containing transmembrane domain (reviewed by Miller and Smart, 2010; see also Chapter 1). This involves displacement of the alpha helices lining the pore and subsequent movement of all subunits to widen the channel and permit flow of ions into and out of the cell (Unwin, 2005; Unwin and Fujiyoshi, 2012; Du et al., 2015). However, pLGIC activation does not constitute a simplistic binary phenomena consisting of purely closed and open states. First, in addition to the principal pathway, interactions between M4 and M1 and M3 (Carswell et al., 2015) and M4, post-M4 and the Cys loop modulate gating. The findings of this thesis, together with the most recent cryo-EM structures of the Torpedo nAChR (Unwin and Fujiyoshi, 2015) add interactions between the fifth subunit and an agonist site as an additional gating element. How do all these gating elements work together to define agonist efficacy? Through structural and functional diversity of receptors as well as ligands, gating can vary e.g. full, partial and super-agonism and be modulated (e.g., allosteric modulators). Gating efficacy is currently thought to be determined by closed states preceding gating (Lape et al., 2009; Mukhtasimova et al., 2009). The structures that underlie the transition to or these closed states themselves are not known but one can surmise that they will likely multiple intra- and inter-subunit interactions. The observation that twisting and blooming involves the whole protein supports this view.

The findings of this thesis shows the importance of the fifth subunit as a gating element, in accord with the interpretation of the most recent cryo-EM structures of *Torpedo* nAChRs by Unwin and Fujiyoshi (2012). These authors propose that both bound-agonist sites asymmetrically push the auxiliary subunit (β1) to gate the channel. Thus, it is the displacement of the fifth subunit that ultimately opens the gate. The functional studies presented here do not fully agree with Unwin and Fujiyoshi (2014). The fifth subunit in the HS α4β2 nAChR appears to increase the efficacy of agonist-driven gating, thus acting like a gating modulator. Thus, the effect of the fifth subunit on agonist efficacy (gating) depends on agonist binding to the agonist site coupled to the fifth subunit, and when the sites are engaged, the fifth subunit increases gating. Indeed, this thesis, through the work carried out on the functional effects of TC-2559, a super-agonist at HS α4β2 nAChRs, shows clearly that agonist binding sites are the principal determinant of agonist efficacy or gating. How this interplay between agonist sites and agonists and coupling between engaged agonist sites and the fifth subunit define gating efficacy remains to be elucidated. However, one can anticipate that gating efficacy, at the structural level, will be complex and comprise many pathways. The gating of pLGICS is likely to be as complex as the physiological functions they mediate.

Gating efficacy, in respect of microscopic receptor kinetics, is determined by how efficiently agonist-bound binding sites reach closed states preceding gating (Lape et al., 2009). Once the flipped or primed states are reached, full and partial agonists gate the channel similarly. Thus, one can surmise that conformational transitions occurring immediately after agonist binding cause the flipping states. It is tempting to speculate that a structural factor underlying the flipping states may be

different degrees of 5th β2 subunit movement, just as the degree of loop C capping has been linked to agonist efficacy (Hansen et al., 2005). This possibility is consistent with REFER data that suggests that agonist dependent differences in gating are likely to be defined by events occurring close to the binding steps, whereas the final activating step of channel opening is very similar between full and partial agonists (Jadey and Auerbach, 2012). Clearly the challenge today for the field of pLGIC is the identification of intermediate activation states such as the "flipped" or "primed" states in which receptors are ligand bound and active but closed provides a basis of understanding how distinct ligands achieve unique responses. As movements and subsequent interactions of the 5th β2 subunit are agonist specific, this thesis suggests there is a structural basis to these intermediate states, determined by the binding sites but propagated at the non-binding subunit interfaces. The flipped receptor has a higher affinity for the agonist than the resting receptor, and in turn, a higher affinity for full over partial agonists low affinity for the flipped state, relative to the resting state, that makes an agonist partial, rather than low affinity for the open state, relative to the resting state. This places interaction energies defining agonist efficacies earlier in the chain of events that follow binding than if the defining state was an open state.

Mukhtasimova (2009) attributed a structural element to the primed 'intermediate states' as the capping of loop C of binding sites. This stated that capping of a single binding site results in one priming state with an intermediate duration that triggers brief channel openings. Capping of two sites results in the second primed state that has a brief duration and leads to longer open states. Significantly, the two closed primed states (one *vs* two liganded binding sites) are

distinct from each other and exhibit conformational changes of loop C that are independent of the agonist eliciting the response. The difference that is conferred by ligands is their ability to prompt receptors to reach this primed state, which in turn depends on bi-directional communication between the binding regions and channel. These findings, taken in conjunction with the findings of this thesis, suggest that although binding interactions within the sites differ between agonists and the sites themselves, eliciting agonist-dependent conformational or energetic transitions in the binding sites, some conformational changes within the sites elicited by ligands are not dependent on the nature of the agonists. Findings here suggest that the functional coupling between agonist site 1 and the fifth subunit has the same effect on gating regardless of whether ACh or TC-2259 occupy the site.

Significantly, this study found that changes in one agonist site through alanine or cysteine mutations affected the function of the other agonist site. Thus, the findings suggest that the sites are somehow functionally coupled. Akk (2002) observed a similar phenomenon for the muscle nAChR. Incorporation of α1Y93F substitutions in a single binding site showed that the receptor behaved functionally as if both agonist sites were mutated. Thus, the agonist sites in the muscle nAChR appear to be coupled, just like the agonist sites in the HS α4β2 nAChR.

Using single channel analysis, Jadey et al. (2012) found that that each binding site in the muscle nAChR appears to undergo two conformational changes following agonist interaction, termed the “catch” and “hold conformations. These conformational changes were suggested to underlie the switching of the sites from a low to high agonist affinity state. This was thought to be due to loop C capping as well as movement of other loops in the binding sites. Agonists that open the channel more effectively bind to resting nAChRs with higher affinity and, this close

correlation between affinity and efficacy implies that binding and the affinity change are two stages of a single integrated process. The energies of these structural re-arrangements leading to affinity changes are able to predict the efficacy of responses and vice versa as they correlate to the gating equilibrium constant (Purohit et al., 2014). A similar correlation between affinity binding and efficacy has been observed in the GABA-$_A$ receptor (Jones et al., 2001). The correlation of agonist affinity and efficacies have been taken to indicate that these catch and hold conformational changes associated with low affinity binding and switching from low to high affinity respectively, are not independent and that all of the intermediate steps in AChR activation including re-arrangement of binding loops comprise a single, energetically coupled process. This work supports notions of intermediate flipped states, and the two mechanisms can be incorporated to give the scheme:

$$\underset{\text{dock}}{\underline{\quad}} \quad \underset{\text{catch}}{\underline{\quad}} \quad \underset{\text{hold}}{\underline{\quad}} \quad \underset{\text{flipped}}{\underline{\quad\quad\quad\quad}} \quad \underset{\text{open}}{\underline{\quad}}$$

$$A+R \leftrightarrow A\text{-}R \leftrightarrow AR^{L} \leftrightarrow \underset{(AF^{1})}{AR^{H}} \leftrightarrow AF^{2} \leftrightarrow AF^{3} \leftrightarrow AR^{*}$$

Considering the findings of this thesis, it is tempting to suggest that movements in the fifth subunit are involved in the process of reaching the flipping states. Functional connection of the 5th β2 with site1 was suggested by the findings of the SCAM and mutagenesis studies reported in Chapter 3 and 4. On the other hand, the only demonstration of functional linkage between the fifth subunit andv agonist site 2 comes mutagenesis studies that perturbed the ACh concentration response curves of the mutant receptors, compared to wild type. This may suggests a weaker functional connection between the fifth subunit and site 2, compared to that with agonist site 1.

Considering the number of functional binding sites of LGIC's from an evolutionary perspective provides leads provoking thoughts on the roles of subunit interfaces and modes of action of these proteins. Within the ancient homomeric Cys-loop receptors, five structurally equivalent interfaces are present, all of which are able to bind agonists. With the development of the more recent heteromeric pentamers incorporating many subunit types, a greater diversity of receptors is seen. However, this is at a cost; subunits shown in this thesis that are incapable of forming functional binding interfaces are introduced to the pentamer and ligand binding site numbers reduced to only 3 and even 2 within a pentamer. As the need for more complex and intricate physiological pathways arises, it fits that multiple receptor subtypes with a variation in the number of binding sites present and thus different modes of action came into existence.

However, more interesting still is that these non-canonical binding interfaces and subunits have not completely lost function but serve a role in receptor activation in an alternate manner. This appears to predominantly be utilisation of the conserved binding sites to exert their modulatory effect as demonstrated in this thesis and more classically in the benzodiazepine binding interface of GABA-$_A$ receptors. These mechanisms of receptor modulation fit with the development of more complex organisms and biological systems as a finer tuning is required. a mechanism of compensation of loss of these orthosteric binding sites making way for modulatory regions may be a factor behind the and functional differences and coupling of conserved binding sites and resultant multiple gating pathways. All these considerations highlight how these receptors function in a complex manner to govern the complex behaviours we know them to govern. This raises the question of how far we can use these multiple pathways of function and gating to our advantage, in order

to understand how brain modulates activity and ultimately use this knowledge to develop theraputic drugs.

Absalom, N. L., Lewis, T. M., Kaplan, W., Pierce, K. D. and Schofield, P. R. (2003) 'Role of charged residues in coupling ligand binding and channel activation in the extracellular domain of the glycine receptor.', *The Journal of biological chemistry*, 278(50), pp. 50151–7.

Agnati, L. F., Zoli, M., Strömberg, I. and Fuxe, K. (1995) 'Intercellular communication in the brain: Wiring versus volume transmission', *Neuroscience*, pp. 711–726.

Albuquerque, E. X., Pereira, E. F. R., Alkondon, M. and Rogers, S. W. (2009) 'Mammalian Nicotinic Acetylcholine Receptors : From Structure to Function', pp. 73–120.

Andreasen, J. T., Olsen, G. M., Wiborg, O. and Redrobe, J. P. (2009) 'Antidepressant-like effects of nicotinic acetylcholine receptor antagonists, but not agonists, in the mouse forced swim and mouse tail suspension tests.', *Journal of psychopharmacology (Oxford, England)*, 23(7), pp. 797–804.

Andreasen, J. T. and Redrobe, J. P. (2009a) 'Antidepressant-like effects of nicotine and mecamylamine in the mouse forced swim and tail suspension tests: role of strain, test and sex.', *Behavioural pharmacology*, 20(3), pp. 286–95.

Andreasen, J. T. and Redrobe, J. P. (2009b) 'Nicotine, but not mecamylamine, enhances antidepressant-like effects of citalopram and reboxetine in the mouse forced swim and tail suspension tests.', *Behavioural brain research*, 197(1), pp. 150–6.

Arevalo, E., Chiara, D. C., Forman, S. A., Cohen, J. B. and Miller, K. W. (2005) 'Gating-enhanced accessibility of hydrophobic sites within the transmembrane region of the nicotinic acetylcholine receptor's ??-subunit: A time-resolved photolabeling study', *Journal of Biological Chemistry*, 280(14), pp. 13631–13640.

Ashare, R. L. and McKee, S. A. (2012) 'Effects of varenicline and bupropion on cognitive processes among nicotine-deprived smokers.', *Experimental and clinical psychopharmacology*. NIH Public Access, 20(1), pp. 63–70.

Azam, L., Winzer-Serhan, U. and Leslie, F. . (2003) 'Co-expression of α7 and β2 nicotinic acetylcholine receptor subunit mRNAs within rat brain cholinergic neurons', *Neuroscience*, 119(4), pp. 965–977.

Bancila, V., Cordeiro, J. M., Bloc, A. and Dunant, Y. (2009) 'Nicotine-induced and depolarisation-induced glutamate release from hippocampus mossy fibre synaptosomes: two distinct mechanisms.', *Journal of neurochemistry*, 110(2), pp. 570–80.

Becchetti, A., Aracri, P., Meneghini, S., Brusco, S. and Amadeo, A. (2015) 'The role of nicotinic acetylcholine receptors in autosomal dominant nocturnal frontal lobe epilepsy', *Frontiers in Physiology*, 6(FEB), pp. 1–12.

Bertrand, D., Picard, F., Le Hellard, S., Weiland, S., Favre, I., Phillips, H., Bertrand, S., Berkovic, S. F., Malafosse, A. and Mulley, J. (2002) 'How mutations in the nAChRs can cause ADNFLE epilepsy.', *Epilepsia*, 43 Suppl 5, pp. 112–22.

Billen, B., Spurny, R., Brams, M., van Elk, R., Valera-Kummer, S., Yakel, J. L., Voets, T., Bertrand, D., Smit, A. B. and Ulens, C. (2012) 'Molecular actions of smoking cessation drugs at α4β2 nicotinic receptors defined in crystal structures of a homologous binding protein.', *Proceedings of the National Academy of Sciences of the United States of America*. National Academy of Sciences, 109(23), pp. 9173–8..

Brown, R. W. B., Collins, A. C., Lindstrom, J. M. and Whiteaker, P. (2007) 'Nicotinic α5 subunit deletion locally reduces high-affinity agonist activation without altering nicotinic receptor numbers', *Journal of Neurochemistry*, 103(1), pp. 204–215.

Bucher, D. and Goaillard, J.-M. (2011) 'Beyond faithful conduction: short-term dynamics, neuromodulation, and long-term regulation of spike propagation in the axon.', *Progress in neurobiology*. NIH Public Access, 94(4), pp. 307–46.

Cadugan, D. J. and Auerbach, A. (2010) 'Linking the acetylcholine receptor-channel agonist-binding sites with the gate.', *Biophysical journal*. Biophysical Society, 99(3), pp. 798–807.

Carbone, A.-L., Moroni, M., Groot-Kormelink, P.-J. and Bermudez, I. (2009) 'Pentameric concatenated (alpha4)(2)(beta2)(3) and (alpha4)(3)(beta2)(2) nicotinic acetylcholine receptors: subunit arrangement determines functional expression.', *British journal of pharmacology*. Wiley-Blackwell, 156(6), pp. 970–81.

Changeux, J.-P. (2012) 'The nicotinic acetylcholine receptor: the founding father of the pentameric ligand-gated ion channel superfamily.', *The Journal of biological chemistry*. American Society for Biochemistry and Molecular Biology, 287(48), pp. 40207–15.

Changeux, J.-P. (2013) '50 years of allosteric interactions: the twists and turns of the models.', *Nature reviews. Molecular cell biology*, 14(12), pp. 819–29

Chavez-noriega, L. E., Crona, J. H., Washburn, M. S., Urrutia, A., Elliott, K. J. and Johnson, E. C. (1997) 'Pharmacological Characterization of Recombinant Human Neuronal Nicotinic Acetylcholine Receptors in Xenopus Oocytes', 280(1), pp. 346–356.

Colquhoun, D. and Lape, R. (2012) 'Allosteric coupling in ligand-gated ion channels', *The Journal of general physiology*, 140(6), pp. 625–34.

Contant, C., Umbriaco, D., Garcia, S., Watkins, K. C. and Descarries, L. (1996) 'Ultrastructural characterization of the acetylcholine innervation in adult rat neostriatum.', *Neuroscience*, 71(4), pp. 937–47

d'Incamps, B. L. and Ascher, P. (2014) 'High affinity and low affinity heteromeric nicotinic acetylcholine receptors at central synapses.', *The Journal of physiology*. Wiley-Blackwell, 592(19), pp. 4131–6.

Daly, J. W., Garraffo, H. M., Spande, T. F., Decker, M. W., Sullivan, J. P. and Williams, M. (2000) 'Alkaloids from frog skin: the discovery of epibatidine and the potential for developing novel non-opioid analgesics.', *Natural product reports*, 17(2), pp. 131–135. Dani, J. A. and Bertrand, D. (2007) 'Nicotinic acetylcholine receptors and nicotinic cholinergic mechanisms of the central nervous system.', *Annual review of pharmacology and toxicology*, 47, pp. 699–729.

Descarries, L., Gisiger, V. and Steriade, M. (1997) 'Diffuse transmission by acetylcholine in the CNS', *Progress in Neurobiology*, 53(5), pp. 603–625.

Descarries, L. and Mechawar, N. (2000) 'Ultrastructural evidence for diffuse transmission by monoamine and acetylcholine neurons of the central nervous system', *Progress in Brain Research*, 125, pp. 27–47.

Dickinson, J. A., Kew, J. N. C. and Wonnacott, S. (2008) 'Presynaptic 7- and 2-Containing Nicotinic Acetylcholine Receptors Modulate Excitatory Amino Acid Release from Rat Prefrontal Cortex Nerve Terminals via Distinct Cellular Mechanisms', *Molecular Pharmacology*. American Society for Pharmacology and Experimental Therapeutics, 74(2), pp. 348–359.

Elgoyhen, A. B., Vetter, D. E., Katz, E., Rothlin, C. V, Heinemann, S. F. and Boulter, J. (2001) 'alpha10: a determinant of nicotinic cholinergic receptor function in mammalian vestibular and cochlear mechanosensory hair cells.', *Proceedings of the National Academy of Sciences of the United States of America*. National Academy of Sciences, 98(6), pp. 3501–6.

Exley, R. and Cragg, S. J. (2008) 'Presynaptic nicotinic receptors: a dynamic and diverse cholinergic filter of striatal dopamine neurotransmission.', *British journal of pharmacology*. Wiley-Blackwell, (Suppl 1), pp. S283-97.

Exley, R., Moroni, M., Sasdelli, F., Houlihan, L. M., Lukas, R. J., Sher, E., Zwart, R. and Bermudez, I. (2006) 'Chaperone protein 14-3-3 and protein kinase A increase the relative abundance of low agonist sensitivity human alpha 4 beta 2 nicotinic acetylcholine receptors in Xenopus oocytes.', *Journal of neurochemistry*, 98(3), pp. 876–85.

Galindo-Charles, L., Hernandez-Lopez, S., Galarraga, E., Tapia, D., Bargas, J., Garduño, J., Frías-Dominguez, C., Drucker-Colin, R. and Mihailescu, S. (2008) 'Serotoninergic dorsal raphe neurons possess functional postsynaptic nicotinic acetylcholine receptors.', *Synapse (New York, N.Y.)*, 62(8), pp. 601–15.

Gao, B., Hierl, M., Clarkin, K., Juan, T., Nguyen, H., Valk, M. van der, Deng, H., Guo, W., Lehto, S. G., Matson, D., McDermott, J. S., Knop, J., Gaida, K., Cao, L., Waldon, D., Albrecht, B. K., Boezio, A. A., Copeland, K. W., Harmange, J.-C., Springer, S. K., Malmberg, A. B. and McDonough, S. I. (2010) 'Pharmacological effects of nonselective and subtype-selective nicotinic acetylcholine receptor agonists in animal models of persistent pain.', *Pain*, 149(1), pp. 33–49.

Garduno, J., Galindo-charles, L., Jime, J., Galarraga, E., Tapia, D., Mihailescu, S. and Hernandez-lopez, S. (2012) 'Presynaptic alpha4 beta2 Nicotinic Acetylcholine Receptors Increase Glutamate Release and Serotonin Neuron Excitability in the Dorsal Raphe Nucleus', 32(43), pp. 15148–15157.

Gatto, G. J., Bohme, G. A., Caldwell, W. S., Letchworth, S. R., Traina, V. M., Obinu, M. C., Laville, M., Reibaud, M., Pradier, L., Dunbar, G. and Bencherif, M. (2004) 'TC-1734: an orally active neuronal nicotinic acetylcholine receptor modulator with antidepressant, neuroprotective and long-lasting cognitive effects.', *CNS drug reviews*, 10(2), pp. 147–66.

Giocomo, L. M. and Hasselmo, M. E. (2007) 'Neuromodulation by Glutamate and Acetylcholine can Change Circuit Dynamics by Regulating the Relative Influence of Afferent Input and Excitatory Feedback', *Molecular Neurobiology*. Humana Press Inc, 36(2), pp. 184–200.

Goldberg, J. A., Ding, J. B. and Surmeier, D. J. (2012) 'Muscarinic modulation of striatal function and circuitry.', *Handbook of experimental pharmacology*, (208), pp. 223–41.

Gotti, C., Clementi, F., Fornari, A., Gaimarri, A., Guiducci, S., Manfredi, I., Moretti, M., Pedrazzi, P., Pucci, L. and Zoli, M. (2009) 'Structural and functional diversity of native brain neuronal nicotinic receptors.', *Biochemical pharmacology*, 78(7), pp. 703–11.

Gotti, C., Moretti, M., Gaimarri, A., Zanardi, A., Clementi, F. and Zoli, M. (2007) 'Heterogeneity and complexity of native brain nicotinic receptors.', *Biochemical pharmacology*, 74(8), pp. 1102–11.

Grady, S. R., Moretti, M., Zoli, M., Marks, M. J., Zanardi, A., Pucci, L., Clementi, F. and Gotti, C. (2009) 'Rodent habenulo-interpeduncular pathway expresses a large variety of uncommon nAChR subtypes, but only the alpha3beta4* and alpha3beta3beta4* subtypes mediate acetylcholine release.', *The Journal of neuroscience : the official journal of the Society for Neuroscience*. NIH Public Access, 29(7), pp. 2272–82.

Grady, S. R., Salminen, O., McIntosh, J. M., Marks, M. J. and Collins, A. C. (2010) 'Mouse striatal dopamine nerve terminals express alpha4alpha5beta2 and two stoichiometric forms of alpha4beta2*-nicotinic acetylcholine receptors.', *Journal of molecular neuroscience : MN*. NIH Public Access, 40(1–2), pp. 91–5.

Grilli, M., Zappettini, S., Raiteri, L. and Marchi, M. (2009) 'Nicotinic and muscarinic cholinergic receptors coexist on GABAergic nerve endings in the mouse striatum and interact in modulating GABA release.', *Neuropharmacology*, 56(3), pp. 610–4.

Han, Z.-Y., Zoli, M., Cardona, A., Bourgeois, J.-P., Changeux, J.-P. and Le Novère, N. (2003) 'Localization of [^{3} H]nicotine, [^{3} H]cytisine, [^{3} H]epibatidine, and [^{125} I]α-bungarotoxin binding sites in the brain of *Macaca mulatta*', *Journal of Comparative Neurology*. Wiley Subscription Services, Inc., A Wiley Company, 461(1), pp. 49–60

Hasselmo, M. E. (2006) 'The role of acetylcholine in learning and memory.', *Current opinion in neurobiology*. NIH Public Access, 16(6), pp. 710–5.

Hasselmo, M. E. and Sarter, M. (2011) 'Modes and models of forebrain cholinergic neuromodulation of cognition.', *Neuropsychopharmacology : official publication of the American College of Neuropsychopharmacology*. Nature Publishing Group, 36(1), pp. 52–73.

Hibbs, R. E., Sulzenbacher, G., Shi, J., Talley, T. T., Conrod, S., Kem, W. R., Taylor, P., Marchot, P. and Bourne, Y. (2009) 'Structural determinants for interaction of partial agonists with acetylcholine binding protein and neuronal alpha7 nicotinic acetylcholine receptor.', *The EMBO journal*. European Molecular Biology Organization, 28(19), pp. 3040–51.

Ito, H. T. and Schuman, E. M. (2008) 'Frequency-dependent signal transmission and modulation by neuromodulators.', *Frontiers in neuroscience*. Frontiers Media SA, 2(2), pp. 138–44.

Jackson, K. J., Marks, M. J., Vann, R. E., Chen, X., Gamage, T. F., Warner, J. A. and Damaj, M. I. (2010) 'Role of alpha5 nicotinic acetylcholine receptors in pharmacological and behavioral effects of nicotine in mice.', *The Journal of pharmacology and experimental therapeutics*. American Society for Pharmacology and Experimental Therapeutics, 334(1), pp. 137–46.

Kawai, H., Lazar, R. and Metherate, R. (2007) 'Nicotinic control of axon excitability regulates thalamocortical transmission.', *Nature neuroscience*, 10(9), pp. 1168–75Kedmi, M., Beaudet, A. L. and Orr-Urtreger, A. (2004) 'Mice lacking neuronal nicotinic acetylcholine receptor beta4-subunit and mice lacking both alpha5- and beta4-subunits are highly resistant to nicotine-induced seizures.', *Physiological genomics*, 17(2), pp. 221–9.

Khiroug, S. S., Harkness, P. C., Lamb, P. W., Sudweeks, S. N., Khiroug, L., Millar, N. S. and Yakel, J. L. (2002) 'Rat nicotinic ACh receptor alpha7 and beta2 subunits co-assemble to form functional heteromeric nicotinic receptor channels.', *The Journal of physiology*. Wiley-Blackwell, 540(Pt 2), pp. 425–34.

Kummer, W., Lips, K. S. and Pfeil, U. (2008) 'The epithelial cholinergic system of the airways.', *Histochemistry and cell biology*. Springer, 130(2), pp. 219–34.

Kurahashi, H. and Hirose, S. (1993) *Autosomal Dominant Nocturnal Frontal Lobe Epilepsy*, *GeneReviews*. University of Washington, Seattle. Available at: http://www.ncbi.nlm.nih.gov/pubmed/20301348 (Accessed: 13 September 2016).

Kuryatov, A., Berrettini, W. and Lindstrom, J. (2011) ‘Acetylcholine receptor (AChR) α5 subunit variant associated with risk for nicotine dependence and lung cancer reduces $(\alpha4\beta2)_2\alpha5$ AChR function.’, *Molecular pharmacology*. American Society for Pharmacology and Experimental Therapeutics, 79(1), pp. 119–25.

Kuryatov, A., Luo, J., Cooper, J. and Lindstrom, J. (2005) ‘Nicotine Acts as a Pharmacological Chaperone to Upregulate Human 4 2 AChRs’, *Molecular Pharmacology*, 68(6), pp. 1839–1851.

Kuryatov, A., Onksen, J. and Lindstrom, J. (2008) ‘Roles of accessory subunits in α4β2* nicotinic receptors’, *Molecular Pharmacology*, 74(1), pp. 132–143.

Labarca, C., Schwarz, J., Deshpande, P., Schwarz, S., Nowak, M. W., Fonck, C., Nashmi, R., Kofuji, P., Dang, H., Shi, W., Fidan, M., Khakh, B. S., Chen, Z., Bowers, B. J., Boulter, J., Wehner, J. M. and Lester, H. A. (2001) ‘Point mutant mice with hypersensitive alpha 4 nicotinic receptors show dopaminergic deficits and increased anxiety.’, *Proceedings of the National Academy of Sciences of the United States of America*. National Academy of Sciences, 98(5), pp. 2786–91.

Lambe, E. K., Picciotto, M. R. and Aghajanian, G. K. (2003) ‘Nicotine induces glutamate release from thalamocortical terminals in prefrontal cortex.’, *Neuropsychopharmacology : official publication of the American College of Neuropsychopharmacology*, 28, pp. 216–225.

Laviolette, S. R. and van der Kooy, D. (2004) ‘The neurobiology of nicotine addiction: bridging the gap from molecules to behaviour’, *Nature Reviews Neuroscience*. Nature Publishing Group, 5(1), pp. 55–65.

Lee, W. Y. and Sine, S. M. (2005) ‘Principal pathway coupling agonist binding to channel gating in nicotinic receptors’, *Nature*. Nature Publishing Group, 438(7065), pp. 243–247.

Léna, C. and Changeux, J. P. (1999) ‘The role of beta 2-subunit-containing nicotinic acetylcholine receptors in the brain explored with a mutant mouse.’, *Annals of the New York Academy of Sciences*, 868, pp. 611–6.

Léna, C., de Kerchove D’Exaerde, A., Cordero-Erausquin, M., Le Novère, N., del Mar Arroyo-Jimenez, M. and Changeux, J. P. (1999) ‘Diversity and distribution of nicotinic acetylcholine receptors in the locus ceruleus neurons.’, *Proceedings of the National Academy of Sciences of the United States of America*. National Academy of Sciences, 96(21), pp. 12126–31.

Lester, H. A., Xiao, C., Srinivasan, R., Son, C. D., Miwa, J., Pantoja, R., Banghart, M. R., Dougherty, D. A., Goate, A. M. and Wang, J. C. (2009) ‘Nicotine is a selective pharmacological chaperone of acetylcholine receptor number and stoichiometry. Implications for drug discovery.’, *The AAPS journal*. Springer, 11(1), pp. 167–77.

Letzkus, J. J., Wolff, S. B. E., Meyer, E. M. M., Tovote, P., Courtin, J., Herry, C. and Lüthi, A. (2011) 'A disinhibitory microcircuit for associative fear learning in the auditory cortex.', *Nature*, 480(7377), pp. 331–5.

Levin, E. D. and Simon, B. B. (1998) 'Nicotinic acetylcholine involvement in cognitive function in animals.', *Psychopharmacology*, 138(3–4), pp. 217–230.

Lips, K. S., Pfeil, U. and Kummer, W. (2002) 'Coexpression of alpha 9 and alpha 10 nicotinic acetylcholine receptors in rat dorsal root ganglion neurons.', *Neuroscience*, 115(1), pp. 1–5.

López-Muñoz, F., Boya, J. and Alamo, C. (2006) 'Neuron theory, the cornerstone of neuroscience, on the centenary of the Nobel Prize award to Santiago Ramón y Cajal.', *Brain research bulletin*, 70(4–6), pp. 391–405.

Luchicchi, A., Bloem, B., Via??a, J. N. M., Mansvelder, H. D. and Role, L. W. (2014) 'Illuminating the role of cholinergic signaling in circuits of attention and emotionally salient behaviors', *Frontiers in Synaptic Neuroscience*, 6(OCT), pp. 1–10.

Lukas, R. J., Changeux, J. P., Le Novère, N., Albuquerque, E. X., Balfour, D. J., Berg, D. K., Bertrand, D., Chiappinelli, V. A., Clarke, P. B., Collins, A. C., Dani, J. A., Grady, S. R., Kellar, K. J., Lindstrom, J. M., Marks, M. J., Quik, M., Taylor, P. W. and Wonnacott, S. (1999) 'International Union of Pharmacology. XX. Current status of the nomenclature for nicotinic acetylcholine receptors and their subunits.', *Pharmacological reviews*. American Society for Pharmacology and Experimental Therapeutics, 51(2), pp. 397–401.

Mansvelder, H. D. and McGehee, D. S. (2002a) 'Cellular and synaptic mechanisms of nicotine addiction.', *Journal of neurobiology*, 53(4), pp. 606–17.

Mantione, E., Micheloni, S., Alcaino, C., New, K., Mazzaferro, S. and Bermudez, I. (2012) 'Allosteric modulators of alpha4beta2 nicotinic acetylcholine receptors: a new direction for antidepressant drug discovery', *Future Med.Chem.*, 4(1756–8927 (Electronic)), pp. 2217–2230.

Marchi, M. and Grilli, M. (2010) 'Presynaptic nicotinic receptors modulating neurotransmitter release in the Central Nervous System: Functional interactions with other coexisting receptors', *Progress in Neurobiology*, 92(2), pp. 105–111.

Markett, S., Montag, C. and Reuter, M. (2011) 'The nicotinic acetylcholine receptor gene CHRNA4 is associated with negative emotionality.', *Emotion (Washington, D.C.)*, 11(2), pp. 450–5.

Maskos, U. (2010) 'Role of endogenous acetylcholine in the control of the dopaminergic system via nicotinic receptors', *Journal of Neurochemistry*. Blackwell Publishing Ltd, 114(3), pp. 641–646.

Maskos, U., Molles, B. E., Pons, S., Besson, M., Guiard, B. P., Guilloux, J.-P., Evrard, A., Cazala, P., Cormier, A., Mameli-Engvall, M., Dufour, N., Cloëz-Tayarani, I., Bemelmans, A.-P., Mallet, J., Gardier, A. M., David, V., Faure, P., Granon, S. and Changeux, J.-P. (2005) 'Nicotine reinforcement and cognition restored by targeted expression of nicotinic receptors.', *Nature*, 436(7047), pp. 103–7.

Mazzaferro, S., Benallegue, N., Carbone, A., Gasparri, F., Vijayan, R., Biggin, P. C., Moroni, M. and Bermudez, I. (2011) 'Additional acetylcholine (ACh) binding site at alpha4/alpha4 interface of (alpha4beta2)2alpha4 nicotinic receptor influences agonist sensitivity.', *The Journal of biological chemistry*. American Society for Biochemistry and Molecular Biology, 286(35), pp. 31043–54.

Mazzaferro, S., Gasparri, F., New, K., Alcaino, C., Faundez, M., Vasquez, P. I., Vijayan, R., Biggin, P. C. and Bermudez, I. (2014) 'Non-equivalent Ligand Selectivity of Agonist Sites in (α4β2)2α4 Nicotinic Acetylcholine Receptors: A Key Determinant of Agonist Efficacy.', *The Journal of biological chemistry*.

McGehee, D. S., Heath, M. J., Gelber, S., Devay, P. and Role, L. W. (1995) 'Nicotine enhancement of fast excitatory synaptic transmission in CNS by presynaptic receptors.', *Science (New York, N.Y.)*, 269(5231), pp. 1692–6.

McKee, S. A., Weinberger, A. H., Shi, J., Tetrault, J. and Coppola, S. (2012) 'Developing and validating a human laboratory model to screen medications for smoking cessation.', *Nicotine & tobacco research : official journal of the Society for Research on Nicotine and Tobacco*. Oxford University Press, 14(11), pp. 1362–71.

McQuiston, A. R. (2014) 'Acetylcholine release and inhibitory interneuron activity in hippocampal CA1.', *Frontiers in synaptic neuroscience*. Frontiers Media SA, 6, p. 20.

Miller, P. S. and Smart, T. G. (2010) 'Binding, activation and modulation of Cys-loop receptors.', *Trends in pharmacological sciences*. Elsevier Ltd, 31(4), pp. 161–74.

Mineur, Y. S., Fote, G. M., Blakeman, S., Cahuzac, E. L. M., Newbold, S. A. and Picciotto, M. R. (2016) 'Multiple Nicotinic Acetylcholine Receptor Subtypes in the Mouse Amygdala Regulate Affective Behaviors and Response to Social Stress', *Neuropsychopharmacology*. Nature Publishing Group, 41(6), pp. 1579–1587.

Mineur, Y. S., Obayemi, A., Wigestrand, M. B., Fote, G. M., Calarco, C. A., Li, A. M. and Picciotto, M. R. (2013) 'Cholinergic signaling in the hippocampus regulates social stress resilience and anxiety- and depression-like behavior.', *Proceedings of the National Academy of Sciences of the United States of America*. National Academy of Sciences, 110(9), pp. 3573–8.

Mineur, Y. S. and Picciotto, M. R. (2010) 'Nicotine receptors and depression: revisiting and revising the cholinergic hypothesis.', *Trends in pharmacological sciences*. NIH Public Access, 31(12), pp. 580–6.

Miyazawa, A., Fujiyoshi, Y. and Unwin, N. (2003) ‘Structure and gating mechanism of the acetylcholine receptor pore.’, *Nature*, 423(6943), pp. 949–55.

Moretti, M., Vailati, S., Zoli, M., Lippi, G., Riganti, L., Longhi, R., Viegi, A., Clementi, F. and Gotti, C. (2004) ‘Nicotinic Acetylcholine Receptor Subtypes Expression during Rat Retina Development and Their Regulation by Visual Experience’, *Molecular Pharmacology*. American Society for Pharmacology and Experimental Therapeutics, 66(1), pp. 85–96.

Moroni, M., Zwart, R., Sher, E., Cassels, B. K. and Bermudez, I. (2006) ‘alpha4 beta2 Nicotinic Receptors with High and Low Acetylcholine Sensitivity : Pharmacology , Stoichiometry , and Sensitivity to Long-Term Exposure to Nicotine’, 70(2), pp. 755–768.

Moroni M, Zwart R, Sher E, Cassels BK, B. I. (2006) ‘Alpha4 Beta2 Nicotinic Receptors With High and Low Acetylcholine Sensitivity: Pharmacology,Stoichiometry, and Sensitivity To Long-Term Exposure To Nicotine.’, *Mol Pharmacol.*, 70(2), pp. 755–768.

Murray, T. A., Bertrand, D., Papke, R. L., George, A. A., Pantoja, R., Srinivasan, R., Liu, Q., Wu, J., Whiteaker, P., Lester, H. A. and Lukas, R. J. (2012) ‘α7β2 nicotinic acetylcholine receptors assemble, function, and are activated primarily via their α7-α7 interfaces.’, *Molecular pharmacology*. American Society for Pharmacology and Experimental Therapeutics, 81(2), pp. 175–88.

Ngolab, J., Liu, L., Zhao-Shea, R., Gao, G., Gardner, P. D. and Tapper, A. R. (2015) ‘Functional Upregulation of α4* Nicotinic Acetylcholine Receptors in VTA GABAergic Neurons Increases Sensitivity to Nicotine Reward.’, *The Journal of neuroscience : the official journal of the Society for Neuroscience*. Society for Neuroscience, 35(22), pp. 8570–8.

Paterson, D. and Nordberg, A. (2000) ‘Neuronal nicotinic receptors in the human brain.’, *Progress in neurobiology*, 61(1), pp. 75–111.

Picciotto, M. R., Addy, N. A., Mineur, Y. S. and Brunzell, D. H. (2008) ‘It is not "either/or": activation and desensitization of nicotinic acetylcholine receptors both contribute to behaviors related to nicotine addiction and mood.’, *Progress in neurobiology*. NIH Public Access, 84(4), pp. 329–42..

Picciotto, M. R., Higley, M. J. and Mineur, Y. S. (2012) ‘Acetylcholine as a neuromodulator: cholinergic signaling shapes nervous system function and behavior.’, *Neuron*. NIH Public Access, 76(1), pp. 116–29.

Poorthuis, R. B., Enke, L. and Letzkus, J. J. (2014) ‘Cholinergic circuit modulation through differential recruitment of neocortical interneuron types during behaviour.’, *The Journal of physiology*. Wiley-Blackwell, 592(19), pp. 4155–64.

Purohit, P., Mitra, A. and Auerbach, A. (2007) ‘A stepwise mechanism for acetylcholine receptor channel gating.’, *Nature*, 446(7138), pp. 930–3.

Rabenstein, R. L., Caldarone, B. J. and Picciotto, M. R. (2006) 'The nicotinic antagonist mecamylamine has antidepressant-like effects in wild-type but not beta2- or alpha7-nicotinic acetylcholine receptor subunit knockout mice.', *Psychopharmacology*, 189(3), pp. 395–401.

Rode, F., Munro, G., Holst, D., Nielsen, E. Ø., Troelsen, K. B., Timmermann, D. B., Rønn, L. C. B. and Grunnet, M. (2012) 'Positive allosteric modulation of α4β2 nAChR agonist induced behaviour.', *Brain research*, 1458, pp. 67–75.

Sarter, M., Parikh, V. and Howe, W. M. (2009) 'Phasic acetylcholine release and the volume transmission hypothesis: time to move on.', *Nature reviews. Neuroscience*. NIH Public Access, 10(5), pp. 383–90.

Scheffer, I. E., Bhatia, K. P., Lopes-Cendes, I., Fish, D. R., Marsden, C. D., Andermann, E., Andermann, F., Desbiens, R., Keene, D. and Cendes, F. (1995) 'Autosomal dominant nocturnal frontal lobe epilepsy. A distinctive clinical disorder.', *Brain : a journal of neurology*, pp. 61–73.

Sgard, F., Charpantier, E., Bertrand, S., Walker, N., Caput, D., Graham, D., Bertrand, D. and Besnard, F. (2002) 'A Novel Human Nicotinic Receptor Subunit, alpha 10, That Confers Functionality to the alpha 9-Subunit', *Molecular Pharmacology*. American Society for Pharmacology and Experimental Therapeutics, 61(1), pp. 150–159.

Srinivasan, R., Pantoja, R., Moss, F. J., Mackey, E. D. W., Son, C. D., Miwa, J. and Lester, H. A. (2011) 'Nicotine up-regulates alpha4beta2 nicotinic receptors and ER exit sites via stoichiometry-dependent chaperoning.', *The Journal of general physiology*. The Rockefeller University Press, 137(1), pp. 59–79.

Steinlein, O. K., Hoda, J. C., Bertrand, S. and Bertrand, D. (2012) 'Mutations in familial nocturnal frontal lobe epilepsy might be associated with distinct neurological phenotypes', *Seizure*. BEA Trading Ltd, 21(2), pp. 118–123.

Tansey, E. M. (2006) 'Henry Dale and the discovery of acetylcholine.', *Comptes rendus biologies*, 329(5–6), pp. 419–25.

Tapper, A. R., McKinney, S. L., Nashmi, R., Schwarz, J., Deshpande, P., Labarca, C., Whiteaker, P., Marks, M. J., Collins, A. C. and Lester, H. A. (2004) 'Nicotine activation of alpha4* receptors: sufficient for reward, tolerance, and sensitization.', *Science (New York, N.Y.)*, 306(5698), pp. 1029–32.

Timmermann, D. B., Sandager-Nielsen, K., Dyhring, T., Smith, M., Jacobsen, A.-M., Nielsen, E. Ø., Grunnet, M., Christensen, J. K., Peters, D., Kohlhaas, K., Olsen, G. M. and Ahring, P. K. (2012) 'Augmentation of cognitive function by NS9283, a stoichiometry-dependent positive allosteric modulator of α2- and α4-containing nicotinic acetylcholine receptors.', *British journal of pharmacology*. Wiley-Blackwell, 167(1), pp. 164–82.

Turrini, P., Casu, M. A., Wong, T. P., De Koninck, Y., Ribeiro-da-Silva, A. and Cuello, A. C. (2001) 'Cholinergic nerve terminals establish classical synapses in the

rat cerebral cortex: synaptic pattern and age-related atrophy.', *Neuroscience*, 105(2), pp. 277–85.

Unwin, N. and Fujiyoshi, Y. (2012) 'Gating movement of acetylcholine receptor caught by plunge-freezing.', *Journal of molecular biology*. Elsevier, 422(5), pp. 617–34.

Verbitsky, M., Rothlin, C. V, Katz, E. and Elgoyhen, A. B. (2000) 'Mixed nicotinic-muscarinic properties of the alpha9 nicotinic cholinergic receptor.', *Neuropharmacology*, 39(13), pp. 2515–24.

Vidal, C. and Changeux, J. P. (1993) 'Nicotinic and muscarinic modulations of excitatory synaptic transmission in the rat prefrontal cortex in vitro.', *Neuroscience*, 56(1), pp. 23–32.

White, B. H. and Cohen, J. B. (1992) 'Agonist-induced changes in the structure of the acetylcholine receptor M2 regions revealed by photoincorporation of an uncharged nicotinic noncompetitive antagonist', *Journal of Biological Chemistry*, 267(22), pp. 15770–15783.

Wilkie, G. I., Hutson, P., Sullivan, J. P. and Wonnacott, S. (1996) 'Pharmacological characterization of a nicotinic autoreceptor in rat hippocampal synaptosomes.', *Neurochemical research*, 21(9), pp. 1141–8.

Wonnacott, S., Irons, J., Rapier, C., Thorne, B. and Lunt, G. G. (1989) 'Presynaptic modulation of transmitter release by nicotinic receptors', *Progress in Brain Research*, 79, pp. 157–163.

Wooltorton, J. R. A., Pidoplichko, V. I., Broide, R. S. and Dani, J. A. (2003) 'Differential Desensitization and Distribution of Nicotinic Acetylcholine Receptor Subtypes in Midbrain Dopamine Areas', *The Journal of Neuroscience*, 23(8), pp. 3176–3185.

Wu, J. and Lukas, R. J. (2011) 'Naturally-expressed nicotinic acetylcholine receptor subtypes.', *Biochemical pharmacology*. NIH Public Access, 82(8), pp. 800–7.

Xiu, X., Hanek, A. P., Wang, J., Lester, H. A. and Dougherty, D. A. (2005) 'A unified view of the role of electrostatic interactions in modulating the gating of Cys loop receptors', *Journal of Biological Chemistry*, 280(50), pp. 41655–41666.

Yu, A. J. and Dayan, P. (2005) 'Uncertainty, neuromodulation, and attention', *Neuron*, 46(4), pp. 681–692.

Zhang, H., Lin, S.-C. and Nicolelis, M. A. L. (2010) 'Spatiotemporal coupling between hippocampal acetylcholine release and theta oscillations in vivo.', *The Journal of neuroscience : the official journal of the Society for Neuroscience*. NIH Public Access, 30(40), pp. 13431–40.

Zhang, J., Xiao, Y.-D., Jordan, K. G., Hammond, P. S., Van Dyke, K. M., Mazurov, A. A., Speake, J. D., Lippiello, P. M., James, J. W., Letchworth, S. R., Bencherif, M. and Hauser, T. A. (2012) 'Analgesic effects mediated by neuronal nicotinic acetylcholine receptor agonists: correlation with desensitization of α4β2* receptors.', *European journal of pharmaceutical sciences : official journal of the European Federation for Pharmaceutical Sciences*, 47(5), pp. 813–23.

Zoli, M., Léna, C., Picciotto, M. R. and Changeux, J. P. (1998) 'Identification of four classes of brain nicotinic receptors using beta2 mutant mice.', *The Journal of neuroscience : the official journal of the Society for Neuroscience*, 18(12), pp. 4461–72.